To cancer patients

and their loved ones

waiting in hope

CHARACTERIZATION OF EXTRACELLULAR PURINERGIC SIGNALING COMPONENTS IN COLORECTAL CARCINOMA

A THESIS SUBMITTED TO

THE GRADUATE SCHOOL OF ENGINEERING AND SCIENCE

OF BILKENT UNIVERSITY

IN PARTIAL FULFILLMENT OF THE REQUIREMENTS FOR

THE DEGREE OF

MASTER OF SCIENCE

IN

MOLECULAR BIOLOGY AND GENETICS

By

Beste Uygur

January 2021

CHARACTERIZATION OF EXTRACELLULAR PURINERGIC SIGNALING COMPONENTS IN COLORECTAL CARCINOMA

By Beste Uygur

January 2021

We certify that we have read this thesis and in our opinion it is fully adequate, in scope and in quality, as a thesis for the degree of Master of Science.

Serkan İsmail Göktuna (Advisor)

Onur Çizmecioğlu

Sreeparna Banerjee

Approved for Graduate School of Engineering and Science:

Ezhan Karaşan

Director of Graduate School of Engineering and Science

ABSTRACT

CHARACTERIZATION OF EXTRACELLULAR PURINERGIC SIGNALING COMPONENTS IN COLORECTAL CARCINOMA

Beste Uygur
M.Sc. in Molecular Biology and Genetics
Advisor: Serkan İsmail Göktuna
January 2021

Colorectal carcinoma is a heterogeneous disease which is the third leading cause of cancer-associated mortalities in the world. It is also reported to be the third most diagnosed cancer among other cancer types. The intracellular functions of purines and pyrimidines in energy transaction and nucleic acid synthesis reactions have been well-known and clarified. Notwithstanding, the extracellular roles played by purinergic signaling components in cancer initiation and progression was not disclosed thoroughly as yet and become more prominent day by day. The extracellular purinergic system may have growth-inhibiting or growth-promoting effects in tumors in a tissue and context-dependent manner. Indeed, the knowledge regarding the impact of these elements in colorectal cancer is immensely limited. Therefore, in this study, we focused on deciphering the involvement of several extracellular purinergic signaling components in colorectal cancer, which are mainly one of the enzymes involved in degradation process of ATP, PSE002, and one of the adenosine receptors, PSC003. To assess their roles in colorectal cancer, we generated stable knockout cell lines targeting these two genes separately by CRISPR/Cas9 gene editing as well as transiently depleted cell lines by RNA interference (RNAi). The depletion of PSE002 and also PSC003 promoted cell proliferation and their anchorage-independent growth *in vitro.* In addition to this, their loss resulted in enhanced epithelial-to-mesenchymal transition (EMT) by upregulating the expression of mesenchymal markers. Moreover, cell line-derived xenograft models (CDX) of PSE002 could corroborate *in vitro* findings and strikingly augmented tumor growth *in vivo.* Interestingly, the effects observed in colorectal cancer cell lines upon

PSE002 silencing could not be seen upon pharmacological inhibition by PSE002-selective antagonist. Contrary to this, PSC003-selective antagonist led to increased proliferative capacity in colorectal cancer cell lines under normal or hypoxic conditions. Ultimately, our findings provide a different perspective to extracellular adenosine signaling and claim that these targets act as tumor suppressor genes in colorectal carcinoma which should be taken into consideration for selecting therapeutic strategies against colorectal cancer.

Key words: Purinergic signaling, colorectal cancer, CRISPR/Cas9, ectonucleotidase, adenosine receptors, adenosine signaling

ÖZET

HÜCRELER ARASI PÜRİNERJİK SİNYALİZASYON BİLEŞENLERİNİN KOLOREKTAL KARSİNOMDA KARAKTERİZASYONU

Beste Uygur

Moleküler Biyoloji ve Genetik Yüksek Lisans

Tez Danışmanı: Serkan İsmail Göktuna

January 2021

Kolorektal kanser, kanser-ilişkili ölümlerin en büyük ikinci sebebi olan ve diğer kanserler arasında üçüncü en çok tanı konulan heterojen bir hastalıktır. Pürin ve pirimidinlerin enerji transaksiyon ve nükleik asit sentez reaksiyonları gibi hücre içi işlevleri oldukça iyi bilinmektedir. Buna karşın pürinerjik sinyalizasyon bileşenlerinin kanser başlangıcı ve ilerlemesindeki hücre dışı rolleri yeterince belirlenememiş olmakla birlikte her geçen gün daha çok öne çıkan bir hal almaktadır. Hücreler arası pürinerjik sinyal yolağı, doku ve bağlam bağımlı olarak tümörlerde büyümeyi teşvik edici veya büyümeyi inhibe edici etki gösterebilmektedir. Bunun yanında, bu bileşenlerin kolorektal kanserdeki etkilerine dair olan bilgi birikimi oldukça sınırlıdır. Dolayısıyla, bu çalışmamızda, ATP degradasyon süreçlerinde rol oynayan enzimlerden biri olan PSE002 ve adenozin reseptörlerinden biri olan PSC003 gibi çeşitli ekstrasellüler pürinerjik sinyalizasyon komponentlerinin kolorektal kanserdeki etkileri üzerine yoğunlaşılmıştır. Bu komponentlerin kolorektal kanserdeki etkilerinin incelenebilmesi için ayrı ayrı olmak üzere CRISPR/Cas9 yöntemi kullanılarak stabil knockout hücre hatları oluşturulmuştur. Buna ek olarak bu genler RNA interferans ile geçici olarak da susturulmuştur. Bu susturulmuş kolorektal karsinoma (KRK) hücre hatları kullanılarak yapılan çalışmalarda PSE002 ve PSC003'nin susturulmasının hücrelerin proliferasyonunu ve yüzeyden bağımsız olarak büyüme oranlarını *in vitro* olarak arttırdığı gözlenmiştir. Buna ek olarak, bu genlerin KRK hücrelerindeki kaybı mezenkimal hücre yüzey belirteçlerinin ekspresyon seviyesini artırıp epitel-mezenkimal

geçişi indüklemiştir. Dahası, KRK hücre hattı kullanımı ile oluşturulan ksenograft modelleri *in vitro* dataları desteklemiş ve tümör büyümesini önemli derecede teşvik etmiştir. İlginç olarak, PSE002-susturulmuş hücre hatları ile görülen etkiler, PSE002 farmakolojik inhibitor kullanımının ardından doğrulanamamıştır. Bunun aksine, PSC003-seçici antagonisti kolorektal kanser hücre hatlarında hücre büyümesini normal veya hipoksik koşullarda desteklemiştir. Sonuç olarak, bulgularımız hücreler arası adenozin sinyal yolağına yeni bir bakış açısı sağlamakta ve bu hedef genlerin tümör baskılayıcı genler olarak fonksiyon gösterdiğini, kolorektal kanseri hedef alan terapötik stratejiler belirlenirken bu bilgilerin de göz önüne alınması gerektiğini işaret etmektedir.

Anahtar kelimeler: Pürinerjik sinyalizasyon, kolorektal kanser, CRISPR/Cas9, ektonükleotidaz, adenozin reseptörleri, adenozin sinyal yolağı

ACKNOWLEDGEMENTS

Firstly, I would like to express my deepest gratitude to my advisor Assist. Prof. Serkan İsmail Göktuna for his patience and guidance throughout my graduate studies. I have considerably improved my skills to become a better scientist and I am grateful to him for always supporting me, creating a productive atmosphere in our lab and sharing his ceaseless knowledge and experiences. It would not be possible to work this hard without his precious supervision and encouragement.

I am deeply indebted to Dr. Tieu Lan Chau for always being available for my questions and discussion about my results, managing every single detail in our lab, creating a peaceful working environment and always being understanding. It would be impossible to progress without her esteemed guidance and tremendous ideas to save the experiments even at the last minute.

I would also like to express my appreciation to committee members, Assist. Prof. Onur Çizmecioğlu and Prof. Dr. Sreeparna Banerjee for their feedbacks and contributions in completion of this thesis.

I would like to express my sincere gratitude to my lovely family for always being understanding in busy times and for their unconditional love and endless support in every decision I have made. I am always going to be grateful to them for being my reason to keep it up. I would also like to express my deepest appreciation and special regard to Javaid Jabbar for always being there for me under any circumstances and coping with the challenges we have faced as if they were his. I would also like to thank Marzana Ishraq, Melike Dinççelik Aslan, Hazal Beril Çatalak and Burçin İrem Arıcı for their great friendship and support. I wish to show my gratitude to my lab mates Zeynep Güneş Tepe and Servin Bagheralmoosavi for providing collaborative research environment, to Pelin Gülizar Ersan for helping me and answering my every single question in detail about *in vivo* work and to my undergraduate student Alperen Baran to relieve my burden and for always being there to help. Lastly, I would like to thank each

member of the department of Molecular Biology and Genetics at Bilkent University for providing a pleasant working environment.

The studies reported here are supported by TÜBİTAK ARDEB 118S399 grant.

Table of Contents

List of Figures

List of Tables

Abbreviations

CRC – Colorectal Carcinoma/Colorectal Cancer

CIN – Chromosomal instability

LOH – Loss of heterozygosity

TP53 – Tumor protein p53

APC - Adenomatous polyposis coli

MMR – Mismatch repair

MSI – Microsatellite instability

MSS – Microsatellite stable

CIMP – CpG island methylator phenotype

CMS – Consensus molecular subtype

EMT – Epithelial-mesenchymal transition

ECM – Extracellular matrix

NF-κB – Nuclear factor kappa B

TGF-β – Tumor growth factor beta

HIF-1 – Hypoxia-induced factor 1

ERKs – Extracellular signal-regulated kinases

MAPKs – Mitogen-activated protein kinases

MEKs – Mitogen-activated protein kinase kinases

TNF-α – Tumor necrosis factor alpha

ATP – Adenosine triphosphate

ADO – Adenosine

E-NTPDase – Ectonucleotide triphosphate disphosphohydrolase

NT5E – Ecto-5’-nucleotidase

ADA – Adenosine deaminase

AMPCP/APCP – α,β-methylene adenosine diphosphate

CRISPR – Clustered Regularly Interspaced Short Palindromic Repeats

Cas9 – CRISPR-associated protein 9

CHAPTER 1

INTRODUCTION

Colorectal cancer is a heterogeneous disease caused by numerous genetic and epigenetic aberrations arising incrementally within cells. In spite of progress in detection and treatment methods, colorectal cancer (CRC) is still known as the third most diagnosed cancer and the second main reason of cancer-related mortalities in the world[1][2][3]. Colorectal cancer incidents are sporadic by 65% meaning that it is independent of family history or conspicuous genetic predisposition[4] whereas 35% of the cases are hereditary which rises with the effect of environmental determinants[4][5].

1.1. Molecular characteristics of colorectal carcinoma

Different subtypes of colorectal cancer can be categorized by distinct clinical and molecular characteristics such as chromosomal instability (CIN) observed in most of the sporadic cases[6][7] which appears as alteration in chromosome structure and number. Chromosomal rearrangements, loss of heterozygosity (LOH) and gain or loss of chromosomal segments may be evaluated as changes which are likely to affect the regulation of genes playing role in cell cycle checkpoints or cell proliferation, and/or tumor-associated genes. These changes, which has been seen 85% of CRC initiation process[6][7][10], may trigger pathways required for colorectal cancer initiation and progression[8][9]. In these tumors, the mutations are accumulated especially in some tumor suppresser genes including TP53 (tumor protein p53) and APC, and in oncogenes such as BRAF (B-Raf proto-oncogene serine/threonine kinase) and KRAS (KRAS proto-oncogene GTPase)[7][9]. According to multistep genetic model of colorectal carcinoma[11], oncogenic KRAS mutations take place after APC is inactivated as first steps of adenoma stage. Ultimately, chromosome 18q starts having deletions and TP53 becomes inactivated

on chromosome 17p which develops transition from benign adenoma to malignancy[1][11][12][13] (Fig. 1). Among all allelic loss of chromosomal regions in tumor-suppressor genes; DCC (DCC netrin 1 receptor), and SMAD2/4 on chromosome 18q, APC on chromosome 5q, and TP53 on chromosome 17p appears to be the remarkable ones[14]. The loss of APC causing Wnt signaling pathway activation can be evaluated as the most important change in the progression of colorectal carcinoma since it is essential and the first mutation taking place in CRC. The mutation in APC gene prevents the destruction complex formation which normally provides degradation of β-catenin. In the mutant state, β-catenin protein accumulates in the cytoplasm as destruction complex cannot be formed to degrade β-catenin. Finally, β-catenin is translocated to the nucleus and hence it binds TCF/LEF transcription factors. As a result, the downstream elements of Wnt signaling pathway are induced, causing increased rate of proliferation and other pathways which may ultimately lead to invasion, migration and metastasis in cancer cells. Moreover, the activating mutations in RAS gene family, which has roles in differentiation, cell proliferation and survival, have high frequency in colorectal cancer, especially KRAS-activating mutations[17][18]. The changes in membrane-bound GTP/GDP binding protein KRAS disrupt its GTPase activity and then KRAS proteins begin accumulating and remaining at GTP-bound active state which leads to constitutively activation of proliferation-related downstream pathways over time. The KRAS overactivation upon mutations has been detected in 35-45% of colorectal carcinoma cases[19][20]. On the other hand, NRAS mutation rates are relatively lower compared to KRAS mutations whereas HRAS-activated mutations have not been identified in CRC[19][21][22]. Furthermore, loss of TP53 mostly caused by missense mutations from AT to GC[16] is frequently observed in CRC which leads to the changes in cell cycle, apoptosis and senescence mechanisms, DNA repair and stress signal responses[15].

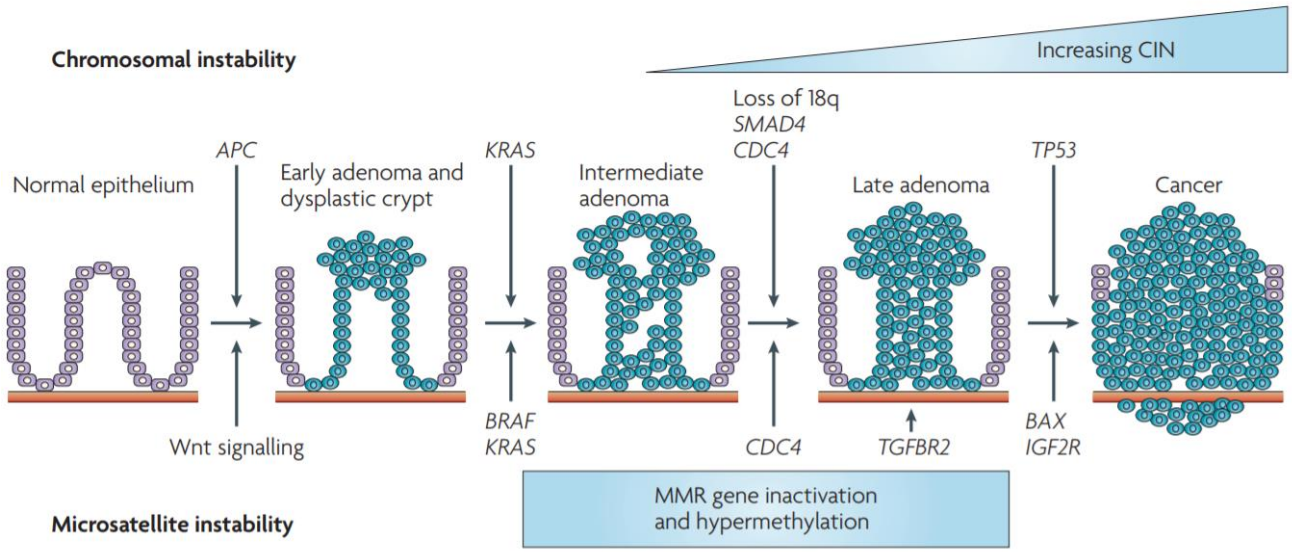

Figure 1: Initiation and progression of colorectal carcinoma. The mutation in APC gene appears to be the first mutation in this transformation which is caused by three main pathways: MSI, *microsatellite instability;* CIN, *chromosomal instability*; CIMP, *CpG island methylator phenotype*[1]. Then, further mutations are observed in proto-oncogenes including KRAS and BRAF followed by loss of heterozygosity on chromosome 18q affecting DCC and SMAD4 in the process from early adenoma to late adenoma. Lastly, loss of chromosomal regions on chromosome 17p and mutations in tumor suppressor genes, namely TGFBR2, BAX, IGF2R, lead to cancer initiation. *Adapted from "Genetic prognostic and predictive markers in colorectal cancer" by Walther A. et. al., 2009.*

In a study, 10 primary and 3 metastatic colorectal tumors have been examined in terms of morphology and mutations for specific genes including TP53, KRAS, APC and MMR (mismatch repair) genes[30]. All cell lines have had high cell viability whereas seven of them have been carrying TP53 frameshift, missense or nonsense mutations and six of them have shown KRAS mutations. Also, nine of these colorectal cancer cell lines have contained mutation in APC gene. In addition, it was shown that most known drug sensitivity genes such as MRP1, MXR, MDR1 and COX2 were highly expressed in most of these CRC cell lines. Lastly, the expression of cancer stem cell biomarkers CD133, CD44 and Lgr5 was detected in these cell lines.

In addition to chromosomal instabilities (CIN), microsatellite instability (MSI) phenotypes are also a type of genomic instabilities seen in some sporadic colorectal cancers and mostly in hereditary cases. Patients with this phenotype show replication errors in these repetitive DNA sequences, microsatellites, which consist of tandem repeats between 1-5 base pairs[23], because of defective mismatch repair mechanism. These nucleotide changes in the microsatellite sequences generate shorter or longer alleles. Bethesda Guidelines[24] recommends five microsatellite markers to evaluate MSI status including three dinucleotide (D2S123, D5S346, and D17S250) and two mononucleotide (BAT26 and BAT25) which are used to categorize tumors depending on the number of instability that microsatellites have. Tumors with ≥30% of the MSI markers are considered as MSI high (MSI-H) and tumors with lower ratio are classified MSI low (MSI-L) whereas ones without any instability are called microsatellite stable (MSS)[24][25]. Furthermore, another well-known mechanism of gene silencing in human carcinogenesis is transcriptionally inactivation of tumor-suppressor genes by hypermethylation of CpG islands at promoter regions[26][27][28] which has been observed in colorectal adenomas by 35%[28][29].

In another study, 24 colorectal cancer cell lines have been analyzed and their MSI and CpG island methylator phenotype (CIMP) status have been stated. The mutations for oncogenes including BRAF, KRAS and PIK3CA and for tumor suppressor genes including PTEN and TP53 have been examined in most known hotspots[31]. 9 cell lines out of 24 colon cancer cell lines have showed MSI after being analyzed by BAT-25 and BAT-26 mononucleotide repeat markers[31] and it has been mutually exclusive with CIN status. In addition, thirteen and nine of them have been detected as CIMP positive by using two different panels, seventeen colon cancer cell lines have been carrying TP53 mutations, which makes TP53 the most frequently mutated gene after APC mutation in CRC, and twenty of them have harbored KRAS or BRAF mutations enhanced by mitogen-activated protein kinase pathway. In 15 cancer cell lines, KRAS has been hyperactivated while five of those have been homozygous in which BRAF mutations have been detected, as expected. Moreover, hyperactivated phosphoinositide 3-kinase (PI3K)/AKT pathway has been detected in thirteen colorectal cancer cell lines due to the mutations in PIK3CA and PTEN genes[31] except one cell line, SW948 which is

homozygous for mutant allele. Despite the fact that these mutations are commonly seen in colorectal carcinoma cases, four cell lines (SW48, Caco-2, COLO 320, and V9P) have not displayed any of these mutations other than TP53. Since HCT-15 and DLD1, and HT29 and WiDr have been obtained from the same patient, there was no genetical difference detected. SW480 primary tumor and its metastatic form SW620 (lymph node) have had the identical profile for mutations but they have varied epigenetically. Besides, SW480 and SW620 have displayed different TP53 mutations leading to contrasting results. In SW480 cells, this mutation is evaluated as tolerated/increased activity whereas it is damaging/non-functional for SW620 cells. The information regarding to the origin and mutation profiles of colorectal cancer cell lines is shown in Table 1 and Appendix A, respectively.

Table 1. The origin of colon cancer cell lines[31].

Cell Line	Patient	Organ	Disease	Stage	Derived from
DLD-1	Male	Colon	Colorectal adenocarcinoma	Dukes'C	HCT-15/DLD-1 misclassified
HT29	44-year-old female	Colon	Colorectal adenocarcinoma	Dukes'C	Primary tumor
LoVo	56-year-old male	Colon	Colorectal adenocarcinoma	Dukes'C	Left supraclavicular region
RKO	-	Colon	Colonic carcinoma	-	Primary tumor
SW480	50-year-old male	Colon	Colorectal adenocarcinoma	Dukes'B	Primary tumor
SW620	51-year-old male	Colon	Colorectal adenocarcinoma	Dukes'C	Lymph node metastasis

Even though molecular characteristics of colorectal cancer cells are well-known, the lack of consensus molecular groups has been problematic in terms of clinical translation and causing inconsistencies in large-scale data. Basically, these tumors can be classified either as hypermutated with microsatellite instability (MSI) because of deficient mismatch repair and/or proof-reading mechanisms[33][34] or non-hypermutated cancers, which are microsatellite stable (MSS), with chromosomal instability (CIN) resulting in mutations in the KRAS, TP53, APC and/or BRAF genes[33][34]. To overcome this issue, four consensus molecular subtypes (CMSs) have been established[32][33]: CMS1 (14% of CRC cells, microsatellite instability immune) for the cells which are hypermutated, and have strong immune activation and microsatellite instability; CMS2 (canonical, 37%) for those which have chromosomal instability (CIN), MYC signaling activation and elevated WNT; CMS3 (metabolic, 13%) belongs to the epithelial cells with metabolic dysregulation; and CMS4 (mesenchymal, 23%) for those with TGF-β activation, angiogenesis and stromal invasion[32][33]. Even in the presence of consensus subtype groups, there are still 13% of the colorectal tumors not belonging to any subtype group on account of their diverse gene expression signatures[33] (Fig. 2). Another classification system depending on gastro-intestinal ssGSEA score has been established by Kaja C.G. Berg et al.[35] which categorizes the cells with low ssGSEA score as undifferentiated cell lines which appear mostly in mesenchymal phenotype such as LoVo and RKO while colon-like cell lines have high gastro-intestinal ssGSEA score[35] (Appendix B). Furthermore, it has been established that MSS tumors show worse prognosis than tumors with MSI[36]. They also have different responses to adjuvant chemotherapy[37].

To sum up, all these changes in genetic and epigenetic levels facilitate adenomas to develop carcinomas, which initiates with normal colorectal epithelium becoming a benign adenoma (Fig. 1). The stage of cancer is extremely critical for the patients with colorectal cancer in terms of survival rate as is for other cancer types.

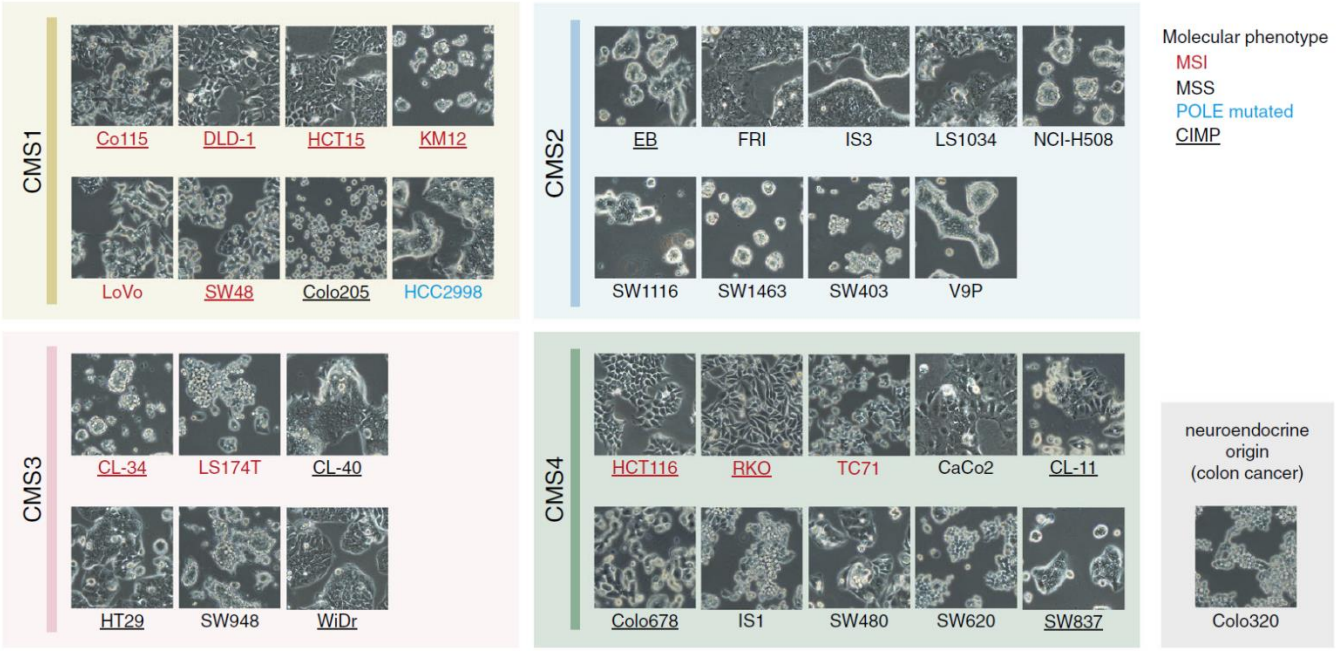

Figure 2: Common molecular subtypes of colorectal cancer cells. These subtypes have been determined based on gene expression except Colo320 cell line with neuroendocrine origin. MSI and MSS status are stated in red and black, respectively. CIMP-positive cell lines are provided as underlined. POLE mutated cell line is shown as blue and implies ultra-mutated tumor phenotype[35]. *Adapted from "Multi-omics of 34 colorectal cancer cell lines – a resource for biomedical studies" by Berg K. C. G. et. al., 2017*

1.2. Epithelial-mesenchymal transition in colorectal carcinoma

After carcinoma has been developed on account of many molecular changes in the cells, the ability for invasiveness and gain of metastatic characteristics may be acquired by epithelial-mesenchymal transition (EMT). Therefore, gaining insights into EMT mechanism is crucial to pinpoint molecular cascade of events providing colorectal cancer progression as seen in other types of cancer. Basically, EMT is a biological process in which epithelial cells lose their own tissue structure including cell-cell adhesions as well as their polarity and begin to have mesenchymal phenotypes such as enhancement in cell movement and migratory characteristics because of less interaction between cells and thus invading the extracellular matrix (ECM). Briefly, the factors playing roles during EMT process can be classified in three groups: EMT effectors (proteins exhibiting

epithelial or mesenchymal phenotype), EMT core regulators (transcription factors), and EMT inducers (extracellular molecules)[58].

1.2.1. EMT Effectors

During EMT process, E-cadherin appears to be a critical molecule since it is an epithelial cell adhesion molecule which is indispensable for junctions between epithelial cells. Therefore, it is likely that this molecule is downregulated throughout the tumor progression by mutations in the gene, transcriptional repression, promoter methylation and phosphorylation[40] as it diminishes intercellular adhesiveness[38][39]. In addition to loss of E-cadherin during EMT process, other changes occur to give mesenchymal properties to the cells such as increased expression of tenascin and fibronectin receptor, αvβ6 integrin, which plays role in the function of mesenchymal cells[39][42]. This increased integrin expression facilitates the escape of carcinoma cells from the basement membrane and spreading into the lamina where the environment is rich in tenascin and fibronectin[43][44]. Furthermore, elevated fibronectin activity provides metastasis of colorectal cancer to the liver by extravasation. In a similar manner, vascular endothelial growth factor (VEGF) has been shown to be a critical factor for the survival of colon carcinoma cells upon EMT[39]. Briefly, elevated ECM components like collagens α1 and α2 and mesenchymal cell surface markers including vimentin, N-cadherin and α-smooth muscle actin (α-SMA), and diminished levels of cytoskeletal elements like cytokeratins and of epithelial markers such as E-cadherin, claudins, ZO-1 are the typical indications of epithelial-mesenchymal transition[45].

Extracellular components like ECM, inflammatory and immune cells, and hypoxic conditions create tumor microenvironment by assisting the progress of cancer and ultimately metastasis. The connection between hypoxia and EMT has been previously known as it affects ZEB1 expression via hypoxia response element 3 (HRE-3)[59] and this knowledge has been reinforced by the discovery about HIF-1 activating Snail and Twist expression[46]. Moreover, stromal activation, which is regulated by multiple pathways including cytokines, growth factors and integrins through EMT, is one of the incidents taking place in tumor microenvironment. Inflammatory cells are found as a

major source of activating factors as well as NF-κB which has roles in controlling Slug and Snail expression[41].

1.2.2. EMT Core Regulators

The transition between epithelial and mesenchymal status of the cells occurs owing to the cooperation between molecular cascades of different signaling pathways and regulators. This regulation has been coordinated by mostly transcriptional machinery in which transcription factors function. Basically, it can be considered that three main groups of transcription factors promote EMT, which are the zinc finger E-box binding homeobox (ZEB) family of transcription factors ZEB1/ZEB2, SNAIL family of zinc-finger transcription factors SNAIL/SLUG, and TWIST family of basic helix-loop-helix (bHLH) transcription factors TWIST1/TWIST2[59]. Accordingly, nuclear translocation and upregulation of these particular transcription factors can be seen upon EMT[46]. As expected, the ability of the cells for metastasis and invasion is contributed by E-cadherin transcriptional repressors including SNAIL and SLUG[41] which bind to E-box on the DNA sequence in the promoter region of E-cadherin[63], and TWIST1[42] which recruits methyltransferases to inhibit E-cadherin expression[64]. Moreover, SNAIL and TWIST1 activates the expression of genes reflecting mesenchymal phenotype such as fibronectin, N-cadherin, and collagen[41][59]. Also, SNAIL can trigger WNT/β-catenin signaling pathway, one of the pathways involving in EMT, by interacting with β-catenin[59][60] together with other pathways, Notch61] and TGF-β[62]. Lastly, ZEB family, ZEB1 and ZEB2, that binds to E-boxes by recruiting co-repressor C-terminal-binding protein (CTBP) is one of the three major groups of EMT-related transcription factors as mentioned before[65]. Additionally, ZEB1 engages SWI/SNF chromatin remodeling protein BRG1 which also suppresses E-cadherin expression[66]. ZEB1 also interacts with the transcriptional coactivator p300/CBP-associated factor (PCAF), leading to a switch from its transcriptional repressor status to the transcriptional activator role which triggers SMAD signaling[67].

Other than these three main groups, other transcription factors such as Prospero Homeobox 1 (PROX1) and forkhead box Q1 (FOXQ1) have been also found to contribute to EMT which has been overexpressed in intestinal epithelium upon attenuated oncogenic effect of TCF/β-catenin signaling and related to lymph node metastasis[68], and to be upregulated in epithelial and stromal tumor subdivisions[59], respectively. In addition, FOXQ1 increases the inhibition of E-cadherin expression in CRC via TWIST interaction[69]. Another forkhead box protein, FOXC2, which increase AKT activity with following GSK-3β phosphorylation and SNAIL stabilization has been shown to be related with patient survival[59]. Furthermore, FOXM1 promotes ZEB1, ZEB2 and SLUG expression which results in diminished E-cadherin levels[70]. An isoform of FOXM1, FOXM1D, also plays role during EMT and consequently metastasis in CRC via Rho-associated kinases (ROCKs) which are known as factors with crucial roles in actin cytoskeleton regulation.

1.2.3. EMT Inducers

One of the striking signaling pathways which is found to be related to EMT is SMAD/STAT3 pathway. Further studies have shown that STAT3 enhances proliferation and survival of the tumor cells and has been claimed as a key regulator for NF-κB activation in colon carcinoma. SMAD4 makes complexes with SMAD2 and SMAD3 after binding takes place between TGF-β and its receptor, which activates the transcription of genes participating EMT such as vimentin[50]. Nonetheless, in the case of blockage of STAT3 phosphorylation via TGF-β activity, the ability for metastasis and invasion is attenuated on pancreatic cancer cells[51]. Hence, invasiveness of these cells has been enhanced by STAT3 activation and SMAD4 seems to be a negative regulator in this function. However, abnormal activation of STAT3 by SMAD4 reduction might be triggering a switch in TGF-β role from tumor suppressive to tumor promoting in colorectal cancer[52] which is also seen in transition between early and late stages. This diversity of cellular responses upon TGF-β activation and its dual role can be explained with the specific expression of transcription factors interacting with SMAD2 and SMAD3 depending on the cell type[53]. Moreover, NF-κB activity is promoted by TGF-β in malignant cells while TGF-β has repressing effect on this activity in normal epithelial

counterparts[54]. It has also been demonstrated that STAT3 regulates cell cycle-related molecules c-Myc, Mcl-1, Cyclin D and Bcl-2 expression[47]. Plus, the role of MSI or MSS status of the cells in the concept of TGF-β1-induced EMT have been demonstrated on colon cancer cells with mutant or wild type TGFBR2[71]. In this study, it has been proved that TGF-β1 can induce EMT in MSS cells, however, TGF-β1-induced EMT does not take place in MSI cells unless the cells harbor wild type TGFBR2. In addition to the importance of TGFBR2 in TGF-β1-induced EMT, the requirement of ERK1/2 phosphorylation for EMT induction in these cells has also been proven by demonstrating that the reduction in the phosphorylation level reverses the morphology from mesenchymal to epithelial by increasing E-cadherin expression considerably[71].

As mentioned before, Ras/ERK1/2 pathway appears to be another crucial pathway affecting EMT. As known, Ras proteins serve as switches between active GTP-bound and inactive GDP-bound status and play role in cell proliferation. Together with activated Ras complex, stimulated growth factor receptors activate Raf kinases, which leads to the activation of MAPKKs, MEK1 and MEK2, resulting in triggered extracellular signal-regulated kinases, ERK1 and ERK2[55]. Then, stimulated ERKs translocate into the nucleus to phosphorylate and trigger the activation of downstream nuclear transcription factors including ATF-2, Elk-1, ETS1/2. In Ras signaling pathway that involves these downstream effectors, many molecular changes take place. First, mutations in one of the members of Raf family, BRAF, are seen in 9-11% of colorectal cancer and related to increased kinase activity. In addition to BRAF, phosphorylated MEK has been found activated in 30-40% of adenomas and in 76% of colorectal cancers in total. Furthermore, elevated ERK levels have been demonstrated in intestinal tumors and colorectal cancer. Besides, suppression of MEK/ERK signaling reduces the proliferation of colon tumors in vivo[45][56]. Further analyses have showed that downstream effector molecules of ERK/MAPK such as Egr-1, Fra-1 and AP-1 regulate MEK1-induced expression of Snail1/2[56]. Additionally, Ras can cooperate with TGF-β through PI3K and Rho-GTPases[57].

In addition to all these mentioned above, tumor necrosis factor alpha (TNF-α) emitted by tumor associated macrophages (TAM) appears to be a key factor to advance the transition to mesenchymal of colon epithelial cells since it suppresses GSK-3β and affect Wnt/β-catenin signaling by disrupting the destruction complex[48] as mentioned before. Additionally, upon TNF-α induction, it has been seen that the expression of Snail, ZEB1 and Twist increase whereas Slug does not get affected by that. They have also showed that upregulated Snail triggers a shift from E-cadherin to N-cadherin in a specific colorectal cancer cell line, HCT116, likewise depletion of Snail counteracting TNF-α induced EMT considerably[49]. All these findings have suggested that Snail has a pivotal role in TNF-α-induced EMT.

Ultimately, due to EMT process, tumor cells begin to lose their epithelial-like phenotype and starts to gain the ability to become more invasive with mesenchymal features. As a consequence of these changes, they can pass through the extracellular matrix and start growing in lymphatic and blood vessels which ultimately leads to metastasis.

1.3.Purinergic signaling

Purinergic signaling has been first speculated in 1972[92]. The intracellular roles of nucleotides and nucleosides have been well-known with their participation in nucleic acid synthesis, a diverse range of biochemical reactions, and energy transactions in intracellular compartments for years. Surprisingly, when they are present as extracellular factors, they regulate an entirely different set of processes than they do intracellularly[136]. In extracellular milieu, they participate in cell proliferation, growth induction/reduction, growth factor secretion, migratory effects, and cell differentiation[145-148]. For instance, adenosine triphosphate (ATP) has been only known to be a fundamental component of nucleic acids and the main energy source of a cell in the beginning. Later on, it was also found to be an anti-neoplastic factor which diminishes cell growth by arresting cell cycle in S-phase[93]. Oppositely, tumor-promoting effect of adenosine was shown in cancer[94]. Almost all cancer cells present receptors for extracellular nucleosides and nucleotides in their plasma membrane.

When there is a damage or stress condition, ATP gets released from the cell into extracellular environment. This ATP release can occur through many mechanisms including vesicle-mediated release, membrane transporters and channels, and purinergic receptors[152][153] (Figure 3). Moreover, adenosine and adenine nucleotides such as AMP can be released into extracellular environment in the inflamed tissues by the uncontrolled leakage[236]. Adenosine is an immunosuppressant mainly functioning through A2A receptors which also regulates cell growth on A3 receptors. Similarly, ATP is also an immunosuppressant and growth-promoting factor with proinflammatory roles[72]. Thus, as expected, tumor microenvironment is immensely rich in ATP and adenosine (ADO)[149][154]. Thanks to the recent findings, the importance of ADO and ATP involving in tumor microenvironment as key regulators of host-tumor interaction has been revealed. Also, it has been demonstrated that they are effective modulators of cytokine release and immune cell responses[72].

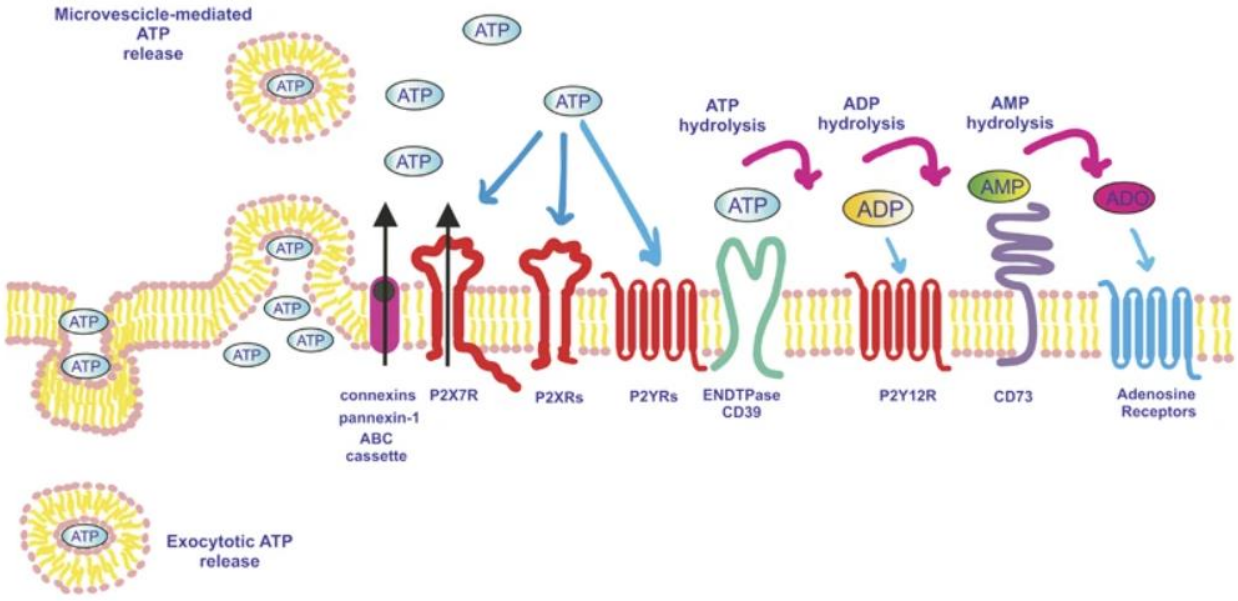

Figure 3: Extracellular purinergic signaling regulation. Upon damage or stress, nucleotides and nucleosides can be liberated to extracellular environments and start acting as signaling molecules. ATP can be released to the extracellular environment through several mechanisms. Once it released, it can bind to multiple receptors including P2Y and P2X receptors or to an ectonucleotidase, CD39. CD39/ENTPD1 can facilitate the conversion of ATP to ADP and/or less efficiently ADP to AMP. CD73/NT5E

activity is induced upon AMP binding which produces adenosine as end product. Adenosine can bind any P1 receptors (adenosine receptors), namely A1, A2A, A2B, and A3 and initiates different signaling pathways. *Adapted from "Extracellular purines, purinergic receptors and tumor growth" by Virgilio F. D. et. al., 2017*

1.3.1. Purinergic signaling components

Purinergic receptors are categorized into two different classes, P1 and P2 receptors. Adenosine receptors, called as P1 receptors, vary depending on the signaling pathway they engage and their sequential differences[136]. P1 receptors consist of 4 components including A1, A2A, A2B and A3. They interact with phospholipase C and adenylyl cyclase through different G proteins. The level of A2B receptors is found to be considerably high in many cancers including lung, prostate, melanoma and breast cancer by microarray analysis[98] whereas A2A receptors are mostly present on immune cells such as T cells, monocytes, natural killer cells, and B cells[138]. The elevated levels of A3 receptors have been also shown in tumor cells[99]. Nucleotide receptors, also named as P2 receptors, subdivide into two different classes, metabotropic P2Y whose function is mediated by metabolic actions, and ionotropic P2X receptors which act through ion channels[73]. P2Y receptors can be divided into two subgroups depending on the G proteins that they are coupling to. P2Y1, P2Y2, P2Y4, and P2Y6 interact with Gq protein to regulate phospholipase Cβ whereas P2Y12, P2Y13, and P2Y14 couple to Gi protein to suppress adenylyl cyclase activity. These receptors trigger calcium release and decline cAMP accumulation[138]. Differently than others, P2Y11 can interact with both Gq, and Gs and cause elevated levels of intracellular Ca^{+2} and cAMP[72]. P2X receptors form ATP-gated plasma membrane channels and they are cation-selective. They comprise 7 different subunits (P2X1-7) to form trimeric receptors. P2X1, P2X2, P2X3, P2X4, and P2X6 subunits can form homotrimeric or heterotrimeric channels, however, P2X5 has less tendency to assemble to homomeric complexes and usually forms heterotrimers with either P2X1, P2X2 or P2X4[74][75]. Also, P2X7 subunit can form homoexamer under certain circumstances as well as assembling into homotrimeric channels[76][77]. P2Y and P2X receptors considerably vary in terms of their ligand selectivity. Almost all tumors present P2 receptors on their cell surface. Numerous

purinergic agonists, a molecule that can bind to a receptor on the cell surface to release a physiological response, can combine with P2Y receptors while ATP is the only identified physiological ligand of P2X receptors as of yet. This ligand variety provides a peculiar plasticity to purinergic signaling.

The tumor microenvironment is rich in ATP and adenosine content as expected by considering that ATP is recognized as proinflammatory signals by cells. Some factors such as concentration, degradation level of ATP to adenosine, and the type of P2 receptors expressed by infiltrating inflammatory cells and by particular tumor cells determines whether ATP accumulation in these cells would be favorable or adverse for the host[72]. ATP concentration in extracellular space is kept steady by consecutive release and degradation activities. This degradation process involves 4 different ectonucleotidase subtypes namely, ectonucleotide pyrophosphatase, ectonucleotide triphosphate diphosphohydrolase (E-NTPDase/CD39), alkaline phosphatase, and ecto-5'-nucleotidase (NT5E/CD73) which produces adenosine as end product (Figure 3). Especially two members of ectonucleotidase family, CD39 and CD73, are pivotal for the interaction between tumor and immune cells. CD39 and CD73 involve in the ATP hydrolysis to adenosine which plays critical roles in tumor progression due to the immunosuppressive nature of adenosine. Adenosine ultimately gets degraded to inosine by the activity of adenosine deaminase enzyme (ADA).

1.3.1.1.CD39/ENTPD1

CD39 belongs to ectonucleoside triphosphate diphosphohydrolase (E-NTPDase) family that consist of four membrane-bound components: E-NTPDase1/CD39, E-NTPDase2, E-NTPDase3, and E-NTPDase4[150]. CD39/ENTPD1 starts a phosphohydrolytic cascade and cleaves either ATP or ADP down into AMP with different affinities in a Ca^{2+} and Mg^{2+}-dependent manner and regulates the level of extracellular nucleotides by this cascade. Human ENTPD1 is a protein with 510 amino acid, 11 cysteine residues, two transmembrane regions, and seven N-linked glycosylation sites[166]. It consists of two structural domains including small cytoplasmic domain and large extracellular hydrophobic domain with apyrase conserved regions (ACRs) that are essential for the catabolic activity[167]. ACR1 and ACR5 comprise phosphate-binding motif stabilizing

interaction of CD39 and its substrates, ATP and less efficiently ADP[168]. For CD39 activation, it is required to be located on the cell membrane. Also, its glycosylation is pivotal for membrane localization, correct protein folding, and ultimately enzymatic activity[169].

In a study, the effect of human CD39 together with P2X7 and P2Y2 has been revealed in human colorectal cancer progression by assessing both CD39 deletion on mice with different genetic background and expression pattern in human CRC biopsies[83]. They have claimed that these mice have shown no difference in terms of tumor size and their metastatic ability in primary colorectal cancer models. Conversely, metastasis has been occurring more in CD39-overexpressed mice than CD39-deficient mice[83]. Furthermore, CD39 has been shown to be present on some human cancer cell lines such as melanoma cell lines, B lymphoma cell lines, and leukemia cell lines, yet, expression of CD39 could not be proven in colon carcinoma, pancreatic cancer, and breast cancer cell lines[173].

1.3.1.2. CD73/NT5E

CD73 is one of the members of metallophosphoesterase super-family[170][176] and 5' ectonucleotidase enzyme family which dephosphorylates 5'AMP to produce adenosine as final product. CD73 is the only cell surface-located one among 5'ectonucleotidases[149][186] and involves two identical 70kDa subunits[168][170]. It is located on plasma membrane through its C-terminal serine residue (Ser523) that is associated to glycosylphosphatidyl inositol (GPI)[170]. In the case of proteolytic cleavage of this GPI-anchor, a soluble form of CD73/NT5E can be released from plasma membrane[171][172]. Mature CD73 is composed of 548 amino acids with a 26 amino acid long signal peptide at the N-terminus, which is around 61 kDa in total. C-terminal domain function as binding site for substrate and provide a dimerization interface whereas N-terminal domain has metal ion binding site and facilitates Zn^{2+} and Co^{2+} ion bindings[170][187]. These two domains are associated to each other by an alpha helix with small hinge region which is pivotal for the ability of enzyme to undergo large domain movements[187]. By the link between C-terminal and N-terminal domains, active site for the enzyme is generated. Although CD73 is a membrane-bound protein and mainly function in the extracellular environment, there are some findings in which it has been proven to be localized also in

the cytoplasm[178][186]. These other three soluble forms present in cytosolic compartment controls intracellular levels of nucleoside 5'-monophosphatases[186]. Dimeric human NT5E shows conformational change with 114° switch between active and inactive forms of the enzyme. Dimerization occurs by the C-terminal domains through an interface along with interchain mobility of up to 13°. The structural control of domains is critical for substrate selectivity[187].

Promoter region of CD73 represents binding sites for several transcription factors such as AP-2, SMAD proteins, SP1, and cAMP-responsive elements[181]. It has been also shown that APC downregulates NT5E in SW480 human colorectal carcinoma cells whereas NF-κB and TNFα leads to NT5E activation and PPARγ causes inhibition of NT5E in HT29 human colon cancer cells[181]. Moreover, HIF-1 can directly interact with NT5E promoter and results in upregulated NT5E levels in tumors[81][181]. Interestingly, ADP and ATP are natural inhibitors of CD73 in low micromolar range. Despite α,β-methylene adenosine diphosphate (AMPCP/APCP) being the commonly used inhibitor[177], many studies have demonstrated that APCP has no effect on cell proliferation or migratory abilities[183][184].

The studies that have been done so far on CD73 have had contradictory outcomes in a diverse range. They have explained this ambiguity by proposing that CD73 effects on the cells may vary depending on whether it is being expressed by tumor cells or host cells[149]. The activation of CD73 on prostate cancer cells suppresses tumor growth which involves NF-κB signaling inhibition through A2BR signaling, however, it triggers cancer cell proliferation when expressed by healthy prostate epithelial cells[151]. Another study in which they have used CD73 overexpression plasmid pcDNA-NT5E has shown that overexpression of CD73 promotes cell invasion as well as cell migration in both breast cancer and cervical cancer cell lines[155-157]. Likewise, CD73 inhibition has diminished cell migration and the expression of genes participating in epithelial-mesenchymal transition in head and neck squamous cell carcinoma (HNSCC)[159] and EMT-related genes have been found to be downregulated in ovarian cancer cells upon CD73 silencing[160]. CD73 activity has also promoted mesenchymal properties of hepatocellular carcinoma cells. Moreover, A2AR function has been able to compensate CD73 inhibition in these cells[161]. Furthermore, upregulation of CD73 and its promoting effect on EMT during metastasis have been shown in gastric cancer. CD73 has been also

involved in RICS/RhoA signaling, suppressed LIMK/cofilin phosphorylation and in β-catenin activation[174]. Moreover, upon CD73 depletion by small interfering RNA, migration of gastric cancer cell lines has been assessed by both transwell migration assay, and wound healing assay and decreased compared to control gastric cancer cells[164]. Plus, even though cell proliferation has not been affected by anti-CD73 monoclonal antibody, treated cells with this antibody have shown less protection to Doxorubicin in triple-negative breast cancer cells. In addition, migratory ability and invasiveness of the cells have been suppressed in both human TNBC and mouse 4T1 cell lines upon CD73 loss[178].

In addition, it is compelling that A2BR and NT5E have been shown to have a feedback loop that promotes CD73 expression by cancer-associated fibroblasts (CAFs) which results in immunosuppressive outcome. However, when A2 receptors are simultaneously suppressed together with CD73, antitumor immunity is improved[175]. Furthermore, CD73 has been shown to produce adenosine independently of CD39 activity as there are other enzymes involved in AMP production such as CD38[179]. The effect of CD73 knockdown in diminished cell growth has been explained by G1 phase arrest through AKT/ERK/Cyclin D signaling and by tumor necrosis factor receptor-2 (TNFR-2) involvement in this signaling in pancreatic dual adenocarcinoma (PDAC)[180]. These cells have shown considerably attenuated pAKT and pERK levels upon CD73 depletion which results in decreased G1/S phase transition due to diminished levels of Cyclin D1[180]. In a similar manner, overexpression of CD73 has shown upregulated CyclinD1 levels as well as nuclear β-catenin levels that can be reversed by suppression of CD73 activity in breast cancer cells[185]. When CD73 knockdown cells are generated in hepatocellular carcinoma, EMT, metastasis of HCC cells, their proliferative ability, migratory behaviors, and invasiveness have been also diminished, which could be recovered upon overexpression of CD73[161]. It has been mechanistically demonstrated that A2AR induces Rap1 activity upon adenosine binding after CD73 degrades 5'AMP to adenosine. Then, p110β is recruited to the plasma membrane that leads to PIP3 generation and thereby, enhanced pAKT levels in HCC cells[161].

In addition to all these mentioned before, therapeutical approaches revealed a compelling fact that one of the most frequently used chemotherapeutic drugs, doxorubicin, strikingly increases CD73 levels and this effect can be reversed by HIF inhibitor in TNBC[182].

1.3.1.3. Adenosine Receptors

Adenosine receptors are known as seven transmembrane glycoproteins coupled with G proteins[90]. They differ from each other as they have different sequences, promote different signaling pathways through different G proteins and have affinity in different levels for adenosine. After the function of four ectonucleotidases that are responsible for ATP degradation, produced and released adenosine to extracellular environment can bind any P1 receptor and trigger a signaling cascade. All adenosine receptors have the same membrane topology which involves seven transmembrane spanning domains and they all are G-protein coupled receptors[136][137] even though they interact with different G proteins. A1 and A3 receptors couple to Gi subunit which leads to attenuated levels of cAMP and limited adenyl cyclase activity whereas A2 receptors are coupled to Gs protein and promote cAMP synthesis by activating adenyl cyclase[152]. Upon adenosine binding to the receptors, second messengers including cAMP and Ca^{2+} are released to deliver the signals from cell-surface receptors, in this case adenosine receptors, to an effector protein. Ultimately, they control different biological events.

Adenosine is reported to decrease cell migration and invasion in breast cancer and prostate cancer cell lines at low concentrations, and in human ovarian and human cervical cancer cell lines[155][162][163]. It is fundamental to state that the group of receptors involved in signaling and the cancer type need to be taken into consideration to understand the effect of signaling triggered by ADO.

1.3.1.3.1. A1 Receptors

Among all adenosine receptors, A1 receptors are prominent with their physiological effects in the brain. As mentioned before, they couple to Gi protein and cause diminished levels of intracellular cAMP. Moreover, they can trigger phospholipase C (PLC) activity[192]. Interestingly, it is reported that A1AR can release both pro- and anti-inflammatory signals in diseases[193-196]. Generally, A1 receptor is responsible for

triggering immune responses from specific type of immune cells including macrophages and neutrophils[193][194]. On the one hand, A1AR effect on neuronal damage upon hypoxic conditions has been proven in A1AR-deficient mice[197]. Therefore, it has been understood that A1ARs regulate adenosine effects under pathophysiological circumstances[197][198]. According to the findings on cancer research related to A1AR, it is reported to promote brain tumor growth especially glioblastoma tumor growth since it is highly expressed by both tumor cells and microglial cells correlated with these tumor cells[199]. In other types of cancer including colorectal cancer, leukemia, breast cancer, and melanoma, A1AR is reported to show antiproliferative effects[209][210] possibly through cell cycle arrest in G2/M phase[90]. On the contrary, there are some studies in which A1AR has been shown to promote cell growth and increase cell survival in MDA-MB-468 breast cancer cell lines[211].

1.3.1.3.2. A2 Receptors

Of all P1 receptors, A2 receptors couple to Gs protein and their expression level gets promoted by immune cell activation. A2AR and A2BR activation produce cAMP in the environment and stimulate protein kinase A (PKA) function. In immune cells, adenosine is less likely to bind A2B receptors compared to A2A receptors. However, A2BR signaling appears to be contributory in inflammation as they are regulated by hypoxia signaling and hypoxia-inducible factors (HIFs)[139]. In addition, A2BRs have been also found to couple to Gq protein as well as Gs protein in some cells[140]. This phenomenal ability of A2B receptors to interact with Gq protein provides them to be involved in wound healing processes including fibrosis and angiogenesis[141][142]. A2BR is reported to have two crucial roles in human epithelial lung cancer. Firstly, it participates in partial EMT through MAPK/ERK and cAMP/PKA pathways. On the other hand, the activation of A2BR by its selective agonist BAY-606583 counteracts TGF-β induced EMT[164].

1.3.1.3.2.1. A2A Receptors

A2ARs are known with their effects by suppressing immune responses such as macrophage-mediated phagocytosis, cytotoxic activity of natural killer cells and proinflammatory cytokine secretion[200][203]. Moreover, A2ARs inhibit effector T cells function through its own activation[201][202]. These immunosuppressant effects of A2ARs has been further proven by *in vivo* data in which A2AR-deficient mice have been able to reject tumor formation more readily in lymphoma and melanoma. The same results could be obtained by A2AR antagonist treatment on mice[192]. The studies on A2ARs in tumors have demonstrated that blockade of A2AR signaling attenuates tumor formation and stimulate T cell functions also including tumor-infiltrating T cells[143] while it improves tumor growth in some cases[144]. Furthermore, A2AR can promote apoptosis in human A375 melanoma cells and in Caco-2 human colorectal cancer cells by inducing caspase-9 and caspase-3 activity[121][189]. In addition to these, A2AR presented by T lymphocytes leads to adenosine accumulation in hypoxic environment and suppress cytotoxic function of T cells[212].

1.3.1.3.2.2. A2B Receptors

A2B receptors are activated by adenosine in higher concentration than the other adenosine receptor subtypes require[204]. Besides, they are not related to physiological incidents caused by adenosine unlike other ARs. Thus, A2BRs are mostly associated with pathophysiological conditions, especially ones in which hypoxia is involved (i.e. ischemia, tumors)[205][206]. Therefore, it is expected that A2BR function is involved in angiogenesis. Interestingly, A2BR significantly induces inhibition of ERK1/2 phosphorylation[90]. These outcomes of A2BR activity pose a problem for therapeutic approaches as inhibition of angiogenesis would be only possible upon blockade of A2BR signaling while cancer cell growth would be controlled by inhibiting MAPK pathway which requires active A2BR signaling. Despite this dilemma, both approaches could be possibly used in combinatorial therapy with other therapeutics depending on the specific case.

1.3.1.3.3. A3 Receptors

A3 adenosine receptors are reported to be a fundamental adenosine receptor subtype engaged in adenosine-induced inhibition of cancer progression by limiting tumor cell proliferation[91][188][189]. More importantly, A3 adenosine receptors are mostly not expressed in normal tissues whereas their expression levels are elevated on tumor cell surface[91][190][191]. They are also reported to regulate cell cycle by diminishing telomerase activity and causing a cell cycle arrest in G0/G1 phase[213-215]. It is claimed that A3AR decreases the proliferation rate of cancer cells by decreasing protein kinase A and B levels and by increasing GSK-3β level through Wnt pathway which results in degradation of β-catenin. Accordingly, it suppresses c-Myc and cyclin D1 expression[123]. Because of decreased PKA function, ERK1/2 activity is also reduced which causes less cancer cell invasiveness and lower NADPH oxidase activity in prostate cancer[108]. A3AR activation has caused a decrease in cell migration and cell invasiveness by blocking AC/PKA signaling also in human breast, colorectal and hepatocellular cancer cell lines[108][165]. However, there are controversial results about the effect of A3 receptors on tumor cells. These receptors seem to be acting either as growth-promoting or growth-inhibiting factor as well as antiapoptotic or proapoptotic factor[90][91].

1.3.2. Purinergic signaling in cancers

The growth inhibitory signals can be triggered by different P2 purinergic receptors and their combinatorial stimulation in the different types of malignant cells, which might directly diminish the ability of cells to be more proliferative and/or indirectly affect cell growth by advancing cell differentiation or cell death[95]. In colorectal cancer, it is shown that P2Y2 receptor leads to cell death by apoptosis[96] whereas it builds up their proliferative ability when it is stimulated in melanoma[97].

ATP release may be taken place by not only infiltrating inflammatory cells but also tumor cells that is triggered by chemotherapeutic drugs which creates an anticancer response according to the recent studies[78][79][80]. Released ATP from tumor cells to tumor microenvironment triggers P2X7 receptor activation on dendritic cells (DC) which leads to IL-1β production in the extracellular space. Therefore, antigen presentation is

reinforced via this pro-inflammatory cytokine, and ultimately antitumor immunity is improved. However, the role of ATP has not always been advantageous for the host cell. Depending on the expression of P1 and P2 receptors on infiltrating inflammatory and tumor cells, and the expression levels of nucleotide-hydrolyzing enzymes, CD39 and CD73, ATP can have immunosuppressive or immunostimulant role [72].

Furthermore, adenosine accumulates in tumor microenvironment because of hypoxic conditions in which ATP hydrolysis gets accelerated. Accordingly, the level of CD39 and CD73 ectonucleotidases is also elevated by hypoxia-induced transcription factors Sp1 and HIF, respectively[81][82]. Gene deletion studies have proven that CD39 and CD73 are crucial for tumor growth. The depletion of either CD39 or CD73 has attenuated tumor growth and prevented metastasis[83-86]. After adenosine is generated by the function of these two ectonucleotidases, it targets $CD8^+$ T lymphocytes and acts as an immunosuppressant. Moreover, the main source of adenosine has been shown as CD39- and CD73-expressing tumor infiltrating T-regulatory cells (Tregs)[87]. Tumor infiltrating T_H17 lymphocytes can also express CD39 and CD73, thus they can inhibit effector T cells functions through adenosine production[88], suggesting that the function of tumor infiltrating T_H17 lymphocytes may vary depending on the ectonucleotidase level that they express. Subsequently, adenosine deaminase (ADA) degrades adenosine to inosine depending on its interaction with ADA-binding protein cell surface serine protease dipeptidyl peptidase IV/CD26. It would be expected that elevated expression of CD26 would cause a decrease in tumor growth since adenosine degradation would also be augmented. However, in reality, there are contradictory results in which it has been shown that diminished CD26 levels provide the cells more aggressiveness in melanoma or in ovarian carcinoma while, in some of them, CD26 increase is directly proportional to tumor growth such as in thyroid carcinoma, and prostate cancer[89].

1.3.2.1. Purinergic signaling in colorectal cancer

Extracellular ATP has caused diminished levels of cell proliferation and advanced apoptosis of colorectal carcinoma primary cultures, claimed through P2Y2 receptors activity[112][113]. It has been suggested that the effect of ATP on decreased cell growth might be through deteriorated protein kinase C activity which affects S-phase of cell cycle[114]. According to another study with two colon cancer lines, HT29 and SW620, it has been also shown that ATP treatment leads to reduced cell proliferation rate[109] whereas another colorectal adenocarcinoma cell line, Caco-2, has shown induced cell growth upon ATP via P2Y receptors[110]. Moreover, CD73 and ADA have been found to be prominently expressed in primary human colorectal tumors[111]. In these tumors, ADA level has been associated to histological type and lymph node metastases while CD73 function has been claimed to be correlated with tumor grade and location[111]. Furthermore, the existence of adenosine in elevated levels in hypoxic tumor microenvironment decreases the expression of ADA-binding protein dipeptidyl peptidase, CD26, in HT29 cell line[115]. Also, upregulated adenosine kinase expression has been found in human colorectal cancer[116].

Adenosine is shown to improve cell growth in poorly differentiated HT29 cells through A1 receptors while cell proliferation is declined upon ADA and A1 receptor antagonists[117]. Similarly, more differentiated cells such as Caco-2 and DLD1 have also shown increased cell growth but with a lower rate compared to poorly differentiated ones[118]. Moreover, all adenosine receptors are found to be expressed in human carcinoma cell lines[119]. Among all these P1 receptors, A2B receptors seem to be the most prominent one because of its elevated levels playing a part in increased colorectal cancer cells proliferation according to the recent literature[120]. On the other hand, adenosine induces apoptosis in Caco-2 cells[121]. Also, A3 receptor agonists are shown to have inhibitory effect on primary colon carcinoma growth[122]. Adenosine also have effect on CD26 cell surface protein expression. Diminished levels of CD26 by adenosine has been shown on HT29 cells and thus, facilitates the survival of tumor cells[123].

1.3.2.2. Purinergic signaling in other cancer types

In breast cancer, anti-CD73 antibody treatments decrease tumor growth and metastasis[84]. Moreover, it has been shown that hypoxic conditions elevate P2X7 receptor level. Upon P2X7 receptor agonist binding, ERK1/2 expression is increased and leads to nuclear translocation of NF-κB[101]. P2X7 receptor activation also causes increased migration and invasion of tumor cells. A1 and A3 receptors are also reported to be expressed by human breast cancer cells. Although adenosine has been shown to facilitate cancer cells' migration and their proliferation[102], activation of A3 receptor by its selective agonist inhibits cell proliferation and ultimately the metastasis of breast tumors[100][103][104]. In addition, depletion studies on A2B receptor have resulted in diminished growth rate in these cells[105]. On the contrary, it has been also claimed that A2BR activation attenuates cell growth through MAPK signaling pathway in MDA-MB-231 cells[90].

Afterwards, it has been proven that the inhibition induced by ATP in tumor growth in prostate cancer (DU145), lung cancer (A549), and pancreatic cancer (Panc-1) is regulated by PI3K pathway that has roles in cell growth and apoptosis[106]. Similar to breast cancer, cell invasiveness has been advanced upon P2Y receptor stimulation by its agonists through ERK1/2 activation and also p38 function in prostate cancer[107]. Additionally, prostate tumors have lost their ability to grow more and metastasize to distal regions upon anti-CD73 antibody[86]. Interestingly, adenosine has had inhibitory effects on prostate tumor growth even though normal cell growth has been advanced by adenosine[95]. Like in breast cancer, A3 receptor activation reduces prostate cancer cell proliferation by arresting cell cycle and leading to apoptosis. Thus, metastatic ability of cancer cells is also decreased[108]. Similar to prostate cancer cells, human gastric carcinoma cell line (HGC-27) has shown lower cell proliferation rate upon ATP, and adenosine and apoptosis has been induced in this cell line[125][126].

Furthermore, different types of lung cancer cells responded to ATP treatment by decreased cell growth in a dose-dependent manner[127]. Tumor-infiltrating immune cells has been claimed to produce factors that suppress immunity and induce angiogenesis owing to high adenosine levels in tumors. After that, it has been argued that A2B

receptors might be playing a role in these outcomes which has been proven by A2B receptor knockout mice in a Lewis lung carcinoma isograft model. These mice have shown considerably diminished growth[128].

In liver cancer, CD39 knockdown mice model has displayed advanced spontaneous and induced hepatocellular carcinoma[129] as it leads to increased extracellular nucleotides[134]. Additionally, both adenosine and A3 receptor agonist, CF101, have been reported to inhibit cell growth *in vitro* and *in vivo*, respectively[130][131]. A3 adenosine receptor has been also found to be involved in promoted cell apoptosis upon ATP and adenosine treatments in human hepatoma cell line Li-7A[131][132]. Also, the expression level of A2B receptor has been significantly high in human hepatoma cellular carcinoma[133]. In glioblastoma, angiogenic factor IL-8 secretion has been risen in a glioblastoma cell line, U87MG, upon A2 receptor agonist and mRNA transcripts for all P1 receptors (adenosine receptors) have been present while only A2B receptors have been found to be functional in these cells. Furthermore, hypoxic conditions have led to elevated mRNA levels of A2B receptor and A2B antagonists have attenuated tumor angiogenesis in a similar manner[135].

1.4.The aim of the study

Extracellular purinergic signaling may have growth-promoting or growth-inhibiting effects in a tissue and context-dependent manner. According to the findings regarding the roles of extracellular purinergic signaling components in cancers so far, these components have tendency to function as oncogenes. Although the relevance of extracellular purinergic signaling is well-known and their elevated levels are reported in multiple cancer types, their comprehensive characterization in colorectal cancer is still not adequate. Therefore, in this study, we mainly focused on elucidating the roles of extracellular purinergic signaling components, namely PSE001, PSE002 and PSC003, in colorectal cancer by demonstrating their effects with *in vitro* and *in vivo* settings. For this purpose, we utilized CRISPR/Cas9 gene editing system to generate loss-of-function models in CRC cell lines as well as we developed preclinical pharmacological inhibition models.

*The names of the target genes in this study are not disclosed and they are stated as PSE001, PSE002, PSC002 and PSC003. The identity of these genes would be revealed in the forthcoming manuscript.

CHAPTER 2

MATERIALS AND METHODS

2.1. MATERIALS

2.1.1. Chemicals

Table 2. *Chemicals used in the study*

Product Name	Catalog Number	Manufacturer
Agarose-Biomax	BHE500	Prona
NaCl	31434-1KG-R	Sigma Aldrich
Yeast extract	1.03753.0500	Merck
Tryptone	48647.02	Serva
Bacto agar	05039-500	Sigma
NP-40	A1694.0250	Applichem
Sodium deoxycholate	302-95-4	Sigma Aldrich
Sodium orthovanadate	13721-39-6	Sigma Aldrich
β-glycerophosphate	G9422	Merck
Sodium Fluoride	106441	Merck
Bovine Serum Albumin	sc-2323	Santa Cruz Biotechnology
Glycine	GLN001.1	BioShop Canada

EDTA	E-5134	Sigma Aldrich
Ethanol	32221	Sigma Aldrich
Methanol	24229-2.5L-R	Sigma Aldrich
2-propanol	100995	Sigma Aldrich
Glycerol	15524	Sigma Aldrich
Sodium dodecyl sulfate (SDS)	822050	Merck
Tween20	777	Ambresco/VWR
Trizma base	T1503	Sigma
Tris hydrochloride	234	Ambresco
Sodium chloride	S9888	Sigma Aldrich
2-Mercaptoethanol	805740	Merck
Ammonium Persulfate (APS)	7727-54-0	Sigma Aldrich
TEMED	1610801	BioRad
Bromophenol Blue	B0126	Sigma Aldrich
DMSO	67-68-5	Applichem
Sodium Azide	S2002-5G	Sigma Aldrich
Cobalt Chloride Hexahydrate ($CoCl_2.6H_2O$)	C8661	Sigma Aldrich
Trichloroacetic acid (TCA)	91228	Sigma Aldrich
Acetic Acid	1.00056.2500	Merck
Crystal violet	42555	Sigma Aldrich
polyHEMA	P3932	Sigma Aldrich

2.1.2. Cell culture media and solutions

Table 3. *Cell culture media and solutions used in the study*

Product Name	Catalog Number	Manufacturer
DMEM Low Glucose	L0064-500	Biowest

DMEM Low Glucose	BI01-050-1A	Biological Industries
RPMI 1640 w/stable L-glutamine	L0498-500	Biowest
McCoy's 5A w/L-glutamine	L0210-500	Biowest
DMEM High Glucose	11965092	Gibco
DMEM High Glucose	B.L0106-500	Biowest
Fetal Bovine Serum Heat Inactivated	S181H-500	Biowest
HyClone L-glutamine	SH30034.01	Cytiva (formerly GE Healthcare Life Science)
Penicillin/Streptomycin mixture	DE17-602E	Lonza
HyClone Phosphate Buffered Saline 10X	SH30258.02	Cytiva (formerly GE Healthcare Life Science)
Phosphate Buffered Saline 10X	X0515-500	Biowest
Phosphate Buffered Saline 10X	P04-53500	PAN-Biotech
Trypsin-EDTA 10X	X0930-100	Biowest
Puromycin	ant-pr-1	Invivogen
Polybrene (10mg/ml)	Sc-134220	SantaCruz
Opti-MEM^{TM} Reduced Serum Medium	31985070	Gibco

2.1.3. Kits

Table 4. *Kits used in the study*

Product Name	Catalog Number	Manufacturer
E.Z.N.A.® Gel Extraction Kit	D2500-01	Omega Bio-Tek
NucleoSpin Gel and PCR Clean-up	740609.50	Macherey-Nagel
E.Z.N.A Plasmid DNA Mini Kit	D6943-01	Omega Bio-Tek
E.Z.N.A Plasmid DNA Maxi Kit	D6922-02	Omega Bio-Tek
E.Z.N.A. Total RNA Kit I	R6834-02	Omega Bio-Tek
iScript cDNA Synthesis Kit	1708891	Bio-Rad
RevertAid First Strand cDNA synthesis kit	K1622	Thermo Scientific
SYBR® Premix Ex Taq^{EM} II	RR820W	Takara Bio
LightCycler® 480 SYBR Green I Master	04 707 516 001	Roche
Pierce BCA Protein Assay Kit	LSG-2322	Thermo Scientific

2.1.4. Buffers

Table 5. *Buffers used in the study*

Name	Contents
2X RIPA Cell Lysis Buffer	6mL of 5M NaCl, 2mL 0.5M EDTA pH 8.0, 10mL of 1M Tris pH 8.0, 2mL of NP-40, 10mL of 10% sodium deoxycholate, 2mL of 10% SDS, up to 100mL with ddH_2O
1X RIPA Cell Lysis Buffer	5mL of 2X RIPA Buffer, 500µl of 100mM sodium orthovanadate (Na_3VO_4), 500µl of 500mM β-glycerophosphate, 500µl of 500mM sodium floride (NaF)
10X Running Buffer	144g Glycine, 10g SDS, 30.2g Tris-Base, up to 1L with ddH_2O
10X Transfer Buffer	144g Glycine, 30.2g Tris-Base, up to 1L with ddH_2O
10X TBS-T	24.2g Tris-Base, 80g NaCl, pH=7.6, 20mL Tween, up to 1L with ddH_2O
Stacking Gel (2 gels)	0.6mL Acrylamide/Bis Solution, 3mL dH_2O, 625µL 1M Tris pH=6.8, 125µL 0.25M EDTA, 100uL 10%SDS, 60µL 10% APS, 10uL TEMED
8% Separating Gel	3.2mL Bis -Acrylamide, 5.8mL water, 1.5mL Glycerol, 3.75mL 1.5M Tris pH=8.8 375µL 0.25M EDTA, 300µL 10% SDS 125µL 10% APS, 15µL TEMED

4X Protein loading dye	250mM Tris-HCl pH 6.8, 10% SDS, 20% β-mercaptoethanol, 40% Glycerol, 0.008% Bromophenol Blue
Ponceau S	
Mild Stripping Buffer	0.2M Glycine, pH=2.5, 0.2% Tween
2X HBSS	0.1081g of 12mM Dextrose (D-glucose), 2.8mL of 5M NaCl, 5 mL of 10X Na_2HPO_4 (10X: 0.1335g in 50mL), 2mL of 250mM KCl, pH=7.01, up to 50mL with ddH_2O
50X TAE Buffer	242g Tris-Base, 57.1mL Acetic Acid 100mL 0.5M EDTA, up to 1L with ddH_2O
LB Broth	10g of NaCl, 5g Yeast Extract, 10g Tryptone, up to 100mL with ddH_2O
LB Agar	10g of NaCl, 5g Yeast Extract, 10g Tryptone, 15g Bacto agar, up to 100mL with ddH_2O
0.5% Crystal violet	0.5g Crystal violet, 25mL methanol, 75mL ddH_2O
Flow Cytometry Fixation Buffer	4% formaldehyde in PBS
Flow Cytometry Permeabilization Buffer	1mL FBS, 0.1g sodium azide, 0.1g saponin, pH=7.4-7.6, filtered with 0.2µm filter
Flow Cytometry Buffer (FACS Buffer)	500mL 1X HBSS, 2% FBS, 125mg sodium azide (0.25%)
10X Phosphate Buffered Saline	17.02g $Na_2HPO_4.2H_2O$, 80g NaCl, 2g KCl, 2g KH_2PO_4, up to 1L with ddH_2O, pH 6.87

2.1.5. Solutions, Pharmacological inhibitors, Agonists & Antagonists

Table 6. *Solutions, Pharmacological inhibitors, Agonists & Antagonists used in the study*

Product Name	Catalog Number	Manufacturer
GeneRuler 1kb DNA Ladder	SM0311	Thermo Fisher Scientific
TriTrack DNA Loading Dye (6X)	R1161	Thermo Fisher Scientific
PSE002-selective antagonist	M3***	Sigma Aldrich
PSC003-selective agonist	4***	Tocris
PSC003-selective antagonist	3***	Tocris
PageRuler Prestained Protein Ladder	SG-2661	Thermo Fisher Scientific
40% Acrylamide/Bis Solution 37.5:1	1610148	BioRad
Matrigel Matrix GFR Phenol Red Free	356231	Corning
Ampicillin	A0839	Applichem

2.1.6. Reagents

Table 7. *Reagents used in the study*

Product Name	Catalog Number	Manufacturer
HiPerfect Transfection Reagent	301705	Qiagen
cOmplete Protease Inhibitor Cocktail	11697498001	Roche

Pierce ECL Western Blotting Substrate	LSG-32106	Thermo Scientific
SuperSignal West Femto Maximum Sensitivity Substrate	34094	Thermo Scientific
CellTiter-Glo® (CTG) Luminescent Cell Viability Assay	G7570	Promega
CellTiter-Glo® 3D Cell Viability Assay	9682	Promega
Sulforhodamine B (SRB) sodium salt	S1402	Sigma Aldrich
WST-1 Cell Proliferation Reagent	11644807001	Roche
Human FC Block	564219	BD Biosciences

2.1.7. Enzymes & Enzyme Buffers

Table 8. *Enzymes and enzyme buffers used in the study*

Product Name	Catalog Number	Manufacturer
BsmBI	R0739	NEB
CIP	M0290	NEB
T4 Polynucleotide Kinase (T4 PNK)	M0201S	NEB
T4 DNA Ligase	M0202S	NEB
10X NEBuffer^{TM} 3.1	B7203S	NEB
10X CutSmart® Buffer	B7204S	NEB
10X T4 DNA Ligase Reaction Buffer	B0202S	NEB

Adenosine deaminase (ADA)	10102105001	Roche

2.1.8. Consumables

Table 9. *Consumables used in the study*

Product Name	Catalog Number	Manufacturer
1.5mL Reaction Tubes	3621	Corning
2mL Reaction Tubes	430659	Corning
1.5mL SafeLock Tubes	30120086	Eppendorf
50mL falcon tubes	227261	Greiner
50mL falcon tubes	62.547.254-300	Sarstedt
15mL falcon tubes	188271	Greiner
15mL falcon tubes	62.554.502-500	Sarstedt
5mL serological pipettes	4487	Corning
10mL serological pipettes	4488	Corning
25mL serological pipettes	4489	Corning
1000uL filter tips	740288	Greiner
200uL filter tips	739288	Greiner
20uL filter tips	774288	Greiner
10uL filter tips	F161630	Greiner
Gel-loading tips	14-222-809	Axygen
1000uL tips	551146	LP Italiana SP
200uL tips	4845	Corning
10uL tips	F161630	Gilson
96-well plates	655180	Greiner
24-well plates	662160	Greiner
12-well plates	665180	Greiner
6-well plates	657160	Greiner
175cm^2 tissue culture flask	660175	Corning

75cm^2 tissue culture flask	658175	Corning
25cm^2 tissue culture flask	690175	Corning
Cryovials	121263	Greiner
Cell Scraper	121.01.013	ISOLAB

2.1.9. Antibodies

Table 10. *Antibodies used in the study*

Product Name	Catalog Number	Manufacturer
ZO1	13663	Cell Signaling
N-cadherin	14215	Cell Signaling
E-cadherin	Sc-8426	Santa Cruz Biotechnology
Integrin α5	4705	Cell Signaling
ZEB1	Sc-515797	Santa Cruz Biotechnology
PSE002	1****	Cell Signaling
Phospho-AKT	4060	Cell Signaling
Total-AKT	9272	Cell Signaling
Phospho-ERK	4370	Cell Signaling
Total-ERK	9102	Cell Signaling
Alpha smoot muscle actin (α-SMA)	Ab5684	Abcam
PSC003	Ab2*****	Abcam
Vimentin	5741	Cell Signaling
Phospho-CREB	9198	Cell Signaling
Total-CREB	4820	Cell Signaling
APC-conjugated PSE001	32****	BioLegend
PE-conjugated PSE002	12-0***-**	Invitrogen
APC-conjugated PSC003	Bs-5****-A647	Bioss Antibodies
Anti-mouse IgG, HRP linked Antibody	7076	Cell Signaling

Anti-rabbit IgG, HRP linked Antibody	7074	Cell Signaling

2.1.10. Others

Table 11. *Other materials used in the study*

Product Name	Catalog Number	Manufacturer
PVDF membrane, 0.45µM	IPVH00010	Millipore
Mr. Frosty™ Freezing Container	5100-0001	Thermo Scientific
0.45µm filter	16555	Sartorius
0.20µm filter	16534	Sartorius

2.1.11. Instruments

Table 12. *Instruments used in the study*

Product Name	Company
Synergy HT Microplate Reader	BioTek
Leica MC120 HD, 2.5 Megapixel HD Microscope Camera	Leica Microsystems
DMi8 S Platform, Inverted Microscope Solution	Leica Microsystems
Eclipse TS100 Inverted light microscope	Nikon
NanoDrop ONE	Thermo Scientific
Polymerase Chain Reaction (PCR) Thermal cycler	Applied Biosystems
The LightCycler® 480 System	Roche
Amersham™ Imager 600	GE Healthcare Life Sciences
CytoExpert	Beckman Coulter

2.1.12. List of guide RNAs

Table 13. *Guide RNA sequences used in the study*

Gene Name	Sequence
PSE002 1 F	GCA**********GCG
PSE002 1 R	CGC**********TGC
PSE002 2 F	CTA**********GCG
PSE002 2 R	CGC**********TAG
PSE002 3 F	ATC**********CAA
PSE002 3 R	TTG**********GAT
PSC003 1 F	GTT**********GCG
PSC003 1 R	CGC**********AAC
PSC003 2 F	GAC**********ACG
PSC003 2 R	CGT**********GTC
PSC003 3 F	TGT**********AGA
PSC003 3 R	TCT**********ACA
SCR	GCACTACCAGAGCTAACTCA

*The guide RNA sequences for the target genes in this study are not disclosed. These sequences would be revealed in the forthcoming manuscript.

2.1.13. List of siRNAs

Table 14. *siRNA sequences used in the study*

Gene Name	Sequence
PSE002 1	GAU**********AGA
PSE002 2	GAU**********AGU
PSC003 1	GUG**********GUG
PSC003 2	GAU**********AUG
PSC003 3	UGC**********ACU

*The siRNA sequences for the target genes in this study are not disclosed. These sequences would be revealed in the forthcoming manuscript.

2.1.14. List of qPCR primers

Table 15. *qPCR primer sequences used in the study*

Primer	Sequence
GAPDH F	GCCCAATACGACCAAATCC
GAPDH R	AGCCACATCGCTCAGACAC
CDH1 F	CCCGGGACAACGTTTATTAC
CDH1 R	GCTGGCTCAAGTCAAAGTCC
CLAUDIN7 F	CCACTCGAGCCCTAATGGTG
CLAUDIN7 R	GGTACCCAGCCTTGCTCTCA
FN F	CTGGCCGAAAATACATTGTAAA
FN R	CCACAGTCGGGTCAGGAG
ZO-1 F	CAGAGCCTTCTGATCATTCCA
ZO-1 R	CATCTCTACTCCGGAGACTGC
CDH2 F	ACAGTGGCCACCTACAAAGG
CDH2 R	CCGAGATGGGGTTGATAATG
VIMENTIN F	GGTGGACCAGCTAACCAACGA
VIMENTIN R	TCAAGGTCAAGACGTGCCAGA
ZEB1 F	GGGAGGAGCAGTGAAAGAGA
ZEB1 R	TTTCTTGCCCTTCCTTTCTG
TWIST F	AAGGCATCACTATGGACTTTCTCT
TWIST R	GCCAGTTTGATCCCAGTATTTT
PSE001 F	AGG**********TAC
PSE001 R	CCA**********CCT
PSE002 F	GCC**********TTG
PSE002 R	TAG**********TCG
PSC002 F	TCC**********GGC
PSC002 R	AAA**********GGA
PSC003 F	CTC**********GTC
PSC003 R	TGG**********TGG

*The primer sequences for the target genes in this study are not disclosed. These sequences would be revealed in the forthcoming manuscript.

2.2. METHODS

2.2.1. Cell Maintenance

All mammalian cell lines were kept under conditions with 5% CO_2 at 37^{o}C. HT29, SW480, RKO and SW48 have been maintained in DMEM low glucose growth medium supplemented with 10% Fetal Bovine Serum (FBS), 1% L-glutamine and 1% Penicillin/Streptomycin. DLD1 and HCT116 have been kept in McCoy's 5A supplemented with 5% FBS and 8% FBS, respectively, and 1% L-glutamine and 1% Penicillin/Streptomycin. SW620 has been maintained in RPMI 1640 with stable L-glutamine supplemented with 10% FBS and 1% Penicillin/Streptomycin. HEK293T human embryonic kidney cells have been maintained in DMEM High Glucose supplemented with 8% FBS, 1% L-glutamine and 1% Penicillin/Streptomycin.

HT29, SW48, RKO and SW620 have been passaged every 3 days by 1:4 or 1:5 ratio, DLD1, and HCT116 have been splitted every 2 days by 1:10 ratio and SW480 has been passaged every 2 days by 1:5 ratio at most, by firstly washing them with 1X phosphate buffered saline (PBS) after removing old culture media and then by using 1X Trypsin-EDTA for trypsinization. After trypsin is discarded, the cells whose attachment to the cell culture plates is weakened by trypsin have been collected in growth media.

PSE002 and PSC003 knock out cell lines by CRISPR/Cas9 have been kept under selection with puromycin in different concentrations.

2.2.2. Cryopreservation of the cell lines

Once PSE002- and PSC003-knockout cell lines had been generated, they were cryopreserved. After the cells were collected by trypsinization, they were centrifuged at 300xg for 5 minutes. Then media was discarded, and the pellet was resuspended in

freezing medium, 90% FBS and 10% DMSO as cryoprotective agent, as it would not exceed 1-1.5 million cells/mL. 1-1.5mL of cell suspension was added to each cryovial and they were placed in Mr. Frosty Cell Freezing Container to provide gradually freezing. The cells were placed in Mr. Frosty at -80^{o}C for short-term and at liquid nitrogen (-170^{o}C) for long-term.

2.2.3. Cloning

Annealed oligos of designed gRNA sequences were inserted to lentiCRISPRv2 vector (Addgene, #52961) which has sgRNA scaffold and hSpCas9 expression cassettes to generate CRISPR constructs. Firstly, lentiCRISPRv2 vector (Addgene, #52961) was cut by BsmBI (NEB, #R0739) under the conditions stated below.

Table 16. *lentiCRISPRv2 digestion reaction used in the study*

Component	Amount
lentiCRISPRv2	5µg
BsmBI	3µl
NEBuffer 3.1	10µl
ddH_2O	Up to 100µl

It was incubated at 37^{o}C, overnight and enzyme was inactivated at 80^{o}C for 10 minutes at the end of the incubation. Next, it was loaded on 1% agarose gel and extracted by using E.Z.N.A Gel Extraction kit (Omega Bio-Tek, D2500-01) by following the protocol provided by manufacturer. Then the vector was dephosphorylated using CIP (NEB, #M0290) at 37^{o}C for 30 minutes as shown in Table 15 and PCR clean-up (Macherey-Nagel, 740609.50) was performed on dephosphorylated vector to remove excessive materials from the vector.

Table 17. *lentiCRISPRv2 dephosphorylation reaction used in the study*

Component	Amount
Cut lentiCRISPRv2	36µl
CutSmart Buffer	5µl
CIP	1µl
ddH_2O	50µl

Moreover, single guide RNA sequence pairs (forward and reverse) were annealed and phosphorylated by T4 Polynucleotide Kinase (T4 PNK) (NEB, #M0201S) in T4 DNA Ligase Buffer (NEB, #B0202S) at 37^{o}C for 30 minutes. Then these oligos were diluted by 1:200 ratio to be used in ligation reaction.

Table 18. *Phosphorylation and annealing reaction of oligos used in the study*

Component	Amount
Forward sequence	0.5µl
Reverse sequence	0.5µl
10X T4 DNA Ligase Buffer	1µl
T4 PNK	0.5µl
ddH_2O	7.5µl

Annealed and phosphorylated oligos were inserted into cut vector using T4 DNA Ligase (NEB, #M0202S) at 16^{o}C, overnight.

Table 19. *Ligation reaction used in the study*

Component	Amount
Cut lentiCRISPRv2	2.77µl
Annealed oligos	1µl
10X T4 DNA Ligase Buffer	1µl
ddH_2O	5.23µl
T4 DNA Ligase	1µl

This ligation product was transformed to NEB® Stable Component *Escherichia coli (E. coli)* bacteria (NEB, #C3040I) which was plated on agar plates with ampicillin for bacterial selection and grown overnight. Next day, two colonies for each construct were separately picked and put in LB broth with ampicillin by 1:1000 ratio to make them grow overnight. After they grew, miniprep was performed using E.Z.N.A.® Plasmid Mini Kit/Maxi Kit (Omega Bio-Tek, D6943-01/D6922-02) by following the instructions provided by manufacturer. Next, each product was checked on the agarose gel for correct size. The ones with correct size were sent for Sanger sequencing by using hU6-F primer (5'-GAGGGCCTATTTCCCATGATT-3'). The constructs with correct sequence for the targeted gene were used to generate knockout cell lines.

2.2.4. Calcium Phosphate Transfection with lentiCRISPRv2 constructs

HEK293T cells were used as recipient cells to produce lentiviral particles harboring generated CRISPR constructs to generated loss-of-function models. HEK293T cells were seeded as $1.3x10^6$ cells/ml in 6cm cell culture dish to have around 70% confluency in the following day. 2 hours before the transfection, the media of culture was changed to fresh media. Then, a mixture containing packaging plasmids VSVG and R891, lentiCRISPRv2-sgRNA plasmids, $CaCl_2$ and autoclaved ddH_2O were prepared and vortexed to mix. Then, this mixture was added onto 2X HBSS dropwise while vortexing. The mixture was incubated at room temperature for 10 minutes. Lastly, the mixture was added on top of culture media dropwise and the dish was gently shook. 16 hours post-

transfection, media was changed to fresh growth medium and the cells were placed in lentiviral room.

Table 20. *The amount of components used in calcium phosphate transfection.*

Component	Amount
lentiCRISPRv2 CRISPR plasmids	9µg
VSVG packaging plasmid	3µg
R891 packaging plasmid	6µg
2M $CaCl_2$	38µl
2X HBSS	300µl
Autoclaved ddH_2O	up to 600µl

2.2.5. Lentiviral Transduction

Following the transfection on HEK293T cell lines, they were incubated 48 hours post-transfection to obtain viral titer and the media with lentiviral particles were collected. 2nd harvesting was done before 72 hours post-transfection. The collected media was centrifuged to remove any dead cells and supernatant was collected which was filtered through 0.45µM filter and given to HT29, DLD1 and SW480 colorectal cancer cell lines together with 7µg/mL polybrene to facilitate transduction. They were transduced for 2-3 days depending on their confluency and cell healthiness. Finally, the media was changed to fresh growth media and the cells were kept under selection with 2µg/mL puromycin at the beginning. Then it was increased to 5µg/mL for HT29 and 4µg/mL for DLD1 and SW480 cell lines.

2.2.6. siRNA Transfection

We generated transiently depleted cell lines for PSE002 or PSC003 via RNAi in addition to stable knockout cell lines. Thus, the cells were seeded in a cell number that the confluency would be approximately 30-40% next day. 100µM siRNA constructs were separately mixed with OptiMEM (1:1000). Then, HiPerfect was added to the mixtures and vortexed for short time. Old media was discarded from the culture and it was

replaced by the mixture. After 6 hours, 800µl growth medium was added. After 24 hours post-transfection, media was changed to the normal medium.

Table 21. *The amount of components used in siRNA transfection.*

Component	Amount
siRNA constructs	0.8µl
OptiMEM	800µl
HiPerfect	10µl

2.2.7. Cobalt Chloride Hexahydrate ($CoCl_2.6H_2O$) Treatment

The cells were seeded as they would not be less than 50-60% confluency next day. Then, required amount for 100µM, 200µM and 300µM was taken from 100mM stock solution of $CoCl_2.6H_2O$ and mixed with growth medium. Then old culture media was replaced with growth medium and $CoCl_2.6H_2O$ mixture. The cells were treated for 8 hours, 16 hours and 24 hours.

2.2.8. PSE002-selective antagonist/PSC003-selective agonist/PSC003-selective antagonist treatments

After cells were seeded in 96-well plate, 10mM PSE002-selective antagonist was added in different concentrations directly to the growth media and the cells were treated for 3-4 days. For PSC003-selective agonist and PSC003-selective antagonist optimization, cells were first treated with adenosine deaminase (ADA) for 30 minutes at RT to prevent its interfering with PSC003-selective agonist function. Then they were treated with PSC003-selective agonist for 30 minutes, 1 hour and 2 hours at 37^{o}C with 5% CO_2. For PSC003-selective antagonist, following ADA and PSC003-selective agonist pre-treatment separately for 30 minutes, the cells were treated with PSC003-selective antagonist for 30 minutes more at 37^{o}C with 5% CO_2. Then they were lysed by RIPA cell lysis buffer for protein sampling. In cell proliferation assays, the treatments were done for 3-4 days and quantified by Sulforhodamine B (SRB) colorimetric assay.

2.2.9. Single Cell Cloning by Serial Dilution Method

Single cell cloning was performed on PSC003-depleted cell lines to be able to have homogenous depleted cell population in 96-well plate format. Firstly, 100µl growth medium was added in each well except A1. Then, 200µl cell suspension containing $0.5x10^4$ cells was added to well A1 and 100µl of cell suspension was quickly taken from A1 and transferred to well B1. The same process was repeated until H1 and lastly 100µl of cell suspension was discarded. Next, 100µl of growth media was added in each well in the first column. After that 100µl was quickly transferred from each well in the first column to the each well in the second column. The same process was repeated until the last column (column 12). At the end 100µl cell suspension was discarded from each well in column 12. Finally, each well was completed to 200µl growth media and plate was incubated at 37ºC, 5% CO_2.

After 4-5 days, the wells with single cells were detected and followed until they could grow enough to be taken into one bigger size plate which is 48-well plate. These single cell colonies were gradually transferred to one bigger size plate every time until 6cm cell culture dishes. Then they were cryopreserved for long-term storage and protein and RNA samples were taken for PSC003 expression screening.

2.2.10. *In vitro* Assays

2.2.10.1.CellTiter-Glo® (CTG) Cell Viability Assay

CellTiter-Glo® Luminescent Cell Viability Assay was conducted to assess the cell proliferation rate of PSE002-depleted and PSC003-depleted cell lines. The depleted CRC cell lines were seeded in 96-well plate format and grown under normal culture conditions with complete growth media for 3-4 days. Their cell proliferation was measured every day by lysing them with CTG according to the protocol provided by manufacturer. Then luminescence reading was done by Synergy HT Microplate Reader.

2.2.10.2.Sulforhodamine B (SRB) Assay

Sulforhodamine B assay was performed to measure the cell growth upon treatments including PSE002-selective antagonist, PSC003-selective agonist and PSC003-selective antagonist treatments. The cells were seeded in 96-well plate format and treated next day for 3-4 days. At the end of treatment, the old media was discarded and replaced by 80µl media. Then 120µl of 4% trichloroacetic acid (TCA) was added on top of it and incubated at 4^{o}C for 1 hour to fix the cells. After incubation time, the mixture was removed and the wells were washed by ddH_2O. Once excessive water was completely removed from the wells, SRB was added to each well to stain the cells for 30 minutes at RT under dark. After that, SRB was discarded and the wells were rinsed with 1% acetic acid. The plate was left for air-dry around 1 hour under fume hood. Once it was completely dry, 50µl of 10mM Tris-Base was added to destain and the plate was read by Synergy HT Microplate Reader.

2.2.10.3.WST-1 Cell Proliferation Assay

WST-1 cell proliferation assay was one of the cell proliferation assays used. The cells were seeded in 96-well plate format. The old media was removed and replaced with 100µl of fresh media. Then, WST-1 cell proliferation reagent was added to the media by 1:10 ratio (100µl medium + 10µl WST1) and incubated for 4 hours at 37^{o}C. Then it was measured at 450nm and 630nm using Synergy HT Microplate Reader.

2.2.10.4.Clonogenic Assay

The cells were seeded in either 6-well plate or 12-well plate format in a few numbers to be able to observe a single cell growing into a colony separately than others. They were kept in culture and grown for around 14 days. Before colonies came together, staining process was done. After removing media, the wells were washed with 1X PBS and it was also discarded. Next, ice-cold methanol was added onto the wells for fixation. For fixation, the plates were kept at -20^{o}C for 10 minutes. After methanol was discarded, the cells were stained by 0.5% Crystal violet for 30 minutes at RT under dark. Once staining was done, crystal violet was collected to discard properly, and the wells were washed

with water until the excessive dye was removed completely. Then, the plates were left for air dry and quantified by Colony Counter tool.

2.2.10.5.Wound Healing Assay

Wound healing assay was conducted to assess the migratory abilities of the cells. The cells were seeded in 24-well plate format as they would cover all the surface in the well. Next day, the gap was created by using a 200µl tip and dead cells was removed by washing with 1X PBS. Then the medium was changed to 1% DMEM for SW480 to be able to slow the closure down and also to eliminate proliferative ability of the cells. The images were captured at the starting point (0H) and at the different time points. At the end, the gaps were compared to their initial size and each of them was quantified by TScratch.

2.2.10.6.Poly(2-hydroxyethyl methacrylate)/polyHEMA

To be able to demonstrate anchorage-independent growth, polyHEMA system, a hydrogel to prevent cellular attachment, was utilized. 120mg/ml stock polyHEMA was diluted by 95% Ethanol as final concentration would be 15µg/mL. Then, 96-well plates were coated by diluted polyHEMA (15µg/mL). The coating was done twice by adding 50µl each time. Between the first and second coating, and also after second coating, the plate was incubated for at least 1 week to dry the coating in a non-humid incubator at 37^{o}C. When the coatings were completely dry, the cells were seeded on polyHEMA and grown over 1 week. They were lysed by CTG 3D every 2 days and the picture of colonies were captured under inverted microscope.

2.2.11. Cell line-derived xenograft models

6 to 8 weeks old athymic nude mice were provided by the animal facility of the Bilkent University, Department of Molecular Biology and Genetics with the ethical permission of local ethics committee of Bilkent University. Depending on the cell line, cells were amplified in a big scale. In the day of injection, cells were trypsinized and counted. Then they were centrifuged at 300xg for 5 minutes and washed with cold 1X PBS. After PBS was removed, they were prepared as $5x10^{6}$ cells/200µl in 1X cold PBS. For SW480

injection, cell suspension was mixed with Matrigel by 1:1 ratio whereas it was not necessary for HT29 cells. After the cells were prepared, the subcutaneous injection was done only in one flank on athymic mice under anesthesia. Their weights and tumor volumes were followed and observed 3 times a week. Tumor volumes were measured by digital caliper and calculated according to the following formula LxW^2 (L: length, W: width). When tumor volumes reached to approximately $2000mm^3$, the experiment was finalized and all mice were sacrificed. Then tumors were collected one by one and washed with PBS. The samples for protein and RNA were taken and the remaining parts were fixed in 4% PFA overnight for histopathological analysis.

2.2.12. Cell Lysis

Cell lysis was performed for protein and RNA sampling for different cell lines upon depletion or treatments. After the old media was discarded, the cells were washed with 1X PBS twice. Then the cells were collected in 1X PBS by scraper. Next, they were centrifuged at 13000rpm for 10 minutes. Supernatant was removed and the pellet was resuspended in RIPA Cell Lysis buffer for protein samples and in TRK Lysis Buffer (R6834, Omega) for RNA samples. Protein samples were incubated on ice at least for 30 minutes by vortexing every 5-10 minutes. Then they were centrifuged in the same conditions. The supernatant was taken as protein sample and kept at -80^{o}C.

2.2.13. RNA Extraction

The samples resuspended in TRK lysis buffer were thawed on ice and placed at RT. After they were completely thawed, 1 volume of 70% EtOH was added onto samples and vortexed thoroughly. Then it was transferred to the column and the protocol provided by manufacturer was followed.

2.2.14. Reverse Transcriptase PCR (RT-PCR)

For cDNA synthesis, both iScript cDNA Synthesis Kit (1708891, Bio-Rad) and RevertAid First Strand cDNA synthesis kit (K1622, Thermo Scientific) were used. The conditions for RT-PCR with both kits are provided below.

Table 22. *Reaction used for RT-PCR with iScript cDNA synthesis kit*

Component	Amount
5X iScript Reaction Mix	4µl
iScript Reverse Transcriptase	1µl
RNA template	1000ng
Nuclease-free water	Up to 20µl

After the reaction mix was prepared, it was incubated in a thermal cycler using the following protocol.

Table 23. *Protocol for cDNA synthesis using iScript cDNA synthesis kit*

Step	Condition
Priming	5 min at 25^{o}C
Reverse transcription	20 min at 46^{o}C
RT inactivation	1 min at 95^{o}C

Table 24. *Reaction used for RT-PCR with RevertAid First Strand cDNA synthesis kit*

Component	Amount
Template RNA	1000ng
Oligo $(dT)_{18}$ primer	1µl
Nuclease-free water	To 12µl
5X Reaction Buffer	4µl
RiboLock RNase Inhibitor	1µl
10mM dNTP Mix	2µl
RevertAid M-MuLV RT	1µl

The mixture was incubated at 42ºC for 60 minutes and the reaction was terminated by heating it to 70ºC for 5 minutes.

2.2.15. Quantitative PCR (qPCR)

After cDNAs were generated from the extracted RNA samples, quantitative PCR was conducted by using these cDNAs after diluting them by 1:4 ratio, required primers, and SYBR green premix according to the protocol stated below.

Table 25. *Reaction used for qPCR in the study*

Component	Amount
cDNA	1µl
10µM Primer	1µl
2X SYBR Premix*	5µl
ddH_2O	3µl

** LightCycler® 480 SYBR Green I Master or SYBR® Premix Ex TaqEM II*

The protocol provided by manufacturer was applied for either SYBR Green Premix reagents.

2.2.16. Protein Quantification

The table provided below was used for protein quantification by using BCA Protein Assay Reagent Kit. 100µl was added to each well from the required dilution. 100µl BCA (Reagent A + Reagent B by 1:50 ratio) was added on top of them and the plate was incubated at 60ºC for 50 minutes and measured after cooling down.

Table 26. *Protein quantification used in this study*

BSA (µl)	ddH$_2$O (µl)
0	400
40	260
80	320
120	280
160	240
200	200
280	120
400	0

Then samples were prepared by mixing with 4X protein loading dye and boiled at 75^{o}C for 10 minutes to denature the proteins.

2.2.17. Western Blot

The stacking and separating gels were prepared as stated in Table 2.1.4. Boiled protein samples were ran in SDS-page gel and transferred to PVDF membrane via wet transfer system. After transfer, the membrane was stained with Ponceau S to check transfer step and it was washed away. Then blocking was performed with 10% skim milk for 30 minutes at RT and washed with 1X TBS-T twice for 5 minutes. Next, it was incubated with primary antibody overnight at 4^{o}C and with secondary antibody for 1.5 hours at RT by washing the membrane three times for 10 minutes between incubations. After secondary incubation membrane was washed again and revealed using Pierce ECL Western Blotting Substrate or SuperSignal West Femto Maximum Sensitivity Substrate by Amersham Imager 600.

2.2.18. Flow cytometry

For surface staining, the cells were collected in PBS and centrifuged at 300xg for 5 minutes. Then washing step with FACS buffer was done and centrifuged again at 300xg for 5 minutes. After supernatant was discarded, the pellet was incubated with FC block diluted in FACS buffer by 1:50 ratio for 15 minutes on ice. Then, antibody staining was performed with APC-conjugated PSE001 antibody, PE-conjugated PSE002 or APC-

conjugated PSC003 by 1:200 ratio for 30 minutes on ice under dark. It was then centrifuged after washing step with FACS buffer, supernatant was discarded and pellet was resuspended in 200µl of FACS buffer. Finally, it was analyzed in CytoExpert.

For intracellular staining, the steps until first washing with FACS buffer were done in the same way. After supernatant was discarded, the cells were fixed with 4% formaldehyde for 30 minutes on ice. Then it was washed with PBS and centrifuged at 300xg for 5 minutes. After supernatant was discarded, the pellet was incubated with FC block diluted in permeabilization buffer by 1:50 ratio for 15 minutes on ice. Then, antibody staining was performed with APC-conjugated PSE001 antibody, PE-conjugated PSE002 or APC-conjugated PSC003 by 1:200 ratio in permeabilization buffer for 40 minutes at RT under dark. Following steps were performed in the same way as surface staining.

CHAPTER 3

RESULTS

3.1. Expression profile of purinergic signaling components was identified in CRC cell lines.

The significance of purinergic signaling components in cancers other than colorectal cancer is well-established and their elevated levels are reported in many cancers including breast, prostate, and lung cancer as mentioned before. However, their comprehensive characterization in colorectal cancer still was not adequate. Therefore, we firstly identified the expression level of each component (PSE001, PSE002, PSC002, and PSC003) at mRNA level in 7 different colorectal cancer cell lines by quantitative PCR (Fig 4A-4D). Immortalized T lymphocyte cell line Jurkat and immortalized B lymphocyte cell line Namalwa were included as reference cell lines to show the relevance of each purinergic signaling components, especially PSE001 and PSC002, at mRNA level in colorectal carcinoma (CRC) cell lines as they are reported to be highly expressed in lymphocytes[138]. As seen in Figure 4A and Figure 4C, the level of PSE001 and PSC002 mRNA transcripts were not high in CRC cell lines compared to lymphocytes, especially to Jurkat cell line. On the other hand, it was shown that PSE002 and PSC003 mRNAs were highly transcribed in CRC cell lines (Fig. 4B and 4D). Yet, some cell lines could not show as high expression as others do, even though their levels were still higher than their PSE001 and PSC002 levels. Thus, PSC002 was found to be irrelevant to colorectal carcinoma since mRNA expression level could not be detected in any of CRC cell lines (Fig. 4C).

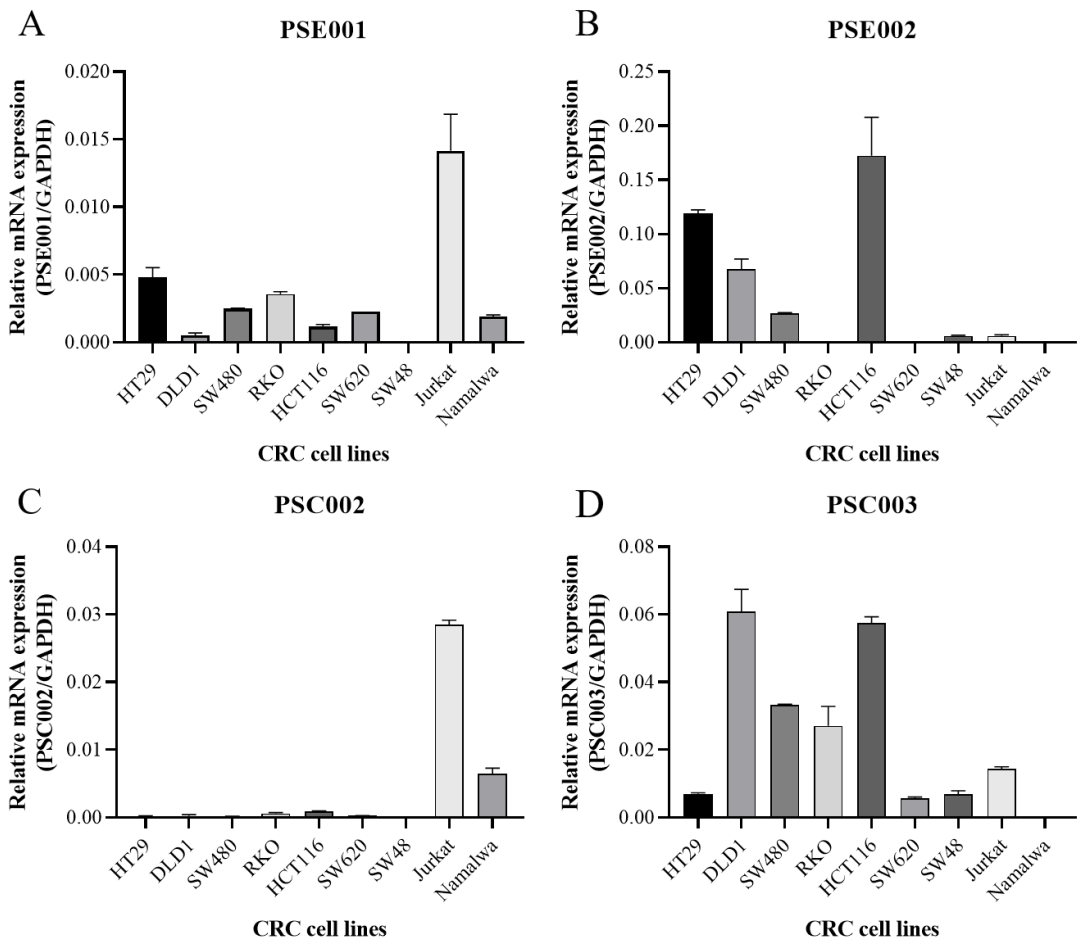

Figure 4: mRNA expression level of purinergic signaling components in CRC cell lines compared to immortalized lymphocyte cell lines. (A) PSE001, **(B)** PSE002, **(C)** PSC002, and **(D)** PSC003 mRNA levels in seven different CRC cell lines, and in Jurkat and Namalwa were compared by quantitative polymerase chain reaction (qPCR). When calculating C_T ($2^{-\Delta\Delta CT}$) values, GAPDH was used for normalization. None of the CRC cell lines showed PSC002 expression at mRNA level whereas PSE001 was expressed in lower levels compared to Jurkat. mRNA expression of PSE002 and PSC003 was detected in almost all CRC cell lines and also in higher levels than immortalized lymphocyte cell lines.

To demonstrate how these transcripts were translated to protein level, Western blot analysis was performed (Fig. 5). Most of CRC cell lines, except RKO and SW620, showed high PSE002 levels while most prominent variant of PSE002 which shows ectonucleotidase activity (upper band) was not expressed on immortalized lymphocyte cell lines (Fig. 5A). Also, it was seen that PSE002 was expressed more in HT29 and DLD1 cell lines compared to others. On the one hand, PSC003 was expressed by all

CRC cell lines in which HCT116 showed the highest expression followed by DLD1 and RKO. Interestingly, PSC003 was expressed in Jurkat almost as much as in CRC cell lines whereas it was expressed by Namalwa in lower levels (Fig. 5B).

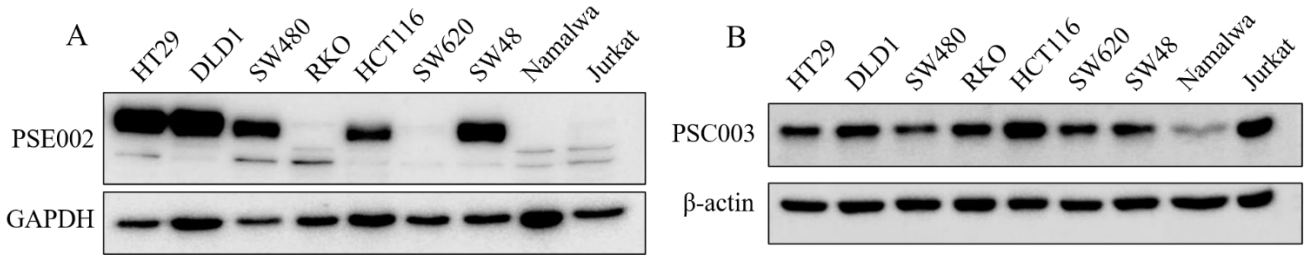

Figure 5: Expression level of purinergic signaling components in CRC cell lines compared to immortalized lymphocyte cell lines. (A) PSE002, **(B)** PSC003 protein levels in seven different CRC cell lines and in Jurkat and Namalwa were detected by Western Blot analysis. GAPDH and β-actin were used as loading controls for PSE002 and PSC003 blots, respectively. Except RKO and SW620, all CRC cell lines highly expressed PSE002 whereas PSE002 variant with ectonucleotidase activity was not present on lymphocytes. PSC003 was expressed by all CRC cell lines as well as immortalized T lymphocyte cell line Jurkat while Namalwa showed this expression in lower levels.

These expression levels were further confirmed in CRC cell lines by flow cytometry. For each cell line, the result for unstained sample is first provided to show noise from the background and it is followed by the result of stained sample by corresponding antibody (Appendix C). PSE001 did not have any expression in CRC cell lines as understood from their signal-to-noise ratios (SNRs) and the population percentages (Fig. 6). SNRs were calculated by dividing MFI values of positive samples (stained samples) by MFI values of negative samples (unstained samples). We showed that all CRC cell lines except SW48 had SNRs around 1.000 meaning that PSE001 was not present on the surface of these cells (Fig. 6A). In addition, to be able to show that there was not any technical issue, peripheral blood mononuclear cells (PBMCs) were included in the analysis. Despite PBMC being a mixed population of T cells, B cells, and NK cells, they could show higher PSE001 level (Fig. 6A). Moreover, the percentage of PSE001-expressing population was also higher in PBMC than CRC cell lines (Fig. 6B). Ultimately, we decided to also exclude PSE001 from our target genes as it does not seem to be relevant in colorectal cancer.

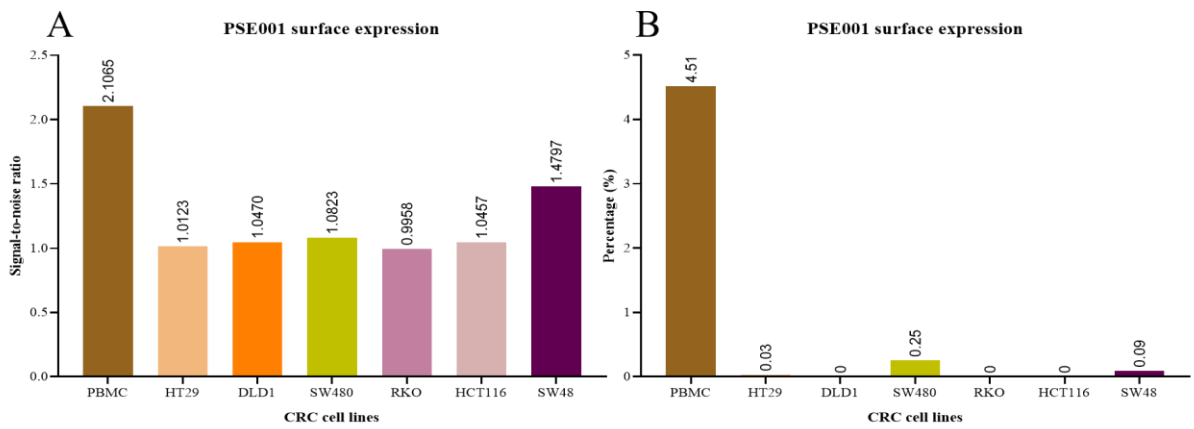

Figure 6: Expression level of PSE001 on the surface of CRC cell lines. (A) Signal-to-noise ratios were calculated by dividing MFI values of positive samples by MFI values of negative samples. Except SW48, all CRC cell lines had SNRs around 1 which was less than SNR of peripheral blood mononuclear cells (PBMCs) **(B)** Percentages are indicating the percentage of PSE001-expressing cell population. As expected, none of the CRC cell lines expressed PSE001 on their cell surface. *MFI; mean florescence intensity, SNR; signal-to-noise ratio, PBMC; peripheral blood mononuclear cell*

To further investigate PSE002 levels in CRC cell lines, we performed both surface and intracellular staining by flow cytometry (Appendix D and Appendix E). It was seen that PSE002 was highly expressed in HT29, DLD1 and SW480 both on the surface and in the intracellular compartment which confirmed the expression profile obtained via Western blot analysis (Fig. 7). Interestingly, HCT116 did not have intracellular PSE002, even though it showed high expression level on the surface. Moreover, PSC003 level was also assessed in CRC cell lines through surface staining and intracellular staining by flow cytometry (Appendix F and Appendix G). We showed that both surface and intracellular expression of PSC003 were strikingly high in all CRC cell lines (Fig. 8). The expression profile obtained by flow cytometry showed the same expression pattern in CRC cell lines as shown by Western blot analysis (Fig. 5). To conclude, we could show that both PSE002 and PSC003 can be potential targets in colorectal carcinoma to elucidate further.

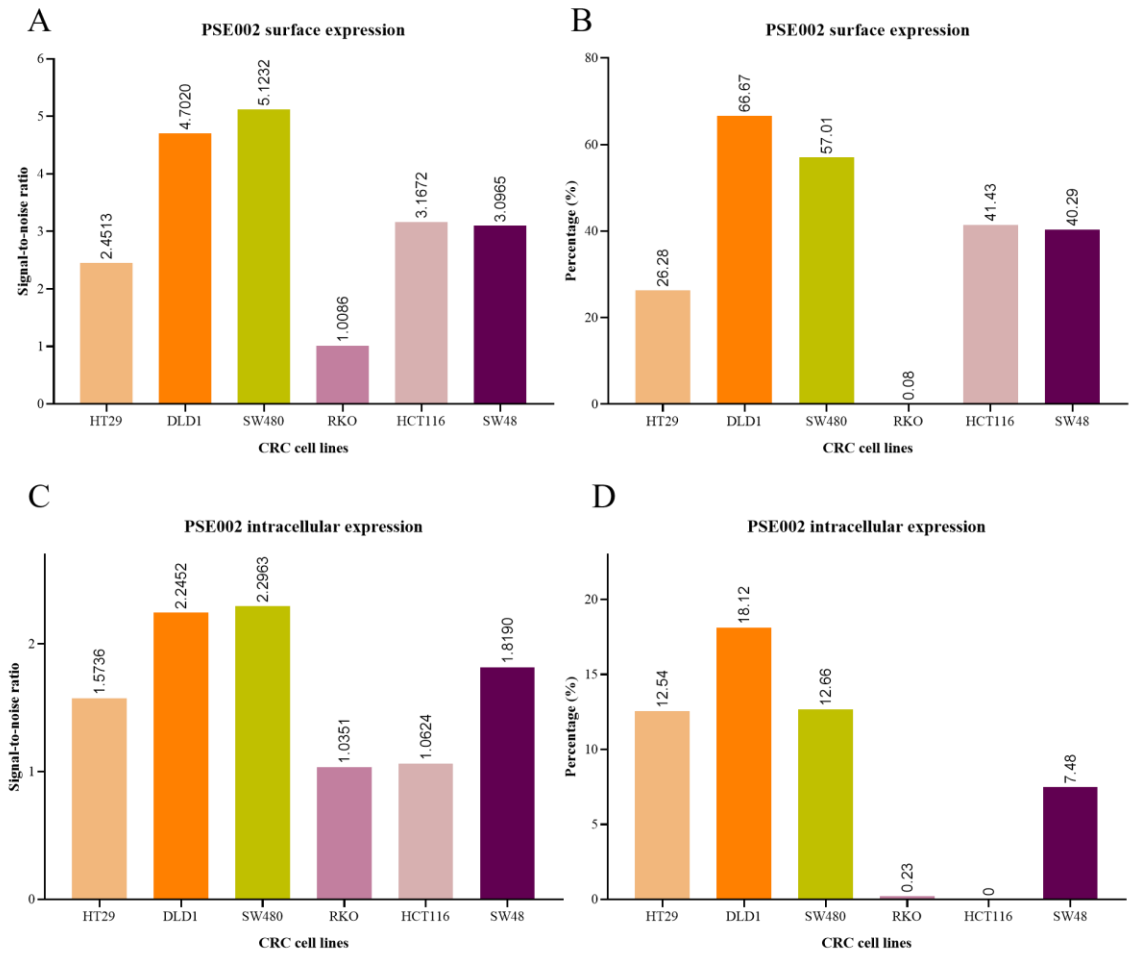

Figure 7: Expression level of PSE002 on the surface and in the intracellular compartment of CRC cell lines. (A)(C) Signal-to-noise ratios were calculated by dividing MFI values of positive samples by MFI values of negative samples. **(B)(D)** Percentages are indicating the percentage of PSE002-expressing cell population. As seen in their SNRs and percentages, PSE002 was highly expressed by all CRC cell lines except RKO on the surface while all CRC cell line showed PSE002 expression in the intracellular compartment except HCT116. *MFI; mean florescence intensity, SNR; signal-to-noise ratio.*

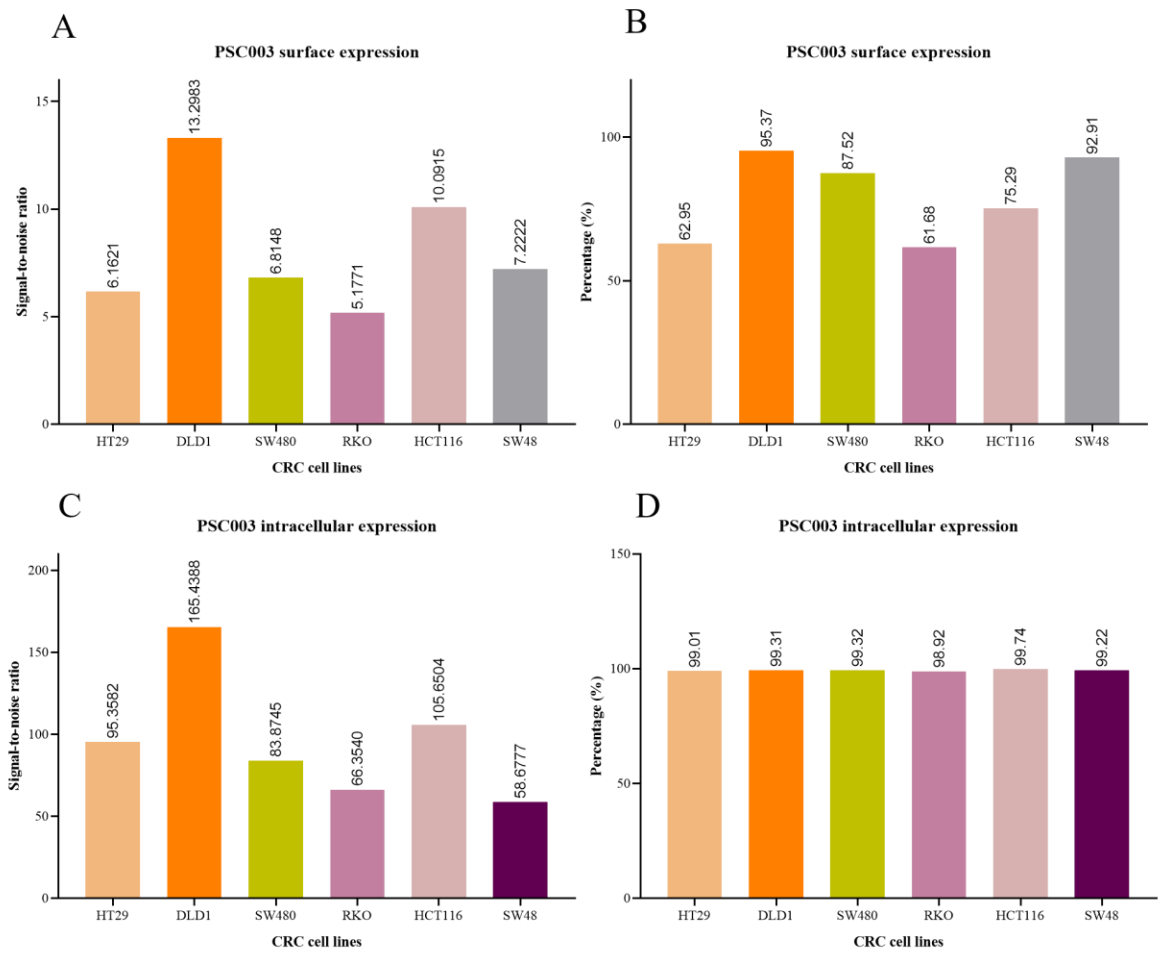

Figure 8: Expression level of PSC003 on the surface and in the intracellular compartment of CRC cell lines. (A)(C) Signal-to-noise ratios were calculated by dividing MFI values of positive samples by MFI values of negative samples. **(B)(D)** Percentages are indicating the percentage of PSC003-expressing cell population. PSC003 was highly expressed by all CRC cell line both on the surface and in the intracellular compartment. *MFI; mean florescence intensity, SNR; signal-to-noise ratio.*

As known, the tumor microenvironment highly displays hypoxic conditions and this feature plays a fundamental role in the progress of colorectal cancer. Additionally, deciphering the correlation between purinergic and hypoxia signaling would be a promising finding to prevent cancer progression as purinergic signaling components have been shown to be regulated by hypoxia-inducible factors in several cancers. For this reason, we also demonstrated the expression profile of our target genes by treating wild-type cells with cobalt (II) chloride hexahydrate ($CoCl_2.6H_2O$) to mimic hypoxic conditions in the cells. We treated the cells with $CoCl_2.6H_2O$ for 8 hours, 16 hours and 24 hours and showed HIF-1α induction. It was seen that $CoCl_2.6H_2O$ treatment successfully induced HIF-1α expression in colorectal cancer cell lines in a concentration-dependent manner (Fig. 9A).

Next, we checked the surface expression level of our target genes under hypoxic conditions. In HT29 cell line, the level of PSE002 was diminished in a dose-dependent manner after 6 hours of $CoCl_2.6H_2O$ treatment whereas its level was enhanced at 24 hours meaning that the effect of hypoxic conditions on PSE002 level may be time-dependent. Moreover, PSE002 level remained steady after 6 hours treatment in DLD1 cell line and then it decreased at 16 hours and 24 hours unlike HT29. In SW480 and RKO, induced HIF-1α decreased PSE002 levels in all concentrations and time points (Fig. 9B). Elevated PSE002 levels in HT29 at 24 hours and attenuated PSE002 in SW480 and HCT116 at 16 hours and 24 hours, respectively were also confirmed by flow cytometry (Fig. 9C). Surprisingly, HIF-1α induction did not alter PSC003 levels in HT29 cell line, however, it resulted in a significant increase of PSC003 level in HCT116 colorectal cancer cell line at 24 hours (Fig. 9D). Even though the induction of HIF-1α was mostly seen in the earliest time point (8 hours) because of its limited half-life, it is apparent that its effect on PSE002 and PSC003 was still present until 24 hours and this effect varies in a wide range depending on the cell type and the duration of treatment.

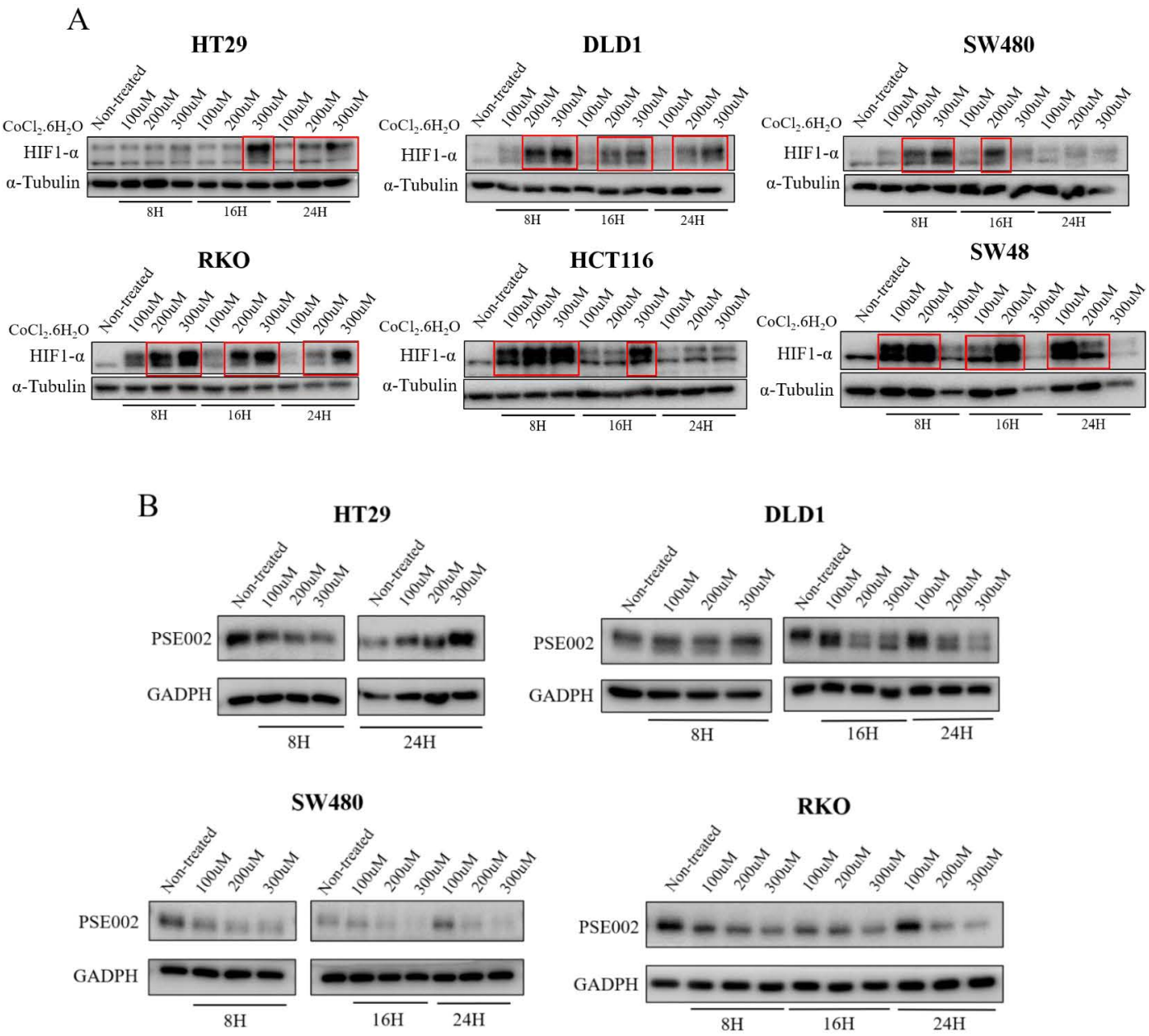
A
HT29
DLD1
SW480
RKO
HCT116
SW48
Non-treated
100uM
200uM
300uM
CoCl2.6H2O
HIF1-α
α-Tubulin
8H
16H
24H
B
PSE002
GADPH

C

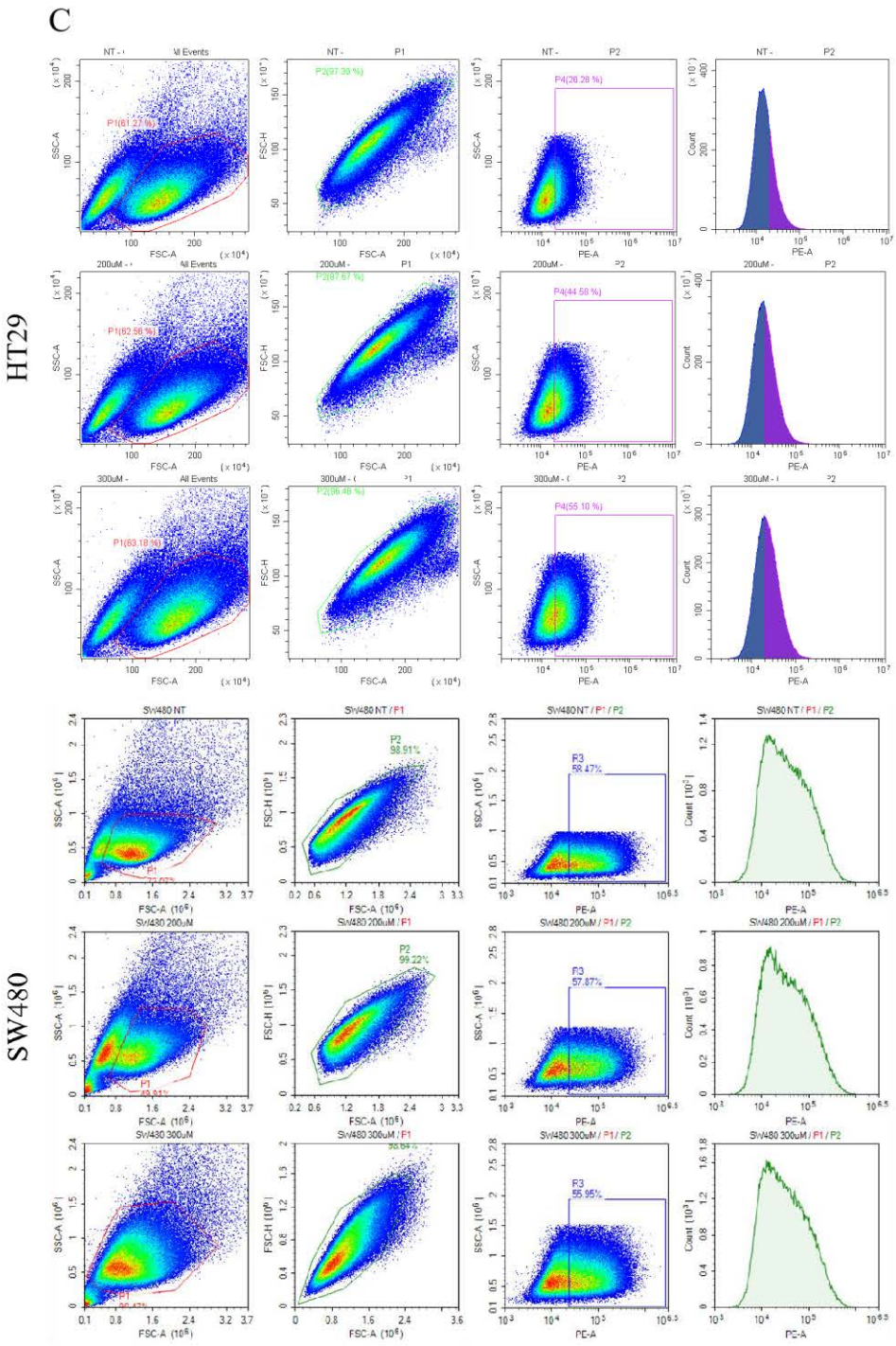
HT29
SW480
NT - All Events
NT - P1
NT - P2
200uM - All Events
200uM - P1
200uM - P2
300uM - All Events
300uM - P1
300uM - P2
SW480 NT
SW480 NT / P1
SW480 NT / P1 / P2
SW480 200uM
SW480 200uM / P1
SW480 200uM / P1 / P2
SW480 300uM
SW480 300uM / P1
SW480 300uM / P1 / P2
SSC-A
FSC-A
FSC-H
PE-A
Count

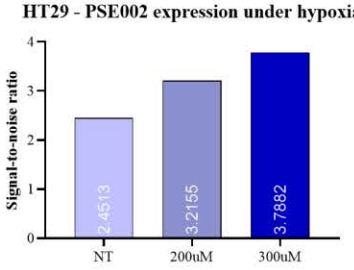
HT29 - PSE002 expression under hypoxia
Signal-to-noise ratio
2.4513
3.2155
3.7882
NT
200uM
300uM

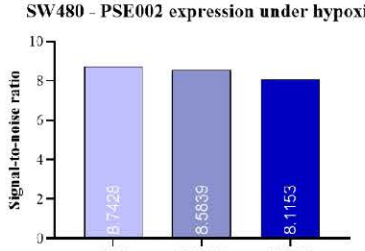
SW480 - PSE002 expression under hypoxia
Signal-to-noise ratio
8.7428
8.5839
8.1153
NT
200uM
300uM

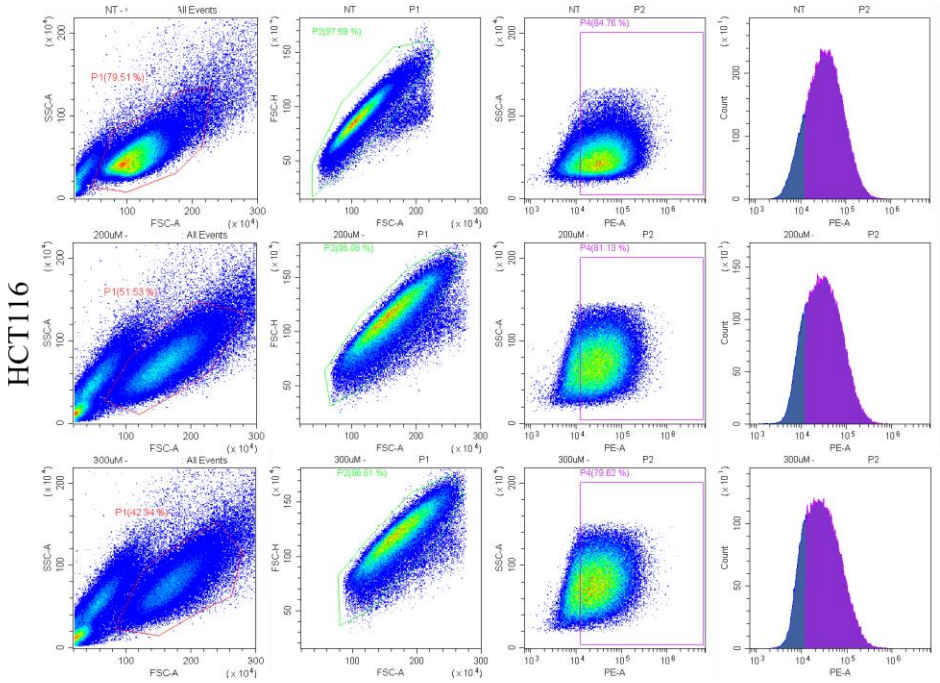
HCT116
NT
All Events
P1(79.51 %)
P2(97.69 %)
P4(84.76 %)
200uM
P1(51.53 %)
P2(85.58 %)
P4(81.13 %)
300uM
P1(42.94 %)
P2(86.81 %)
P4(79.62 %)
SSC-A
FSC-A
FSC-H
PE-A
Count

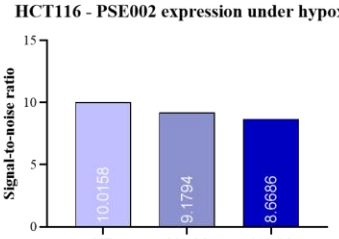
HCT116 - PSE002 expression under hypoxia
Signal-to-noise ratio
10.0158
9.1794
8.6686
NT
200uM
300uM

D

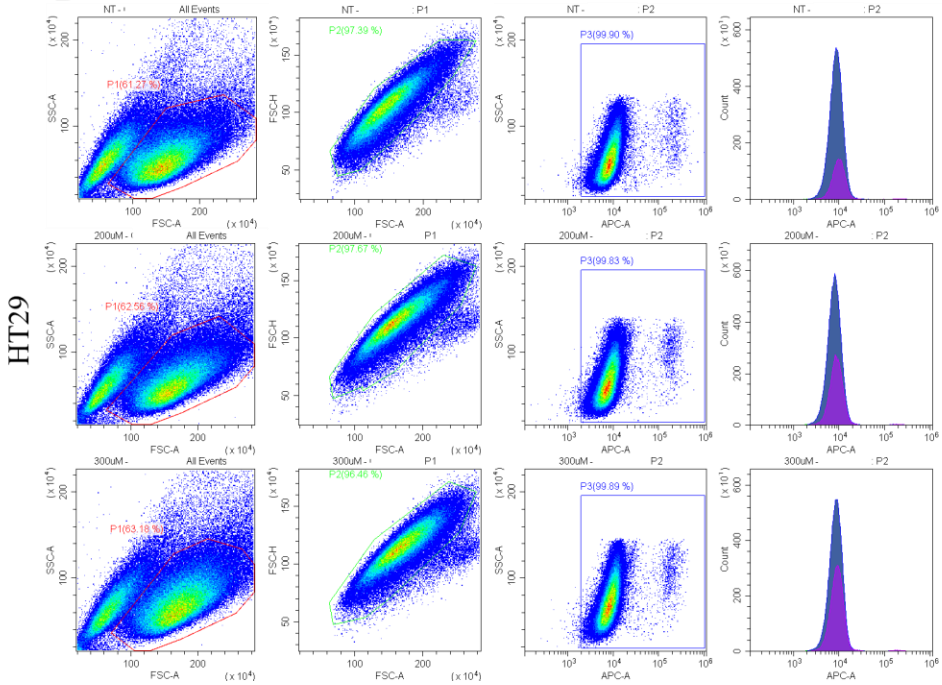
HT29
NT
All Events
P1(61.27 %)
P2(97.39 %)
P3(99.90 %)
200uM
P1(62.58 %)
P2(97.67 %)
P3(99.83 %)
300uM
P1(63.18 %)
P2(96.46 %)
P3(99.89 %)
SSC-A
FSC-A
FSC-H
APC-A
Count

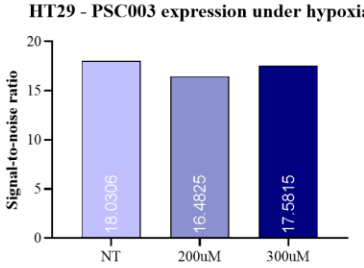
HT29 - PSC003 expression under hypoxia
Signal-to-noise ratio
18.0306
16.4825
17.5815
NT
200uM
300uM

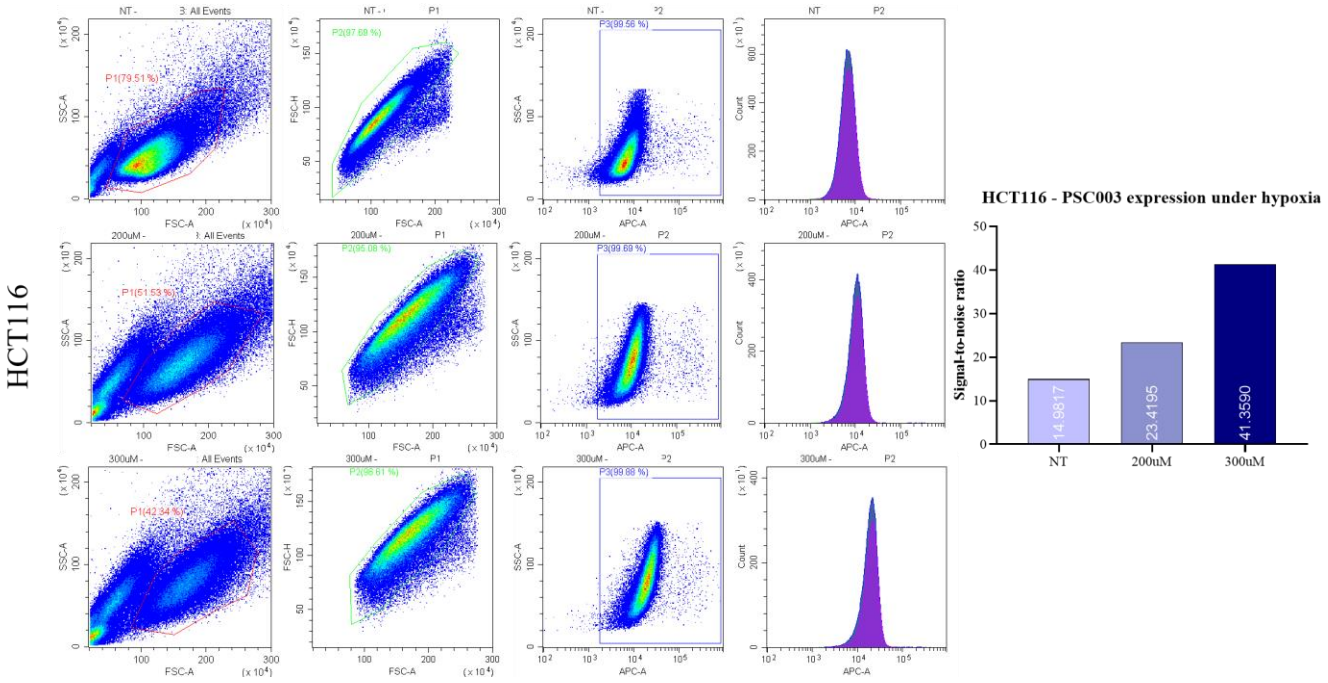

Figure 9: Hypoxia via $CoCl_2.6H_2O$ treatment changed PSE002 and PSC003 levels in colorectal cancer cell lines. (A) CRC cell lines were treated by $CoCl_2.6H_2O$ for 8 hours, 16 hours and 24 hours. Then, HIF1-α induction was detected dose-dependently. **(B), (C)** Changes in PSE002 levels were demonstrated upon $CoCl_2.6H_2O$ treatment in some of CRC cell lines. **(D)** The effect of hypoxia on PSC003 levels were observed.

3.2. The sgRNA sequences for target genes, PSE002 and PSC003, were inserted to lentiCRISPRv2 plasmid to generate CRISPR knock out constructs.

After literature and available single guide RNA (sgRNA) design tool search, we set some criteria to find the best sgRNA sequences for the target genes. First, the target genes were identified for their protein-coding transcript variants since the best depletion efficiency could be reached only if all present variants were targeted by sgRNA sequences. PSE002 was found to have 5 protein-coding variants including 3 computational variants whereas PSC003 had only one protein coding transcript. Computationally mapped potential isoforms were not included for sgRNA design. Then, we exported all the candidate sequences from available online sgRNA design tools (i.e. Horizon Dharmacon[218], Synthego[219], E-CRISP[220], CRISPR-Era[221], ChopChop[222], CRISPOR[223], Benchling[224], Deskgen[225]). Depending on their efficiency and specificity scores, top ranked ones were chosen to continue further by eliminating the

ones with high off-target scores. These off-targeted genes were further assessed by CasOFFinder[226]. The sequences with 2 or less mismatches were excluded[227] since the similarity between target sequence and off-target sequences would be too high and it would lead to increased off-target outcomes. These mismatches were further assessed for their position in the sequence and the ones which are in PAM-distant region (5' of gRNA) were preferred[227]. Also, PAM sequence was preferably chosen as 5'-CGG-3' if possible. Even if not, except sgPSC003-2, 5'-TGG-3' was avoided to be chosen as PAM sequence because thymine is disfavored by SpCas9[228]. Lastly, the sequences with 40-80% GC content were preferred. We chose the common sequences between different design tools by considering the position in the gene sequence that sgRNAs would target. Finally, we chose three sequences with the highest efficiency (Doench et al. 2016[216]) and specificity (Hsu et al. 2013[217]) scores for each gene which will also recognize the target sequence in exon 1 to disrupt whole gene sequence (Appendix H).

Next, we generated CRISPR constructs by cloning annealed oligos of sgRNA sequences into lentiCRISPRv2 plasmid which has two expression cassettes including the chimeric guide RNA (crRNA and tracrRNA), in which we cloned sgRNA sequences and created sgRNA scaffold, and hSpCas9 (Appendix I) by following Zhang et al. "Target Guide Sequence Cloning Protocol". The oligos were synthesized with some additional nucleotides at the ends for the compatibility to the digested plasmid by *BsmBI* according to the protocol[229][230] (Appendix J). After lentiCRISPRv2 plasmid was digested by *BsmBI*, it was run on agarose gel to purify vector backbone which is around 13kb from the 2kb filler sequence (Fig. 10A). Next, annealed sgRNA oligos were inserted into this vector through ligation reaction. The constructs were checked on agarose gel and sent for single-direction Sanger sequencing using hU6 forward primer to show that they were successfully cloned (Fig. 10B and 10C). Subsequently, they were used for colorectal cancer cell lines to generate knockout cell lines for the target genes.

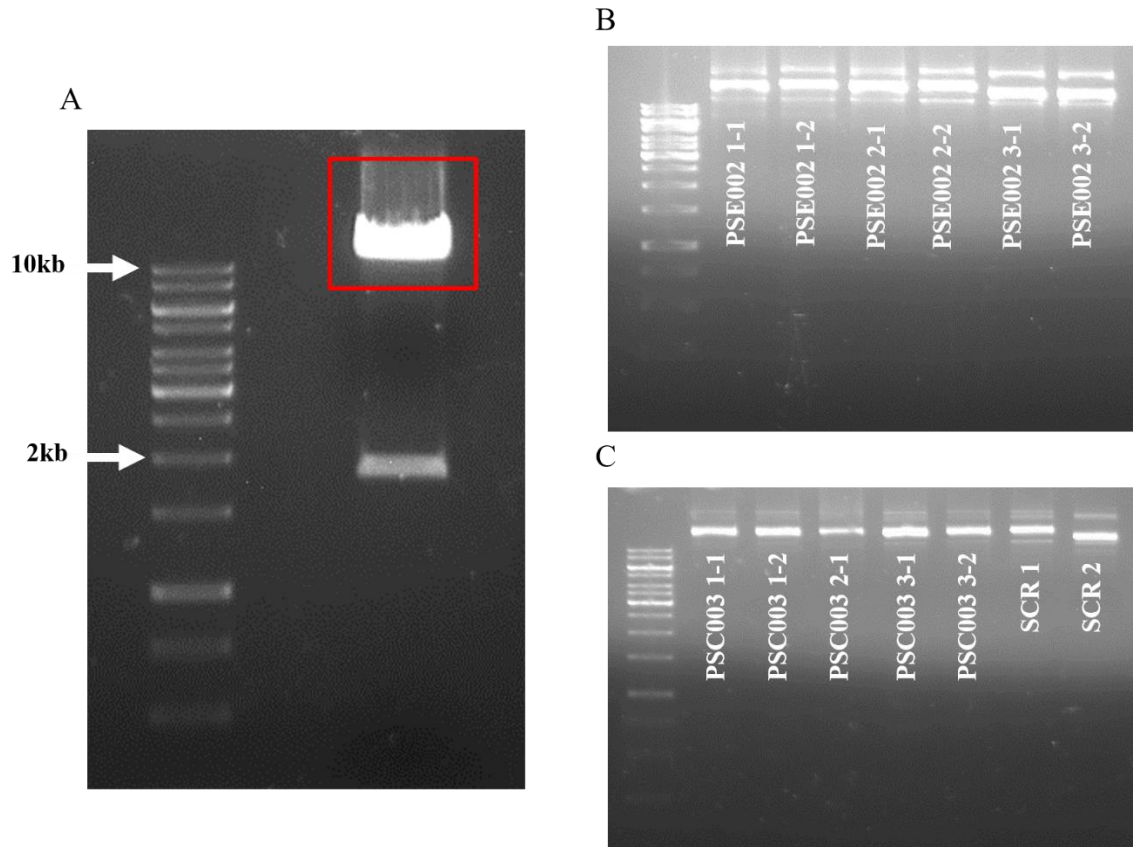

Figure 10: Cloning of sgRNA sequences into lentiCRISPRv2. (A) LentiCRISPRv2 was digested by *BsmBI* and ran on 1% agarose gel. After digestion, two fragments were appeared on the gel, 13kb vector (shown by red) and 2kb filler sequence between *BsmBI* restriction sites. 13kb fragment was extracted from the gel and used for cloning later on. **(B)** PSE002 and **(C)** PSC003, and scramble (SCR) constructs were checked for their sizes (≈13kb) on agarose gel after they were inserted in cut lentiCRISPRv2 plasmid.

3.3. PSE002 and PSC003-depleted colorectal cancer cell lines were generated by CRISPR/Cas9 expression system as well as by RNA interference.

HEK293T cells were transfected with the generated CRISPR plasmids together with packaging plasmids to produce lentiviral particles. After viral titer reached to a certain quantity, they were given to colorectal cancer cell lines to transduce them. Apart from generated stable depleted cells using CRISPR/Cas9, some of these cells were transiently depleted using siRNA constructs. The list of depleted cells for two genes by both methods is provided in Table 27. For some cell lines, depletion could be achieved by both CRISPR/Cas9 and RNAi (i.e. DLD1 and SW480 for PSE002) while some of them

could be silenced only using CRISPR/Cas9 (i.e. DLD1 and HT29 for PSC003 and HT29 for PSE002).

Table 27: The list of depleted cells by CRISPR/Cas9 and/or RNAi. *For some cell lines, depletion could be achieved by both CRISPR/Cas9 and RNAi (i.e. DLD1 and SW480 for PSE002) while some of them were silenced only using RNAi (i.e. HT29 for PSE002), which are all indicated by green color. Red color implies that the depletion was not performed on that specific cell line by the specified method.*

Cell Line	Gene			
	PSE002		PSC003	
	CRISPR	RNAi	CRISPR	RNAi
HT29				
DLD1				
HCT116				
SW480				

We could show that CRISPR constructs generated by the specified CRISPR strategy could marvelously work for PSE002 on all cell lines in which depletion was performed. The efficiency of depletion on HT29, SW480 and DLD1 could be shown at both mRNA level by qPCR and at protein level by Western blot analysis and flow cytometry (Fig. 11). In flow cytometry, PSE002-depleted cell lines have had MFI values as low as negative control which indicates unstained sample and shows the noise caused by background (Fig. 11A, 11B and 11C).

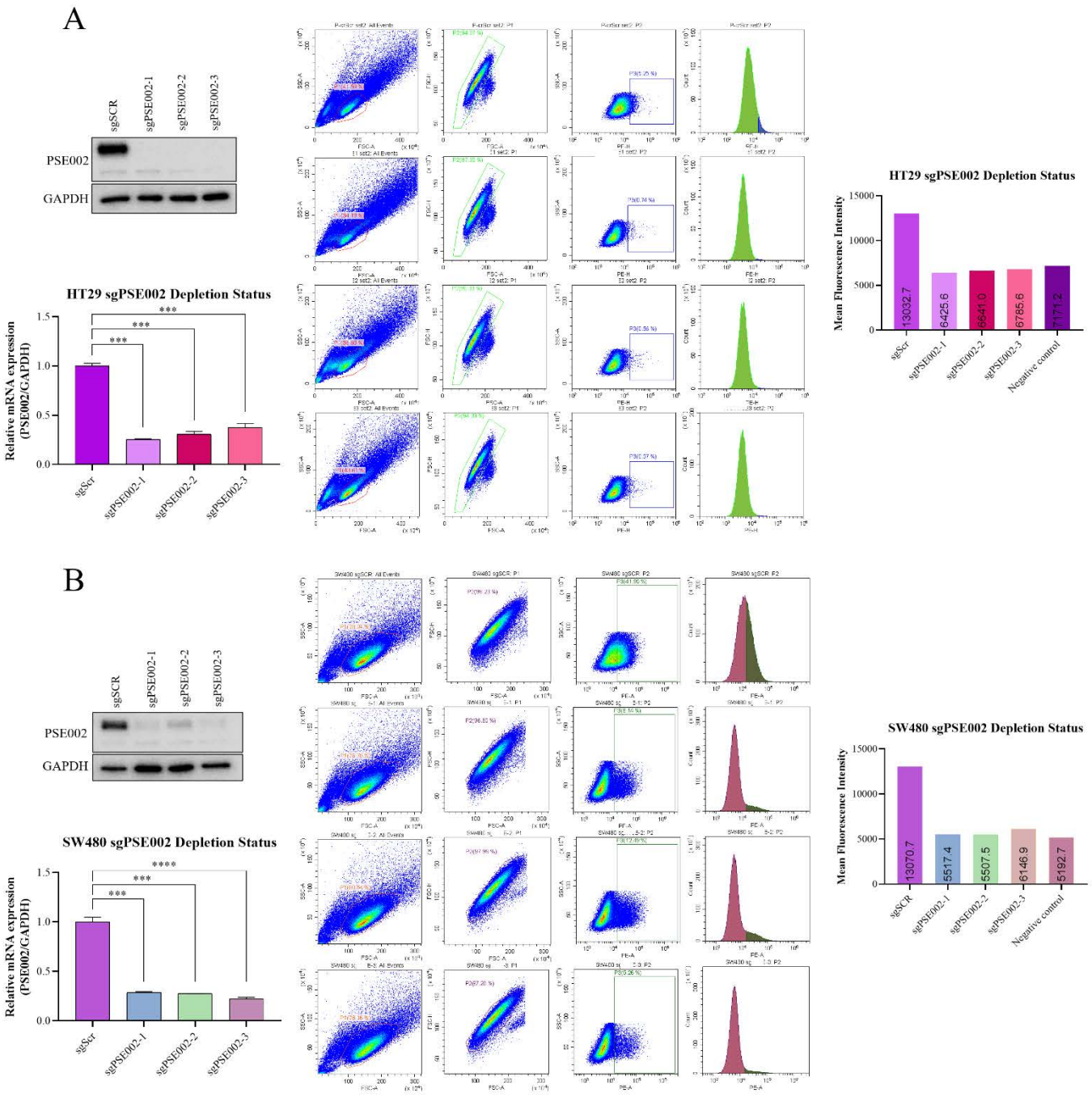
A
sgSCR
sgPSE002-1
sgPSE002-2
sgPSE002-3
PSE002
GAPDH
HT29 sgPSE002 Depletion Status
Relative mRNA expression (PSE002/GAPDH)
sgScr
sgPSE002-1
sgPSE002-2
sgPSE002-3
HT29 sgPSE002 Depletion Status
Mean Fluorescence Intensity
13032.7
6425.6
6641.0
6785.6
7171.2
Negative control
B
SW480 sgPSE002 Depletion Status
13070.7
5517.4
5507.5
6146.9
5192.7

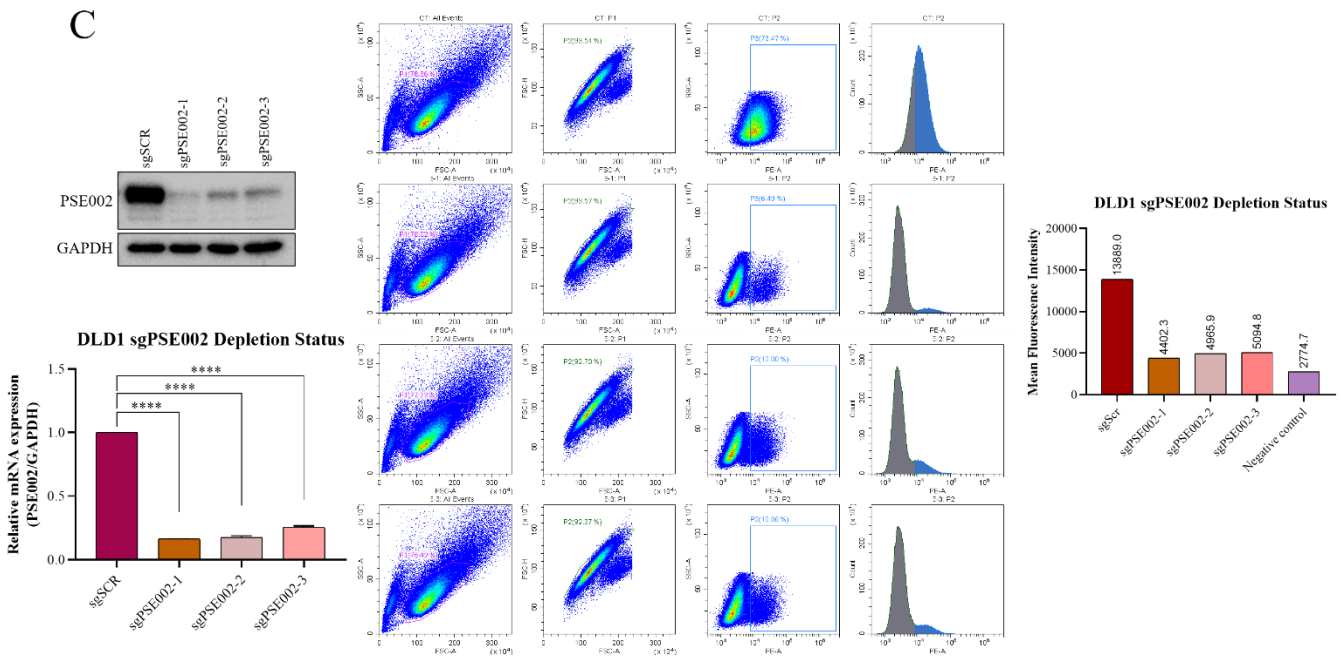

Figure 11: PSE002-depleted CRC cell lines by CRISPR/Cas9 expression system. Silencing of PSE002 gene in **(A)** HT29, **(B)** SW480, and **(C)** DLD1 was successfully done and the depletion statuses were shown by qPCR, Western blot (WB) and flow cytometry. Negative control is unstained sample and shows background. For each cell line, the first row in flow cytometry results is representing control cells (sgSCR). Then, the results for sgPSE002-1, sgPSE002-2, and sgPSE002-3 are shown, respectively. GAPDH was used as internal control for both WB and qPCR analyses. (*Ordinary one-way ANOVA, *** p=0.0001, **** p<0.0001)*

Transiently depleted DLD1 and SW480 CRC cell lines for PSE002 were also successfully generated by RNAi and the depletion efficiency was shown at mRNA and protein level (Fig. 12).

A

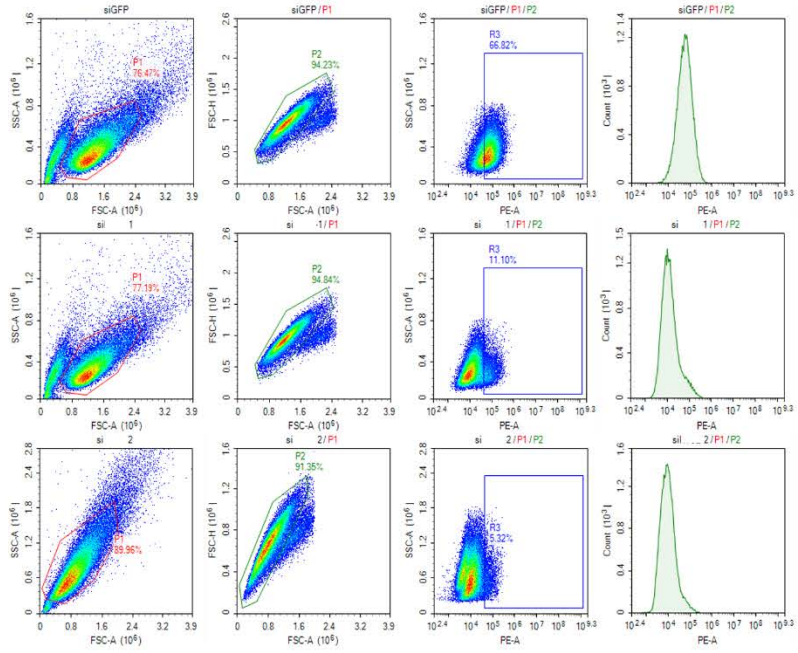
siGFP
siGFP/P1
siGFP/P1/P2
P1
76.47%
P2
94.23%
R3
66.82%
si 1
si 1/P1
si 1/P1/P2
P1
77.19%
P2
94.84%
R3
11.10%
si 2
si 2/P1
si 2/P1/P2
P2
91.35%
R3
5.32%
SSC-A (10⁴)
FSC-A (10⁶)
FSC-H (10⁶)
PE-A
Count (10³)

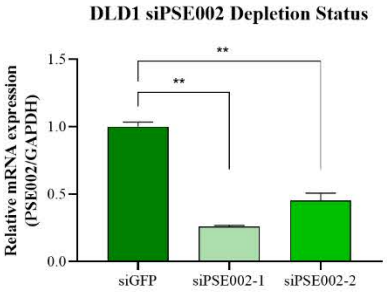
DLD1 siPSE002 Depletion Status
Relative mRNA expression (PSE002/GAPDH)
1.5
1.0
0.5
0.0
**
**
siGFP
siPSE002-1
siPSE002-2

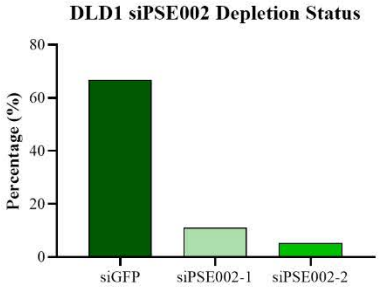
DLD1 siPSE002 Depletion Status
Percentage (%)
80
60
40
20
0
siGFP
siPSE002-1
siPSE002-2

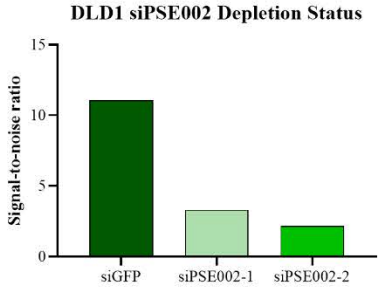
DLD1 siPSE002 Depletion Status
Signal-to-noise ratio
15
10
5
0
siGFP
siPSE002-1
siPSE002-2

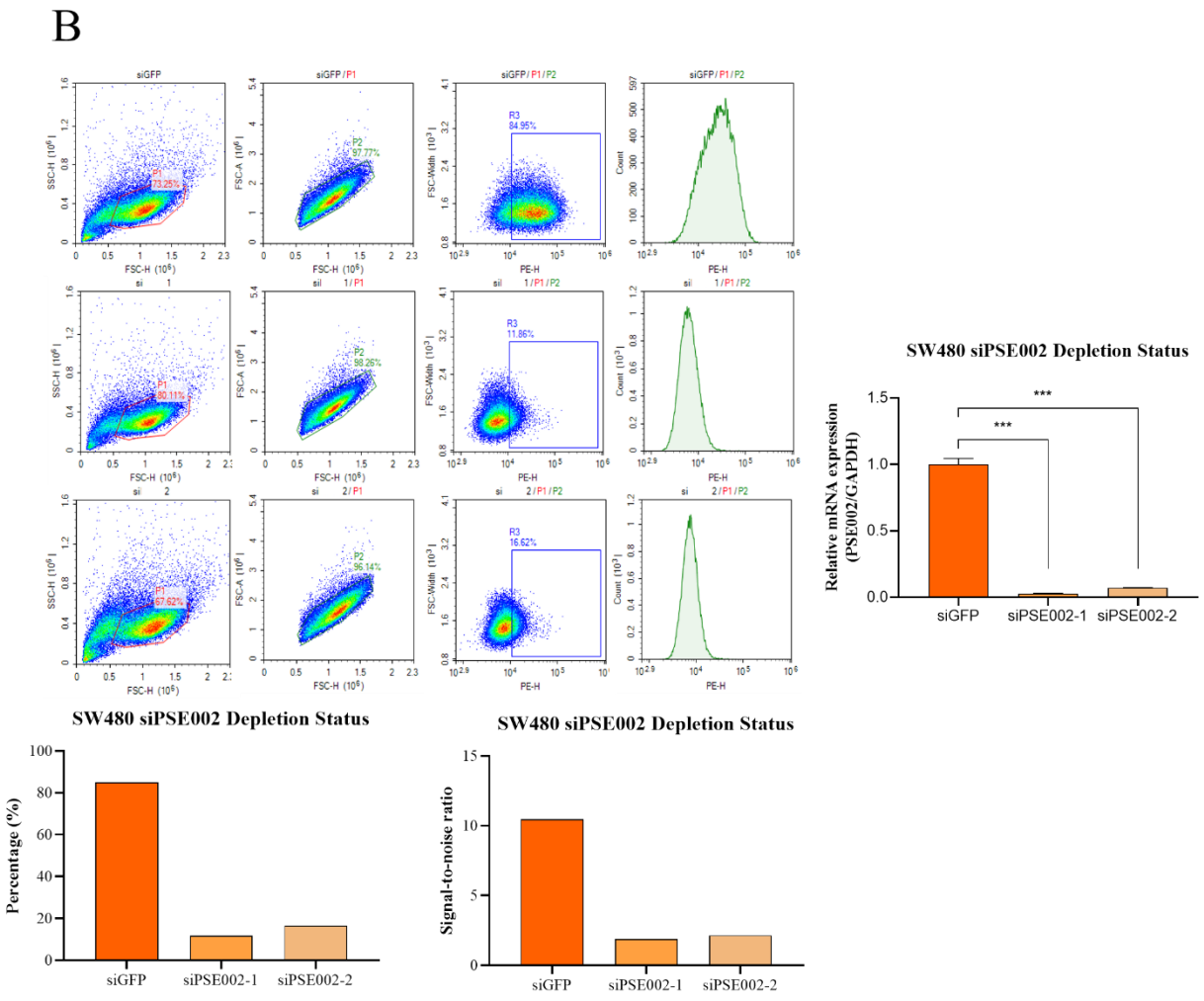

Figure 12: PSE002-depleted CRC cell lines by RNAi. Transiently suppression of PSE002 was shown in **(A)** DLD1, and **(B)** SW480 colorectal cancer cell lines both at mRNA level and protein level. For each cell line, the first row in flow cytometry results is representing control cells (siGFP). Then, the results for siPSE002-1 and siPSE002-2 are shown, respectively. GAPDH was used as internal control in qPCR analyses. *(Ordinary one-way ANOVA, ** p=0.0013, *** p=0.0002)*

On the other hand, PSC003 was challenging to suppress as its expression level is extremely high in CRC cell lines. Most of the attempts by both CRISPR/Cas9 and RNAi resulted in low depletion efficiency (data not shown). Therefore, we performed single cell cloning on HT29 sgPSC003 and DLD1 sgPSC003 cell lines to obtain homogeneous depleted population originated from one single cell and ultimately to improve depletion efficacy. After isolating single cells from the pool by serial dilutions, they were grown in culture until they form their colonies (Fig. 13A). Next, we performed screening for PSC003 expression on these single cell-derived colonies at mRNA and protein level (Fig. 13B and 13C). As expected, PSC003 mRNA and protein levels for individual colonies of HT29 sgPSC003 significantly varied in all the constructs. Some colonies had extremely low PSC003 expression whereas some of them showed higher expression even than control cells (sgSCR) which explains the low depletion efficiency in pool cells. Finally, we chose the best depleted two colonies from each construct to perform *in vitro* assays, which are 112A2 and 121A2 for sgPSC003-1, 231A1 and 231A3 for sgPSC003-2, and 334A1 and 334A3 for sgPSC003-3 (Fig. 13C, last panel). In these colonies, it can be seen that upper band, which is the correct protein size, completely disappeared.

Similar to HT29 sgPSC003, the colonies derived from DLD1 sgPSC003 cells were firstly screened at mRNA level. Then, we defined the potential colonies to be confirmed also in protein level before using in *in vitro* analyses (Fig. 13D). These colonies were namely DA11D6 and DA12G2 for DLD1 sgPSC003-1, DA21H2 for DLD1 sgPSC003-2, and DA31E6 and DA32C10 for DLD1 sgPSC003-3. We checked PSC003 protein level of these single cell-derived colonies by Western blot and could show that depletion efficiency could be improved using single cell cloning.

A

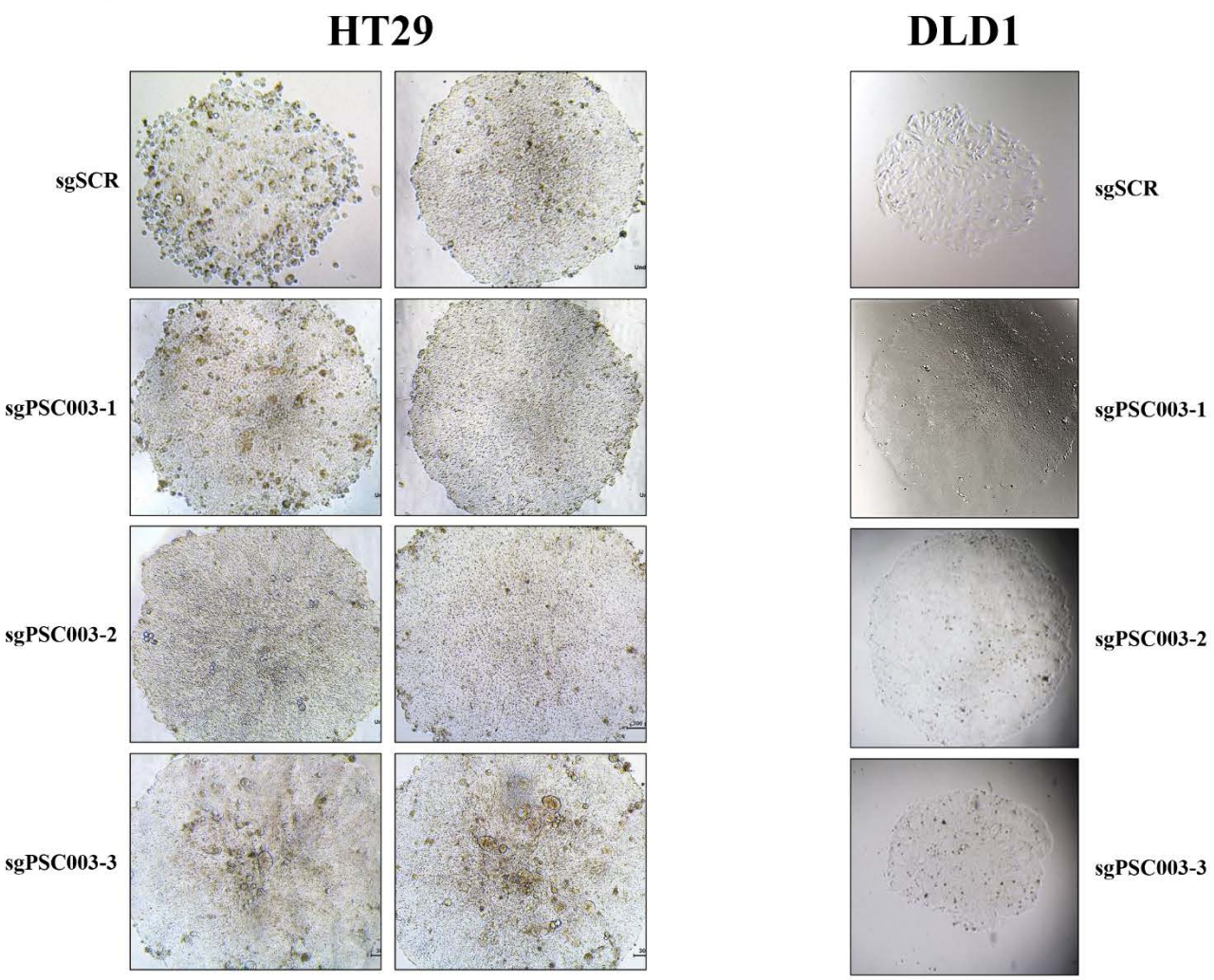
HT29
DLD1
sgSCR
sgPSC003-1
sgPSC003-2
sgPSC003-3
sgSCR
sgPSC003-1
sgPSC003-2
sgPSC003-3

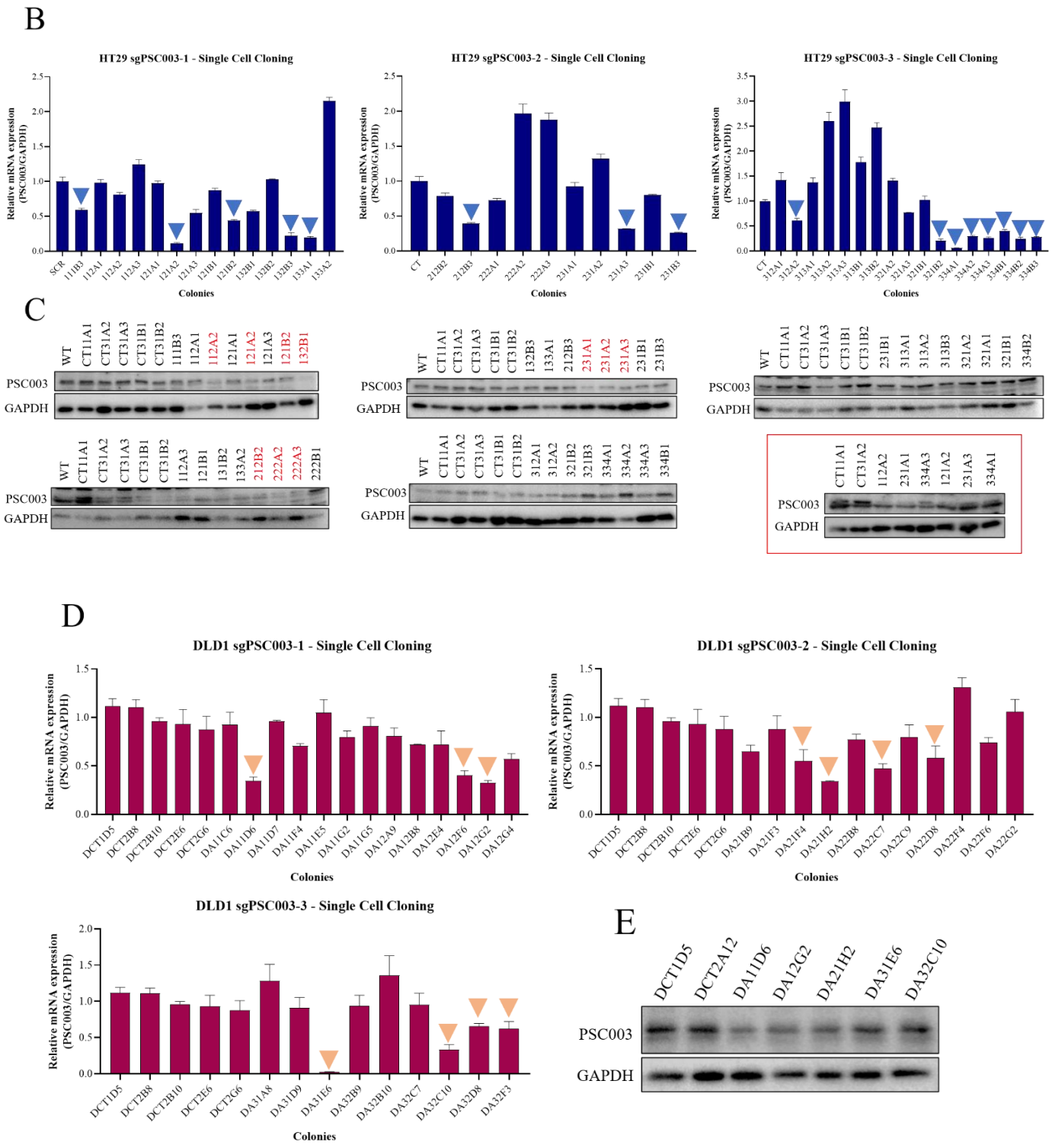

Figure 13: Single cell cloning on PSC003-depleted cell lines. (A) Individual colonies formed by isolated single cells from the pool of PSC003-depleted HT29 and DLD1 were observed under inverted microscope. **(B)** The colonies isolated from HT29 sgPSC003-1, sgPSC003-2, and sgPSC003-3 pool cells were screened for PSC003 expression at mRNA

level. The colonies with better depletion efficiency are marked with blue arrow. **(C)** The colonies were also screened by Western blot for their protein expression. The candidate colonies to be continued with are marked as red. Finally, the chosen colonies are shown in the last panel with red frame. **(D)** PSC003 mRNA level of DLD1 sgPSC003 colonies were shown by qPCR. The potential colonies to be used for *in vitro* analyses are shown by arrows. **(E)** The PSC003 level of potential single cell-derived colonies belonging to DLD1 sgPSC003 cells was checked at protein level.

3.4. The effects of PSE002 loss in colorectal cancer cell lines

3.4.1. Cell proliferation and colony-forming ability of cells were advanced *in vitro* upon PSE002 depletion.

After the cells were depleted by either CRISPR/Cas9 or RNAi and their depletion status were checked, we seeded the cells in a certain number and performed cell proliferation assays by quantifying their growth every day over 3-4 days using CellTiter-Glo® Luminescent Cell Viability Reagent (CTG) which determines the number of metabolically active cells by quantifying ATP concentration or WST1 Cell Proliferation Reagent that quantifies formazan dye produced by metabolically active cells. Then, we calculated their fold change at the defined time points. We demonstrated that the loss of PSE002 resulted in augmented cell proliferation and significantly promoted cancer cell growth in HT29 (Fig. 14A), DLD1 (Fig. 14B), and SW480 (Fig. 14C) cell lines.

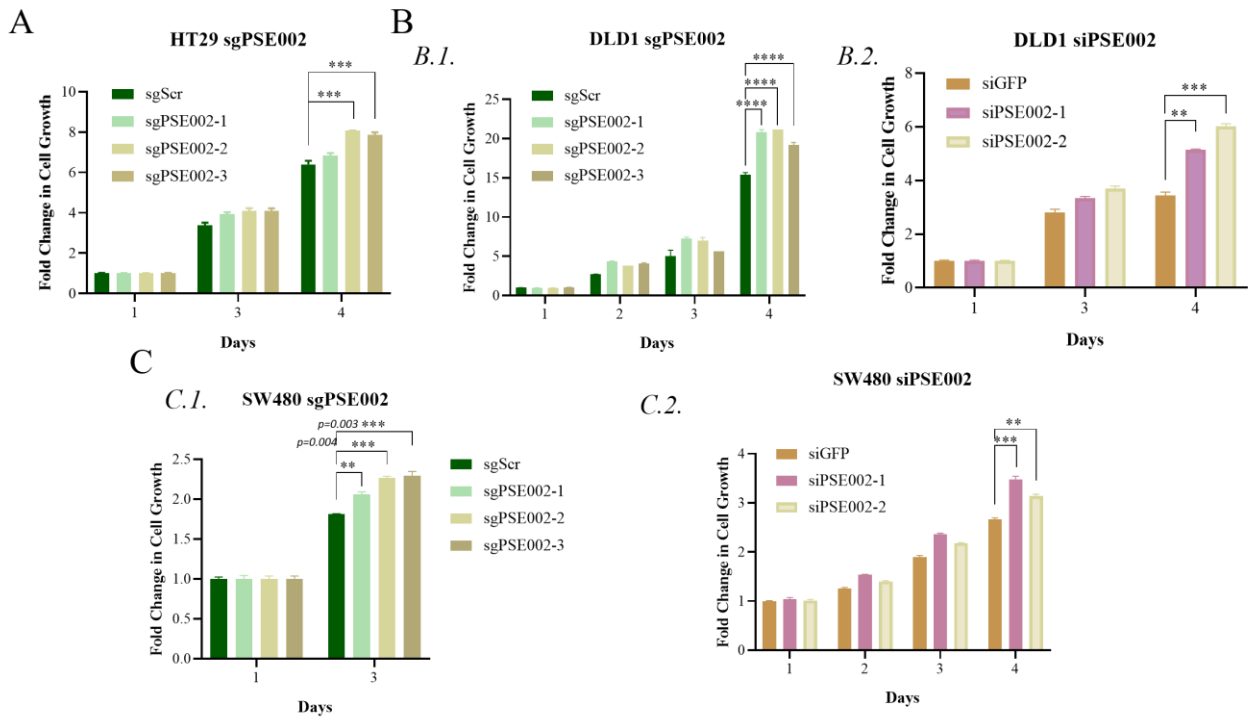

Figure 14: Cell growth was enhanced upon PSE002 depletion. Cell proliferation was measured on CRISPR/Cas9 or RNAi-depleted cells at the specified time points by CellTiter® Glo Cell Viability Reagent. **(A)** HT29 sgPSE002 *(n=3)* **(B)** *(B.1.)* DLD1 sgPSE002 and *(B.2.)* DLD1 siPSE002 **(C)** *(C.1.)* SW480 sgPSE002 *(n=2)* and *(C.2.)* SW480 siPSE002. *(n: biological replicates; Ordinary one-way ANOVA, ** p=0.0017, *** p=0.0005, **** p<0.0001)*

Next, we performed clonogenic assay to assess the ability of PSE002-depleted cell lines to grow into colonies from a single cell. For this purpose, we seeded the cells in 6-well or 12-well plates in a smaller number (300-500 cells/mL in 6-well, 100-150 cells/mL) to be able to observe single cells growing. Then, we followed their growth for at least following 14 days and finalized the assays by staining the colonies with 0.5% crystal violet. We could show that PSE002 depletion provided more ability to the cells to form colonies in HT29 (Fig. 15A), and in SW480 (Fig. 15B). Ultimately, we concluded that PSE002 has cell growth-inhibiting effect on colorectal cancer cell lines and its depletion leads to increased cell proliferation capacity.

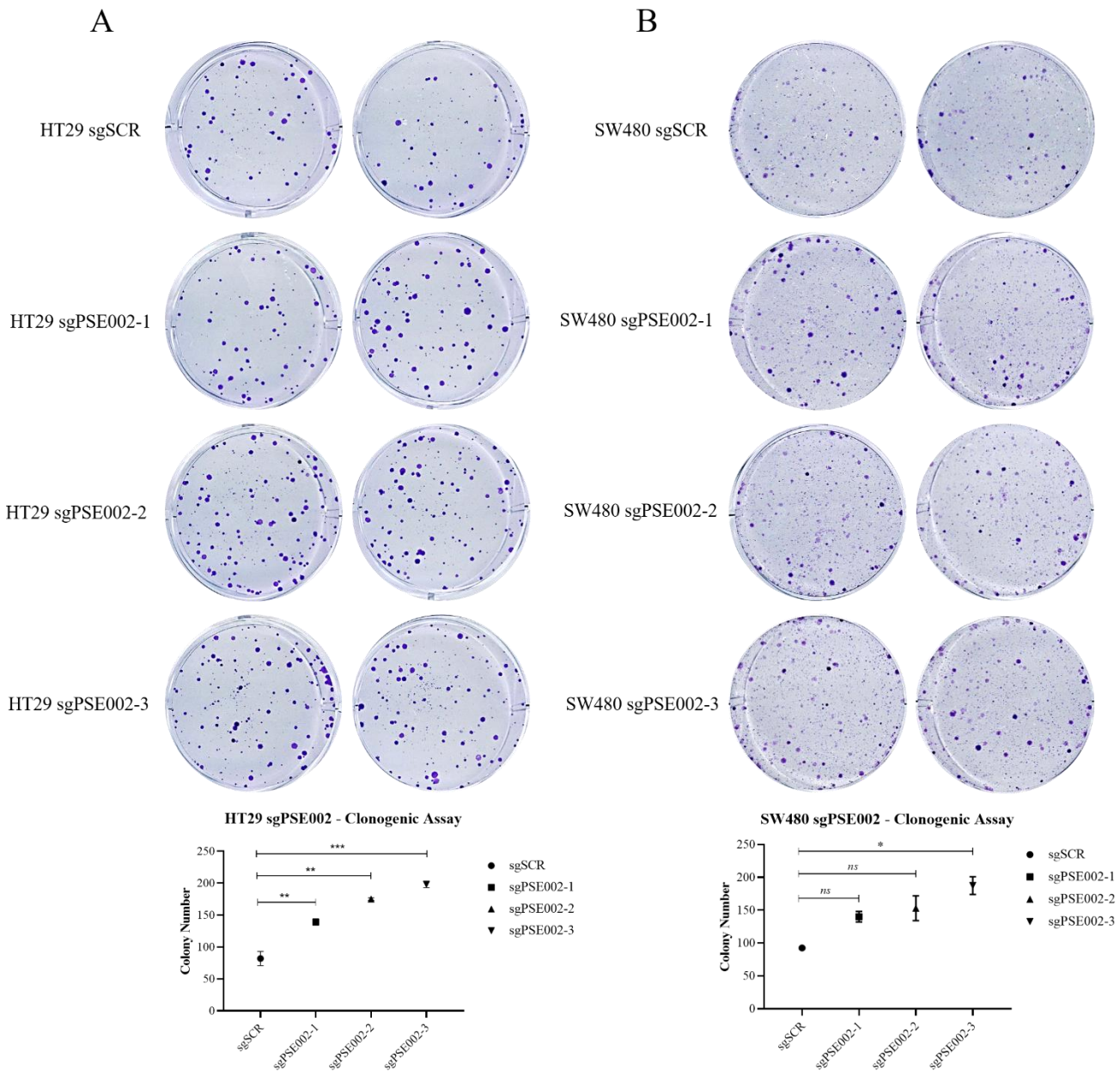

Figure 15: Colony-forming ability of cells were increased on PSE002-depleted CRC cell lines. Clonogenic assay was performed to assess colony-forming ability in **(A)** HT29 sgPSE002 *(n=2)* and **(B)** SW480 sgPSE002 *(n=2).* After colonies reached to a certain size, they were stained by crystal violet and quantified by Colony Counter. *(n: biological replicates; Ordinary one-way ANOVA, * p=0.0127, ** p=0.0013, *** p=0.0006)*

3.4.2. PSE002-depleted cells had more capacity to grow anchorage-independently *in vitro*.

We assessed the ability of cells to grow independently of a surface that they can attach. For this purpose, we coated plates with a hydrogel called polyHEMA to prevent cellular attachment and conducted polyHEMA assay in which we observed them growing into colonies without spreading and measured their growth every 2 days by lysing them with CellTiter-Glo 3D Cell Viability Assay Reagent over 5-7 days. The cells were not seen in their usual morphology as expected, since they grew anchorage independently (Fig. 16). The control cells could not grow into as many colonies as depleted cells form. Also, PSE002 depleted cells could form colonies in greater sizes. Therefore, the loss of PSE002 in colorectal cancer cell lines, HT29 (Fig. 16A), DLD1 (Fig. 16B), and SW480 (Fig. 16C and 16D), caused advanced anchorage-independent growth.

A

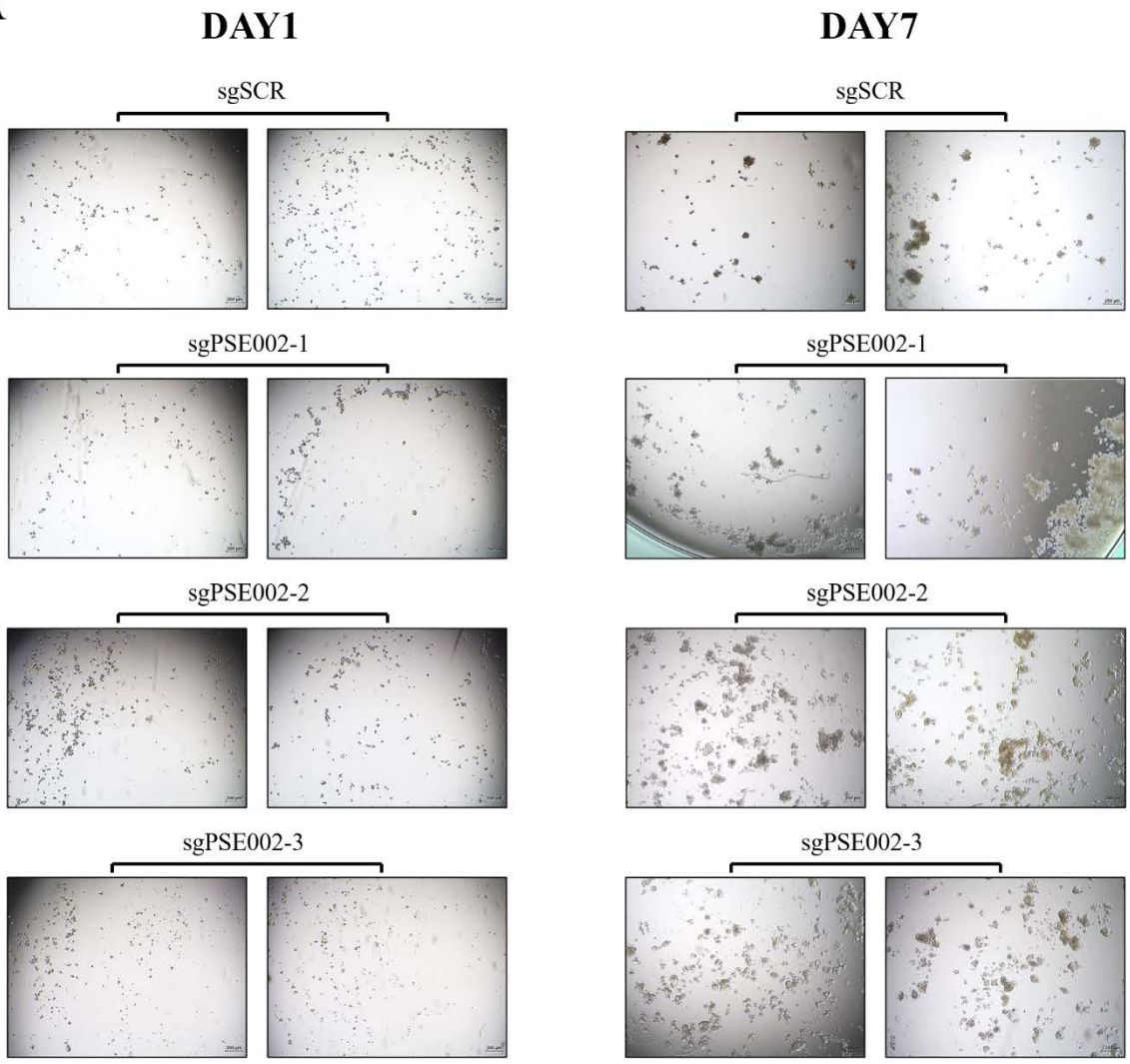
DAY1
DAY7
sgSCR
sgPSE002-1
sgPSE002-2
sgPSE002-3

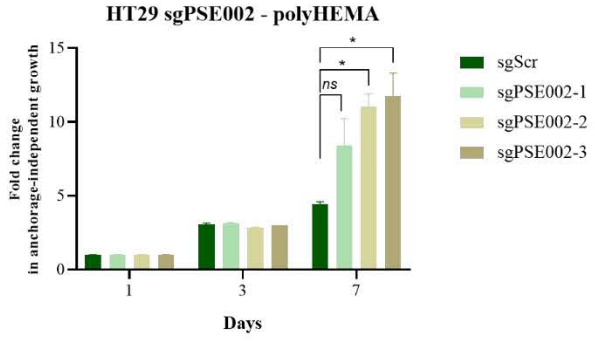
HT29 sgPSE002 - polyHEMA
Fold change in anchorage-independent growth
15
10
5
0
1
3
7
Days
ns
*
*
sgScr
sgPSE002-1
sgPSE002-2
sgPSE002-3

B

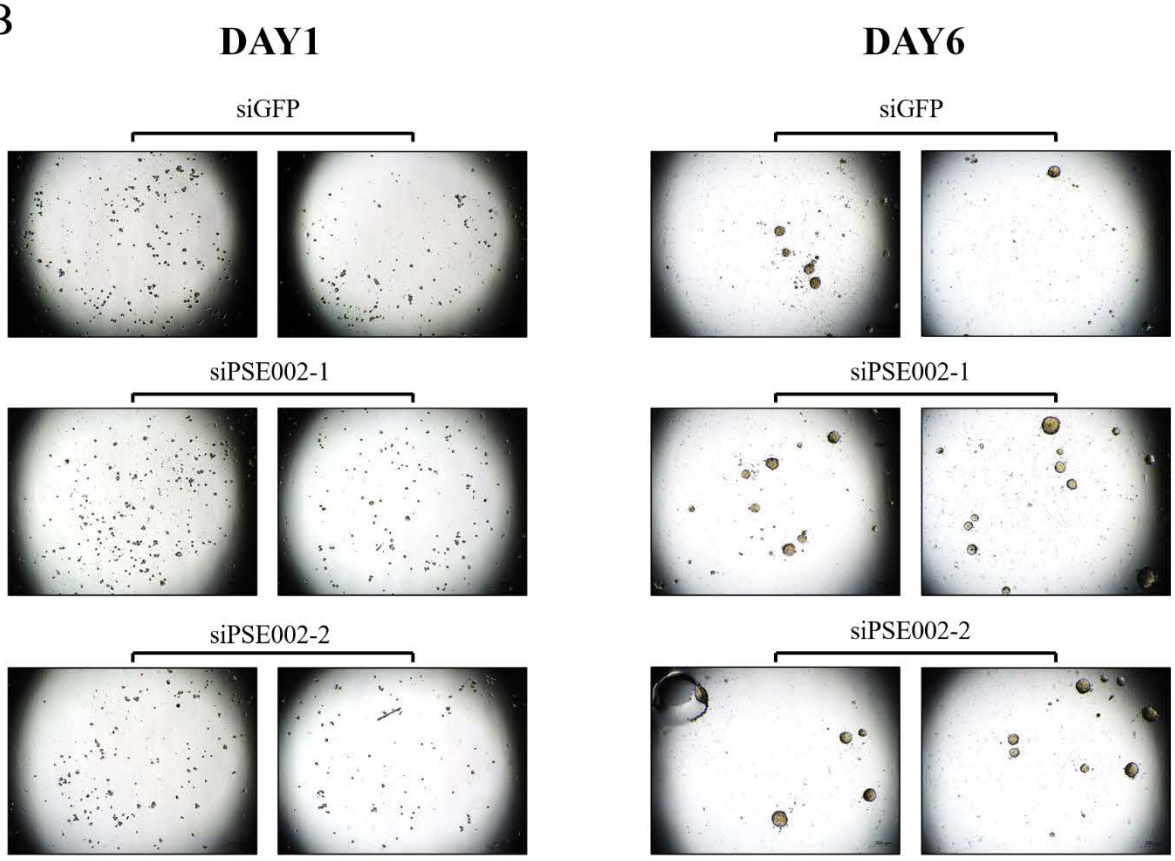
DAY1
DAY6
siGFP
siGFP
siPSE002-1
siPSE002-1
siPSE002-2
siPSE002-2

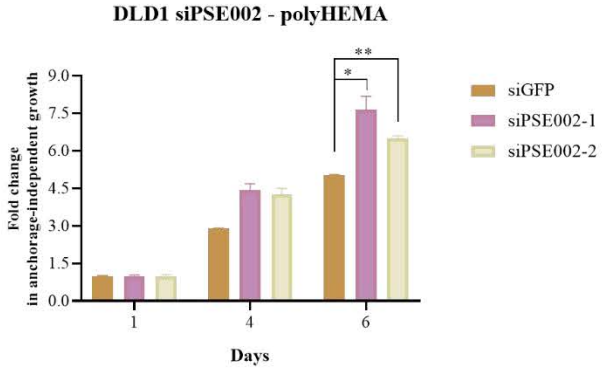
DLD1 siPSE002 - polyHEMA
Fold change in anchorage-independent growth
9.0
7.5
6.0
4.5
3.0
1.5
0.0
1
4
6
Days
**
*
siGFP
siPSE002-1
siPSE002-2

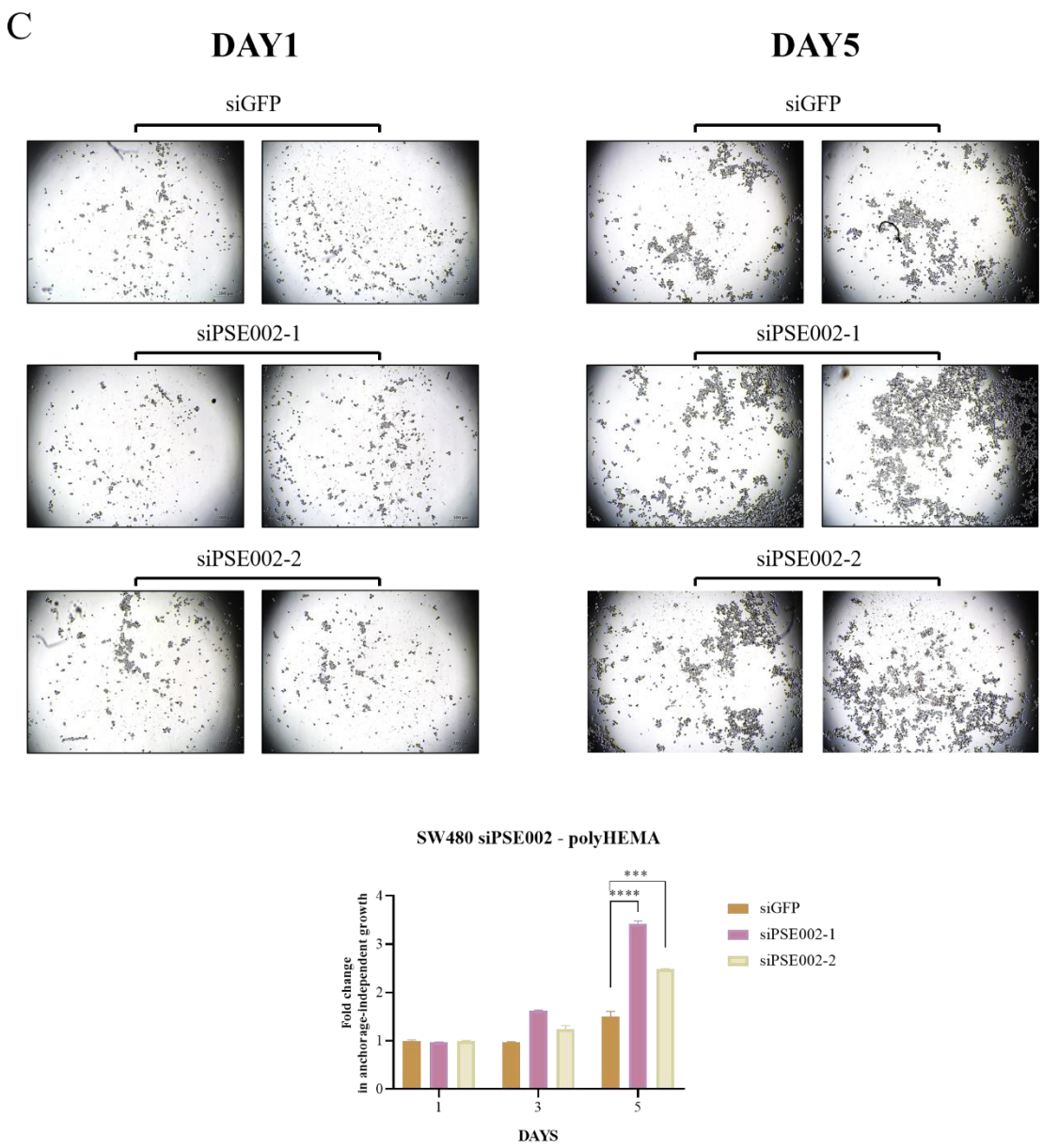

Figure 16: PSE002 loss led to advanced anchorage-independent growth. Representative pictures for **(A)** HT29 sgPSE002 *(n=2)* **(B)** DLD1 siPSE002 **(C)** SW480 siPSE002 are shown in the upper panel. Their quantification was performed by lysing them with CellTiter Glo® 3D Cell Viability Reagent and taking luminescence reading. *(n: biological replicates; Ordinary one-way ANOVA, * p=0.0284, ** p=0.0056, *** p=0.0010, **** p<0.0001)*

3.4.3. Cell line-derived xenograft models showed promoted tumor growth upon PSE002 knockout.

We generated cell line-derived xenograft models (CDX) by injecting HT29 sgPSE002 and SW480 sgPSE002 cell lines in the subcutaneous region of athymic mice to demonstrate the role of PSE002 *in vivo*. We observed their weight change and followed increase in tumor volumes every 3 days over the specified time. HT29 sgPSE002-transplanted mice developed much greater tumors than control mice as seen in representative images (Fig. 17A). It was finalized when one of the tumor volumes reached to approximately 2000 mm^3. At the end of 60 days, PSE002-depleted cell line-derived xenografts formed bigger tumors by 2-2.5-fold than control cells in HT29 (Fig. 17A). These results were confirmed in another CDX model with the second cell line, SW480 (Fig. 17B).

A

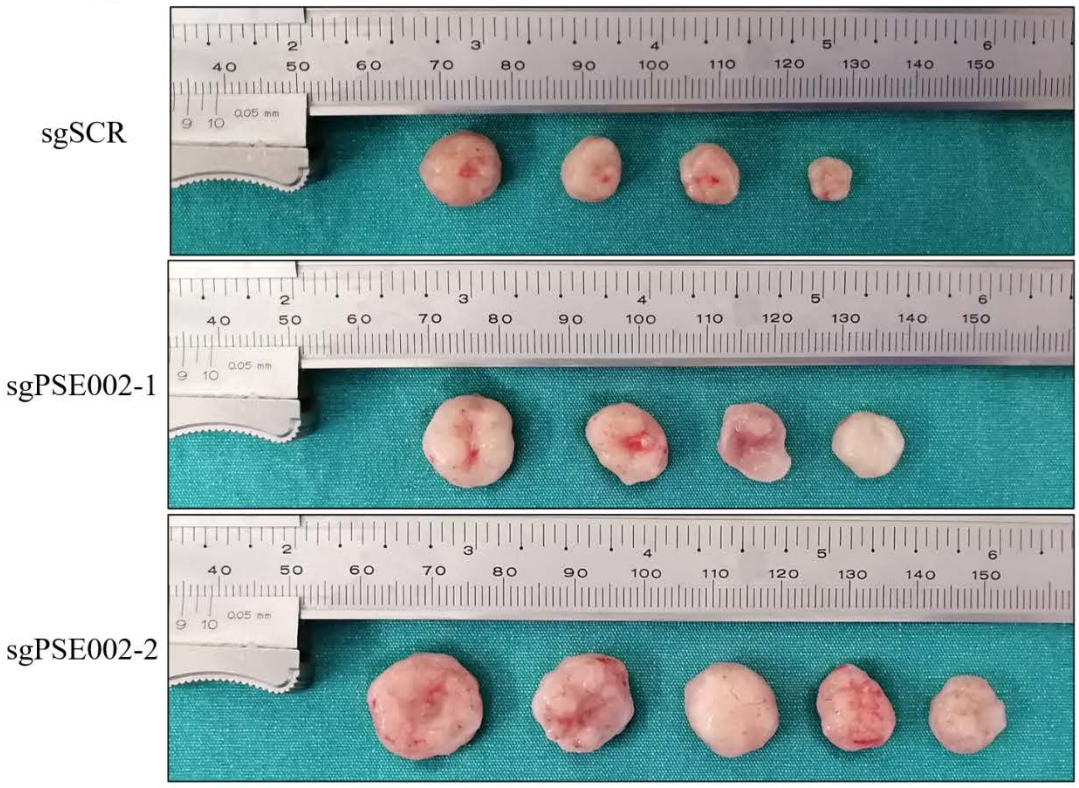

HT29 sgPSE002 - Xenograft

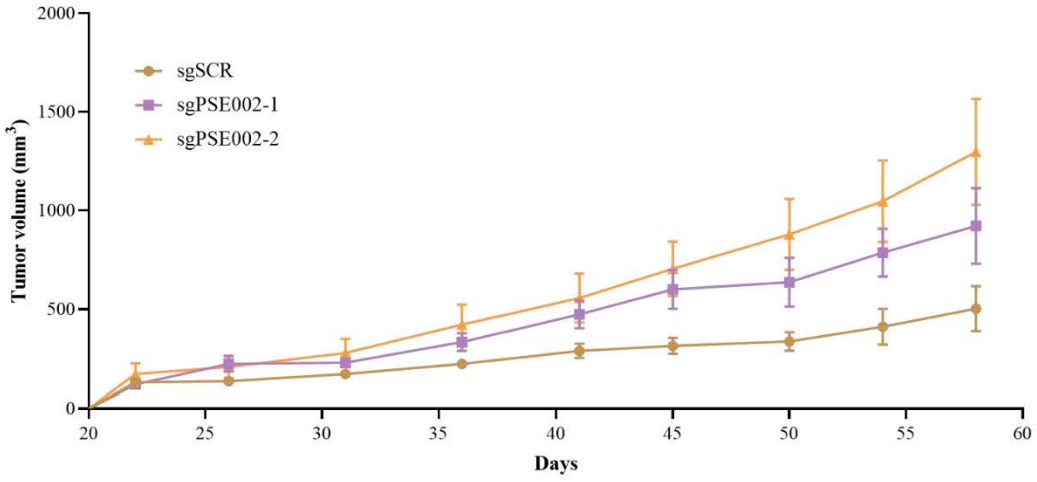

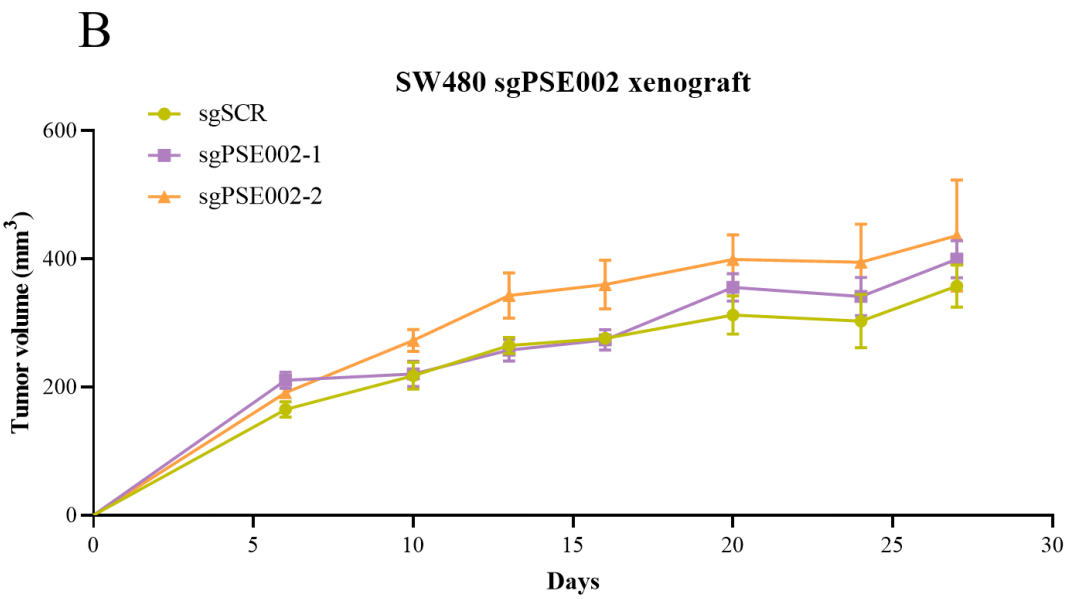

Figure 17: Depletion of PSE002 promoted tumor growth *in vivo*. Tumor volumes were measured over the time in **(A)** HT29 sgPSE002 and **(B)** SW480 sgPSE002. Tumor volumes were calculated using the following equation: $(L*W^2)/2$. *L: length, W: width*

3.4.4. Migration of colorectal cancer cell lines was enhanced in the absence of PSE002 expression.

In the line with the findings about colorectal cancer cells becoming more proliferative, we questioned whether or not their migratory abilities were affected by PSE002 loss. Therefore, we conducted wound healing assay by creating a gap between the cells. Then, we took pictures of each gap at the beginning which is stated as 0 hour (Fig. 18) and observed them during the time they gradually closed the gap. We also captured the gaps at the end point to compare with the gap sizes when they were created . Then, the differences between gap closures were quantified by TScratch. Representative pictures are provided in the starting (0h) and the end points, 7 days for HT29 sgPSE002 (Fig. 18A) and 48 hours for SW480 sgPSE002 (Fig. 18B). As a conclusion, we demonstrated that PSE002-depleted cells could migrate faster and closed the gap before control cells.

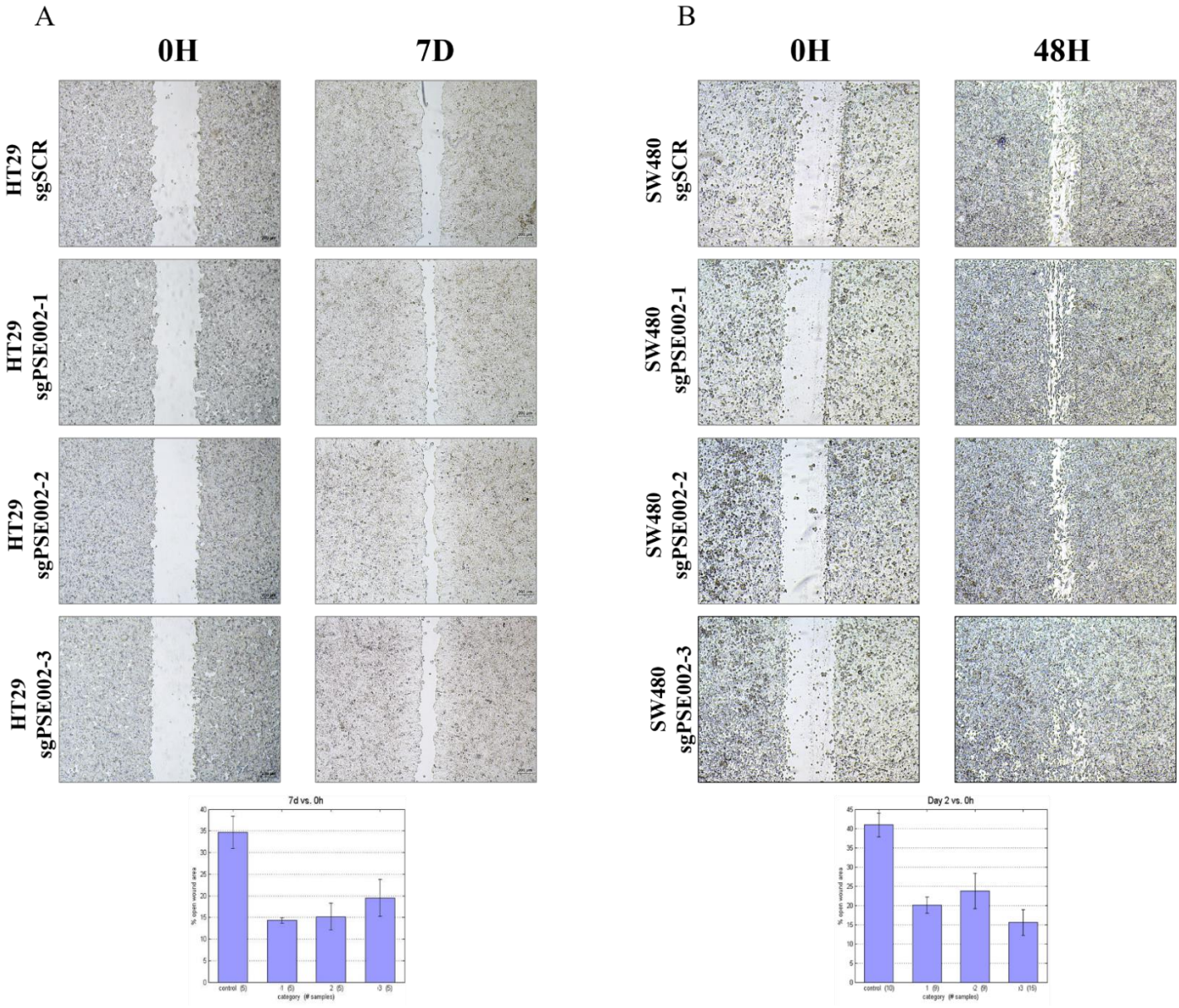

Figure 18: PSE002-depleted cell lines migrated with higher rate compared to control cells. Wound healing assay was conducted to assess the migration ability of **(A)** HT29 sgPSE002, and **(B)** SW480 sgPSE002. Their representative pictures are provided in the upper panel.

3.4.5. Loss of PSE002 promoted epithelial-to-mesenchymal transition in colorectal cancer cell lines.

After checking their proliferative capacity and migration ability, we showed molecular changes at mRNA and protein level. In HT29 colorectal cancer cell line, PSE002 loss resulted in induced EMT. These cells showed slightly decrease in epithelial markers including CDH1, ZO1, and Claudin-7 while mesenchymal markers such as vimentin and ZEB1 were increased and some of them including CDH2, ZEB2, and Twist were found to be significantly augmented at mRNA level (Fig. 19A). Similarly, upregulation of mesenchymal markers including integrin α5, N-cadherin, ZEB1 and α-smooth muscle actin (α-SMA) was seen in addition to the decline in epithelial marker E-cadherin, a fundamental component of epithelial cell-cell junctions, at protein level (Fig. 19B). Interestingly, ERK1/2 and AKT phosphorylation were considerably enhanced upon PSE002 depletion whereas total expression of these proteins did not change. Similarly, SW480 colorectal cancer cell line demonstrated the same effect as HT29 by attenuating E-cadherin level and enhancing the level of vimentin and a-SMA upon PSE002 depletion (Fig. 19C). Induced AKT phosphorylation was also observed in these cells.

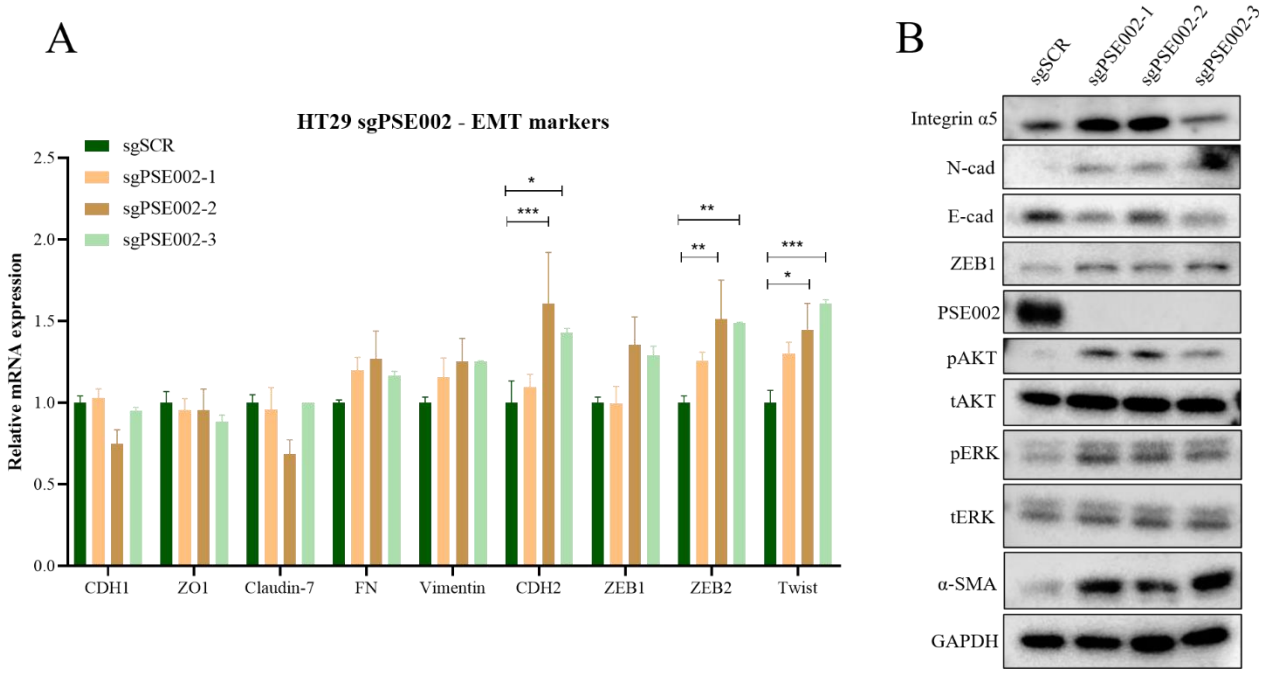

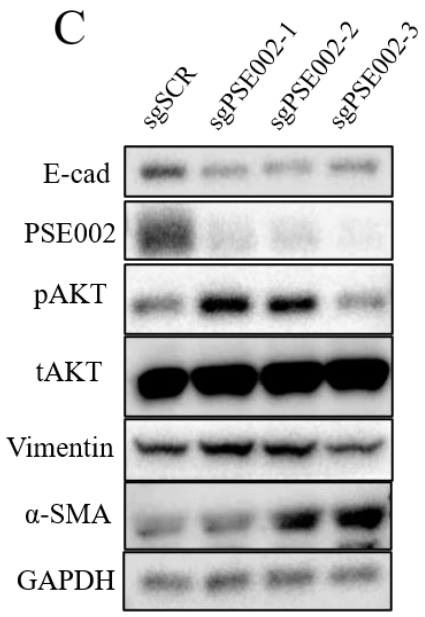

Figure 19: PSE002 knockout cell lines promoted EMT. EMT markers were checked on HT29 sgPSE002 cells at **(A)** mRNA and **(B)** protein level. (* *p=0.0139*, ** *p=0.0045*, *** *p=0.0008)* **(C)** The changes in EMT markers were also observed in SW480 sgPSE002.

3.4.6. Enzymatic activity of PSE002 was not directly responsible for the effects on cell proliferation of colorectal cancer cell lines.

PSE002 knockout colorectal cancer cell lines tended to be more proliferative and thus showed tumor-promoting effects as mentioned earlier. We questioned whether or not we could prove these effects by pharmacological inhibitors. Therefore, we used non-hydrolyzable ADP analog, PSE002-selective antagonist, which binds to the active site and blocks catalytic activity of PSE002. HT29 was treated with PSE002-selective antagonist in a wide range of concentrations (10µM-1mM) for 4 days and then, the cell proliferation was measured by sulforhodamine B assay (SRB). Interestingly, PSE002-selective antagonist treatment on HT29 did not cause any change in cell growth (Fig. 20A). Next, we repeated the same treatment on two more CRC cell lines, DLD1 and HCT116. The cell proliferation of DLD1 also stayed the same while there was a slight increase in HCT116 with 5µM PSE002-selective antagonist even though the change was not statistically significant (Fig. 20B and 20C). Based on this, we conducted PSE002-selective antagonist treatment on HCT116 with 5µM under hypoxic conditions by using

$CoCl_2.6H_2O$ to demonstrate if hypoxia could improve the effect of PSE002-selective antagonist on these cells. The cells were pretreated with $CoCl_2.6H_2O$ for 24 hours and then removed from the media. After that, PSE002-selective antagonist treatment was conducted for 2 days and quantified by CTG. However, it could not show any significant effect (Fig. 20C). In the line of these findings, we can claim that enzymatic activity of PSE002 might not have a major role in cell growth as we have shown earlier with PSE002 knockout cell lines.

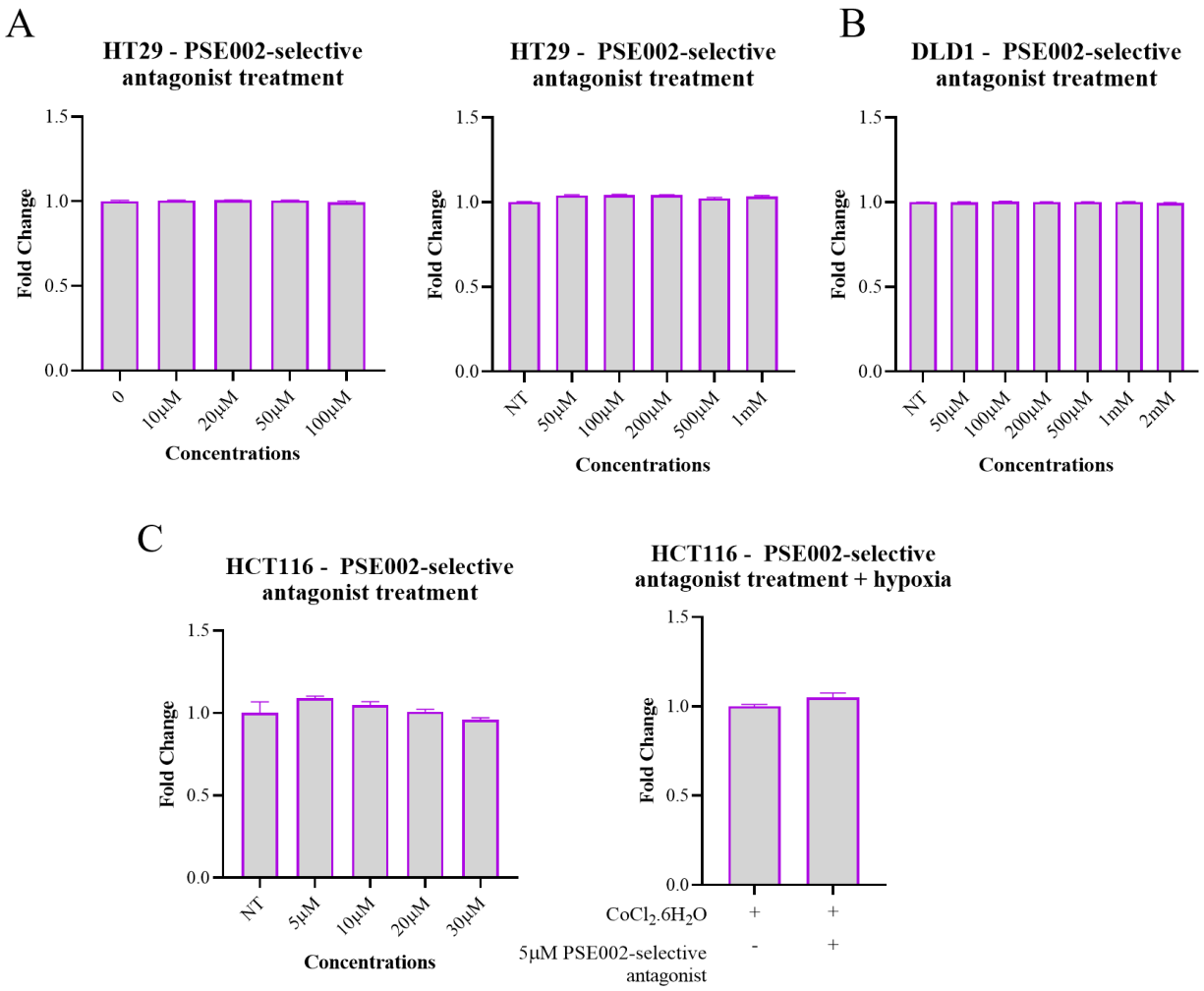

Figure 20: Disruption of PSE002 enzymatic activity did not have any effect on cell growth. After **(A)** HT29 (*n=2*) and **(B)** DLD1 (*n=2*) cell lines were treated with PSE002-selective antagonist, cell growth was quantified. **(C)** Cell proliferation rate of HCT116 cell line was assessed upon PSE002-selective antagonist treatment under normal and hypoxic conditions, separately.

3.5. The effects of PSC003 loss in colorectal cancer cell lines

3.5.1. Cell proliferation and colony-forming ability of cells were advanced *in vitro* upon PSC003 depletion.

The obtained colonies of HT29 sgPSC003 cells after single cell cloning (Fig. 13C) were used to conduct *in vitro* experiments. First, we assessed the effect of PSC003 loss in cell proliferation rate of these cells. The cell growth was measured every day by CTG for 4 days and fold change was calculated. The cell proliferation rate was significantly enhanced upon PSC003 depletion (Fig. 21A). Also, this increase in cell growth was confirmed with PSC003-depleted cells using CRISPR/Cas9 expression system after PSC003-negative population was sorted via FACS (Fig. 21B).

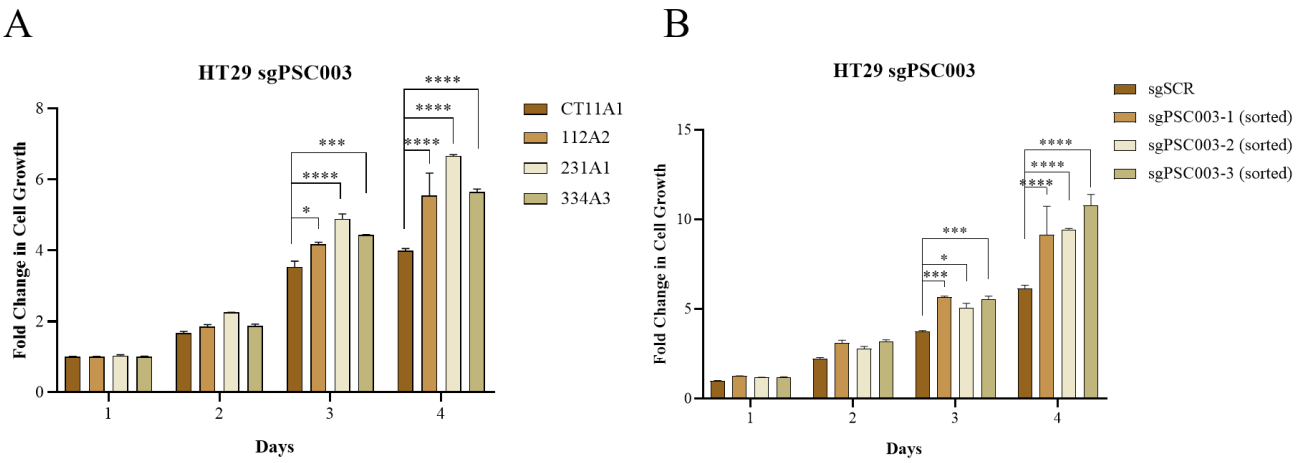

Figure 21: The growth of PSC003-depleted cells were more than control cells. (A) Cell growth was measured in HT29 sgPSC003 single cells for 4 days. *(n=4)* **(B)** Cell proliferation rate of sorted HT29 sgPSC003 was shown by CTG cell proliferation assay. *(n=2) (n: biological replicates, Ordinary one-way ANOVA, * p=0.0160, *** p=0.0005, **** p<0.0001)*

After we showed the cell growth-promoting effect of PSC003 depletion, we performed colony formation assay to assess their colony-forming ability in these cells. They were grown for 14 days and then stained by 0.5% crystal violet. Clonogenic assay demonstrated that PSC003 loss in both single cells and sorted cells strikingly enhanced their colony-forming ability (Fig. 22A and 22B).

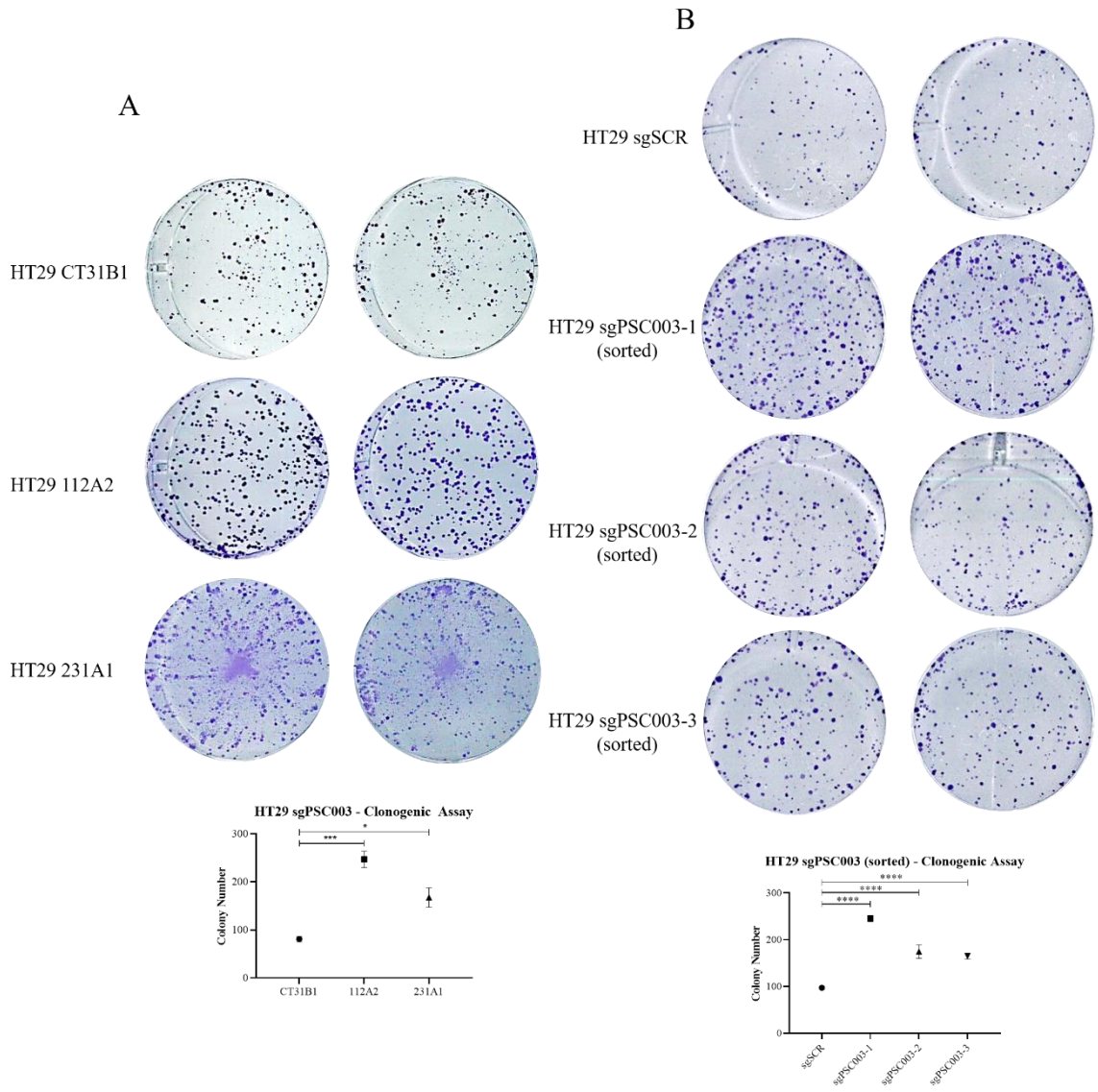

Figure 22: Colony-forming ability of cells were increased on PSC003-depleted HT29 cell lines. Clonogenic assay was performed to assess colony-forming ability in **(A)** HT29 sgPSC003 single cells *(n=2)* and **(B)** sorted HT29 sgPSC003. After colonies reached to a certain size, they were stained by 0.5% crystal violet and quantified by Colony Counter. *(n: biological replicates, Ordinary one-way ANOVA, * p=0.0141, *** p=0.0006, **** p<0.0001)*

3.5.2.Anchorage-independent growth was enhanced in PSC003-depleted cells.

The cells were seeded on polyHEMA-coated plates to prevent cell attachment to the plate and provide them a matrix to grow anchorage-independently. Their growth was measured and quantified by CTG 3D Cell Viability Assay Reagent every 2 days for 5 days. Ultimately, we showed that the anchorage-independent growth of PSC003-depleted HT29 cells was significantly augmented (Fig. 23).

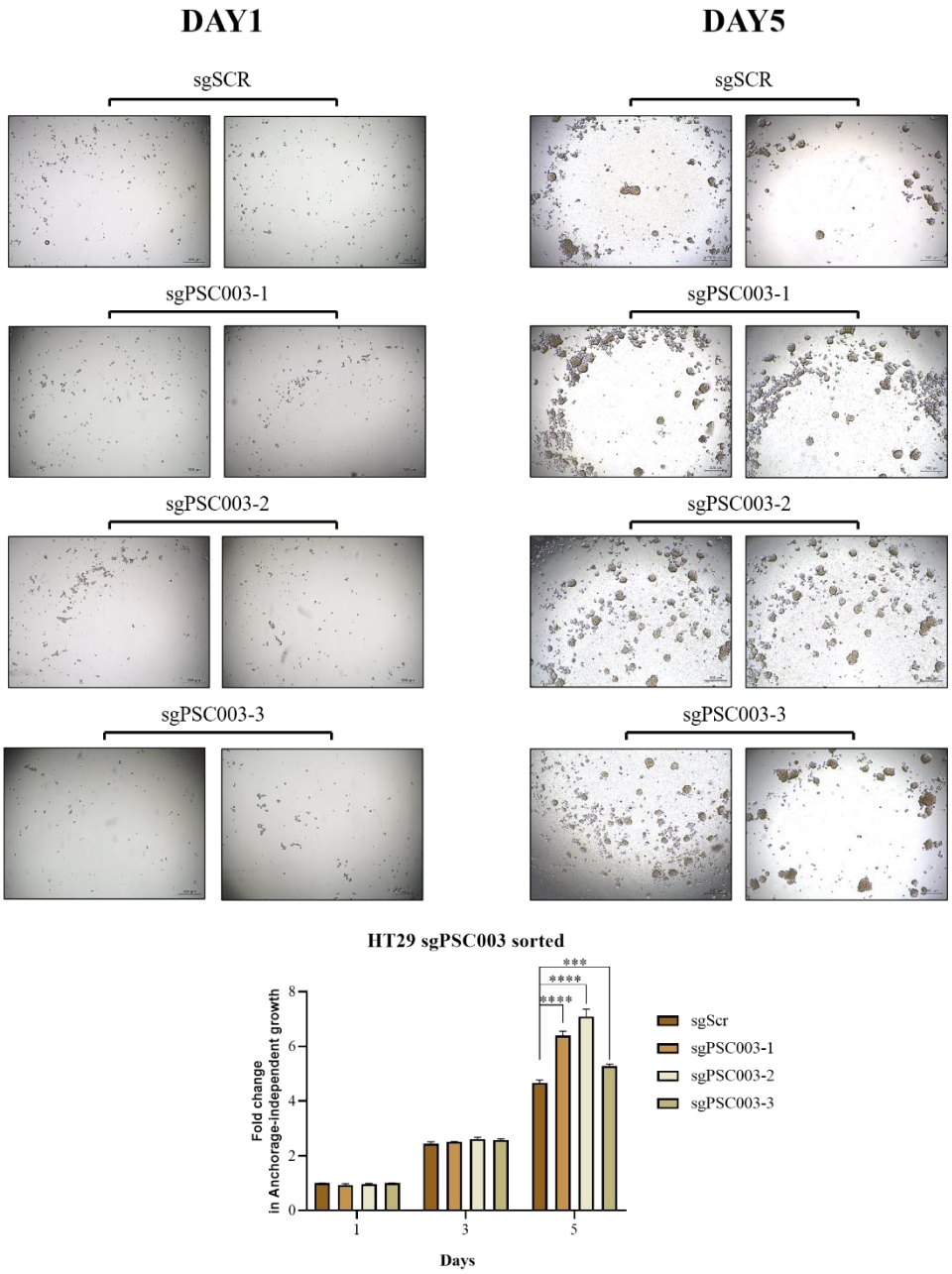

Figure 23: PSE002 loss led to advanced anchorage-independent growth. Representative pictures for HT29 sgPSC003 cells in Day 1 (starting point) and Day 5 (end point) are provided in the upper panel. *(Ordinary one-way ANOVA, *** p=0.0002, **** p<0.0001)*

3.5.3. Migratory ability of the cells was enhanced in the absence of PSC003 expression.

We conducted wound healing assay to demonstrate whether or not the lack of PSC003 affects the migratory abilities of the cells. After the gaps were created for each construct, the pictures were captured and observed until they close the gaps. At the end of 96 hours, the gaps belonging to PSC003-depleted cells were almost closed while control cells could not migrate as much as depleted cells did. Accordingly, it was seen that PSC003 showed considerable effect on migration and the cells could migrate faster upon its depletion (Fig. 24).

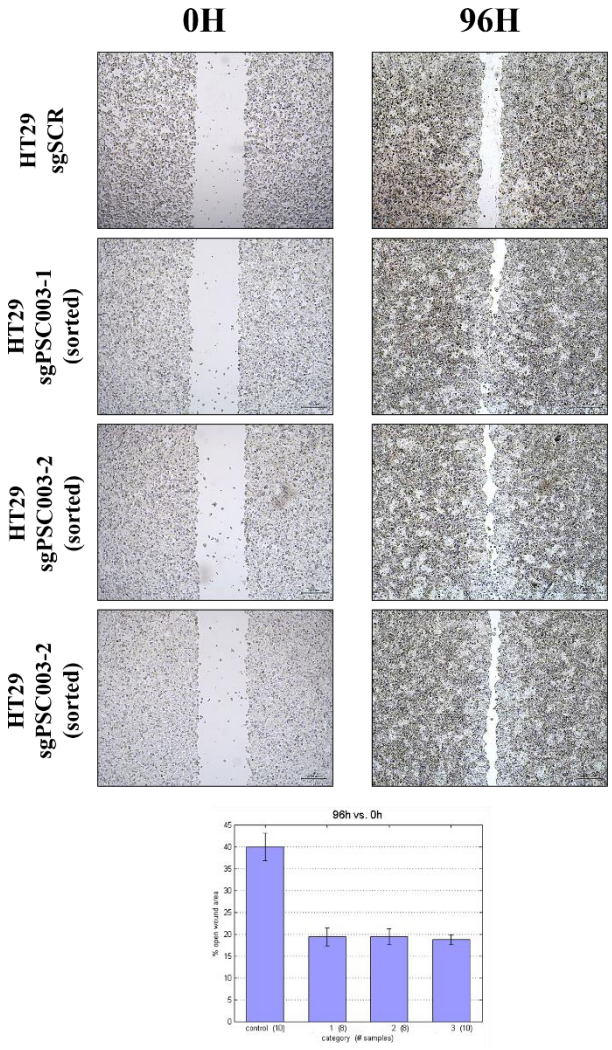

Figure 24: PSC003-depleted cells migrated faster than control cells. Wound healing assay was performed to assess the migration ability of HT29 sgPSC003.

3.5.4. Deterioration of PSC003 expression promoted mesenchymal molecular characteristics rather than epithelial markers.

PSC003 expression was proven to show growth-inhibiting effect in colorectal cancer cell line HT29. Moreover, we investigated the molecular changes in EMT markers and the downstream proteins of PSC003 at protein level upon depletion. At protein level, mesenchymal marker α-smooth muscle actin (α-SMA) level, integrin α5 and vimentin were remarkably enhanced as well as ZEB1, one of the major EMT regulators. Furthermore, ERK and AKT phosphorylation were also considerably promoted in these cells while total protein levels were the same. We checked cAMP response element-binding protein (CREB) levels as CREB is in the downstream of Gs-coupled-PSC003. CREB phosphorylation was strikingly improved while total CREB levels were the same in addition to cAMP-dependent activating transcription factor 1 (ATF-1) increase (Fig. 25). These findings are quite compelling since the downstream genes of PSC003 are upregulated upon PSC003 loss.

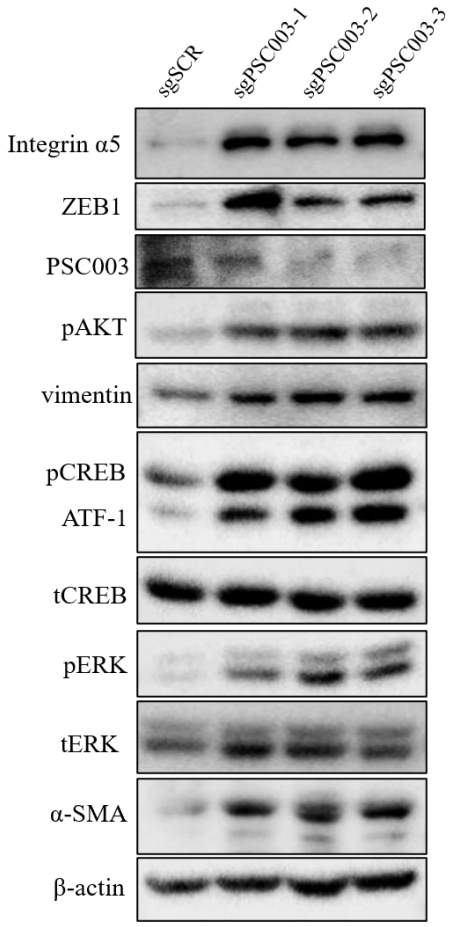

Figure 25: Epithelial-mesenchymal transition was induced upon PSC003 depletion. Molecular changes upon PSC003 depletion were shown at protein level. PSC003 loss enhanced EMT status of these cells by increasing the expression of mesenchymal markers.

3.5.5. Induction of PSC003 signaling caused decreased cell growth whereas inhibition of PSC003 led to increased cell proliferation rate.

In the line of the findings with PSC003-depleted cells, we conducted cell proliferation assays upon PSC003-selective agonist and PSC003-selective antagonist treatments to sort out if or not PSC003 receptor activity was responsible for the effects we had shown earlier. Thus, we optimized the effective doses for both selective-agonist and selective-antagonist by checking phospho-CREB level upon treatment since pCREB is directly in the downstream of PSC003. First, we had used NECA, non-selective adenosine receptor agonist, in different concentrations in which 20µM NECA showed the highest activity in

all cell lines (data not shown). Then, we decided to use PSC003-selective agonist in 20μM final concentration since non-selective agonist was already effective in this concentration. We showed that the activity of PSC003-selective agonist was in its highest point at 30 minutes (Fig. 26A). After optimizing PSC003-selective agonist concentration and the duration of this treatment, we determined the effective dose of PSC003-selective antagonist in HT29, DLD1 and HCT116 CRC cell lines. This dose was 2μM for DLD1 while PSC003-selective antagonist functioned better at 5μM concentration in HT29 and HCT116 (Fig. 26B).

Next, we conducted cell proliferation assays upon agonist-antagonist treatments by SRB method. In HT29 and DLD1, PSC003-selective agonist treatment decreased cell proliferation, as expected (Fig. 26C). In a similar manner, PSC003-selective antagonist treatment resulted in augmented cell growth with two different concentrations in HT29 cell line. However, it did not show any effect in HCT116 and DLD1 CRC cell lines (Fig. 26D). Thereafter, we questioned whether or not hypoxic conditions could improve antagonist activity. We conducted these treatments under hypoxia by pre-treating them with $CoCl_2.6H_2O$ for 24 hours and then we measured their cell proliferation. In DLD1 cell line, we treated the cells with selective antagonist for 3 days and could show that hypoxic conditions improved the effect. Therefore, cell growth was enhanced upon selective antagonist treatment in these cells. Hypoxic conditions were extremely effective in HCT116 cell line such an extent that the effect of both PSC003-selective agonist and PSC003-selective antagonist were seen after 1 day-long treatment and cell growth was increased upon antagonist treatment and attenuated by agonist treatment, respectively (Fig. 26E). We could also demonstrate that PSC003-selective antagonist treatment considerably improved the colony-forming ability of HT29 cells (Fig. 26F).

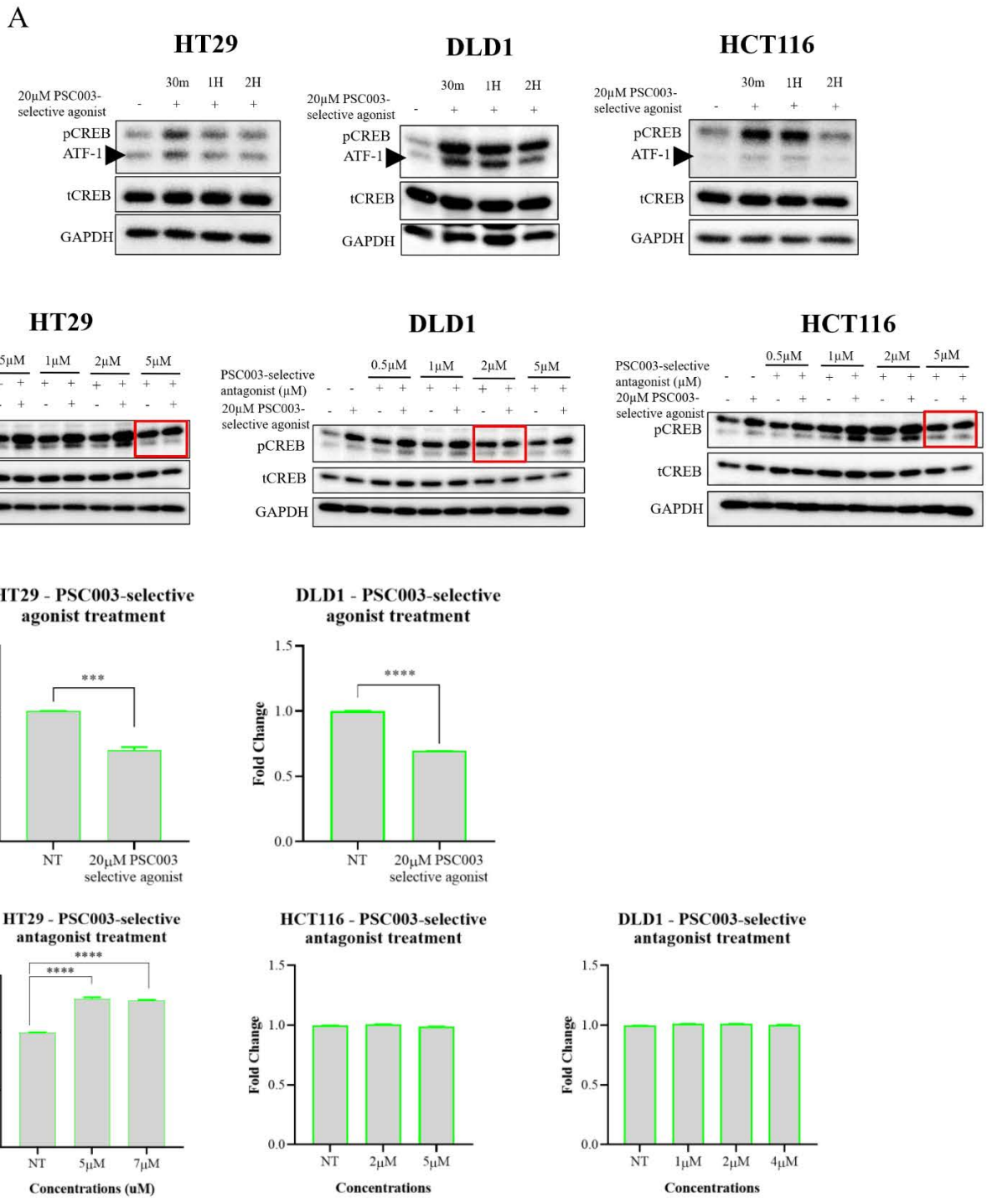
A
HT29
DLD1
HCT116
20μM PSC003-selective agonist
30m
1H
2H
pCREB
ATF-1
tCREB
GAPDH
B
HT29
DLD1
HCT116
PSC003-selective antagonist (μM)
0.5μM
1μM
2μM
5μM
20μM PSC003-selective agonist
pCREB
tCREB
GAPDH
C
HT29 - PSC003-selective agonist treatment
DLD1 - PSC003-selective agonist treatment
Fold Change
***
****
NT
20μM PSC003 selective agonist
D
HT29 - PSC003-selective antagonist treatment
HCT116 - PSC003-selective antagonist treatment
DLD1 - PSC003-selective antagonist treatment
Concentrations (uM)
Concentrations
NT
5μM
7μM
2μM
1μM
4μM

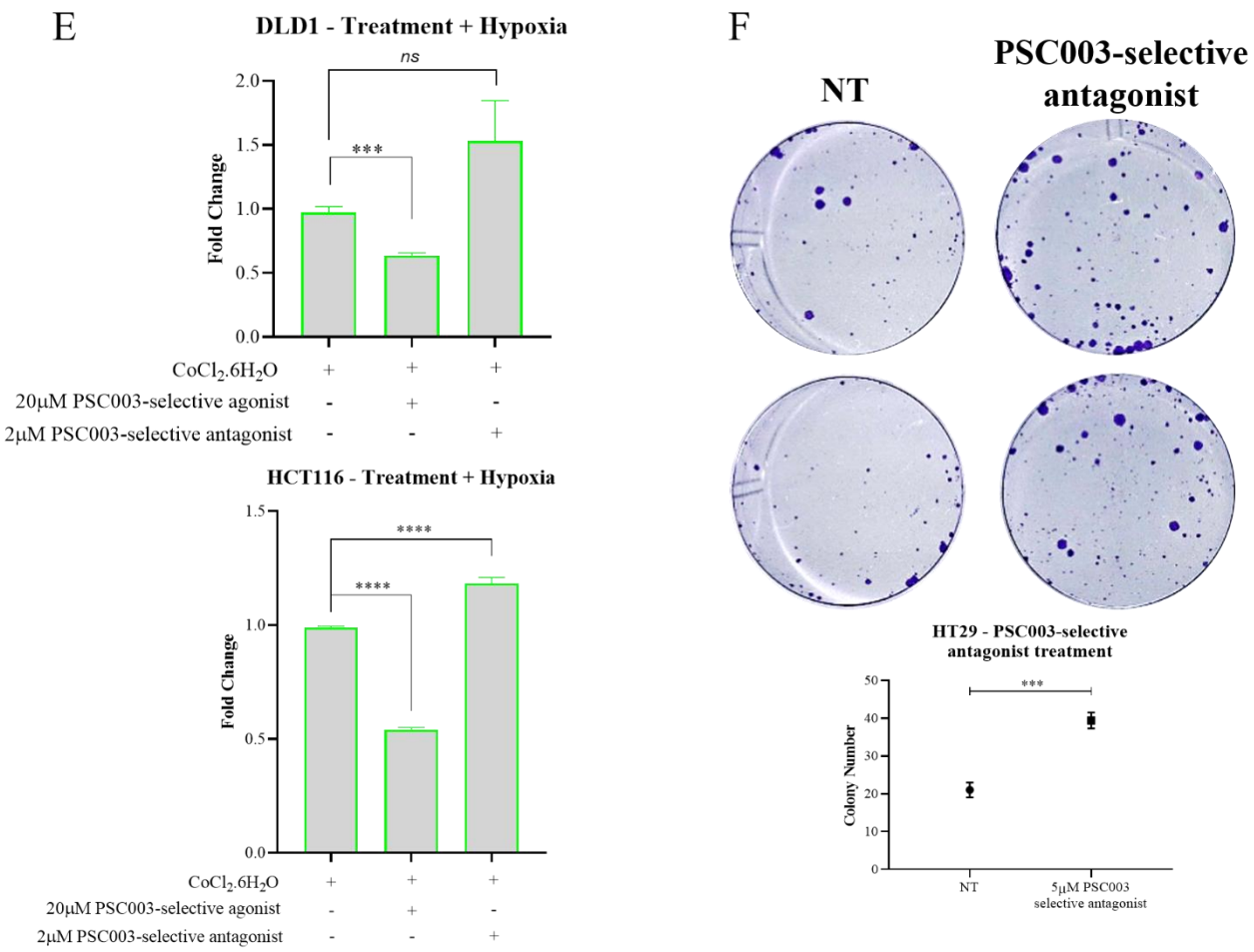

Figure 26: The effects of agonist and antagonist against PSC003 were assessed. Effective dose for both **(A)** selective agonist and **(B)** selective antagonist were detected for each cell line. **(C)** Cell growth upon selective agonist treatment was measured in HT29 (*n=3*) and DLD1 CRC cell lines. *(*** p=0.0002, **** p<0.0001, n=2)* **(D)** Cell proliferation was shown after treatment with PSC003-selective antagonist in HT29 (*n=2*), DLD1 (*n=3*) and HCT116 CRC cell lines. *(**** p<0.0001, n=3)* **(E)** The effect of agonist and antagonist was shown in DLD1 and HCT116 cell lines under hypoxic conditions. *(*** p=0.0005, **** p<0.0001)* **(F)** Colony-forming ability of HT29 cells was assessed upon PSC003-selective antagonist treatment. *(*** p=0.0001) Ordinary one-way ANOVA*

CHAPTER 4

Discussion

Colorectal cancer (CRC) is becoming a greater risk every year with its increased incidence and prevalence, and mortality rates. Only in 2020, 1.148.515 colorectal cancer incidence in both sexes with 50% mortality were reported which comprises 10% of the new cancer cases and 9.4% of the cancer-associated deaths worldwide[231]. Profuse clinical evidences could show that cancer cure is possible when only multiple receptors and their related factors in the pathways are targeted. Purinergic signaling is one of the signaling pathways in which this can be clearly seen since different cell types express different P1 and P2 receptors in a wide range of concentration in addition to that the level of adenosine and ATP in the cells may vary due to pathological and physiological incidents they undergo. Therefore, depending on these factors, purinergic signaling may have opposite outcomes. The complications purinergic signaling lead to because of its extensive effect area can be only overcame by comprehensive molecular and biochemical studies. Purines and pyrimidines have noteworthy roles as building blocks of nucleic acids and as energy transporters. They are also involved in the synthesis of nucleotide cofactors when they are present as intracellular messengers. Surprisingly, in extracellular milieu, they engage in a different set of reactions affecting growth factor secretion, cell differentiation mechanisms and migratory abilities[145-148] which are compelling effects to investigate in cancer context. Therefore, deciphering the roles of purinergic signaling in cancer may provide different perspectives in understanding tumor microenvironment and manipulating this environment for the therapeutical purposes.

In this study, we mainly focused on adenosine signaling in colorectal cancer. Even though pyrimidine nucleotides, UDP and UTP, are also reported to function as extracellular messengers, the reason why we concentrated on the roles of adenosine is diversified amount of activity that ATP is involved compared to UTP or UDP[149] and adenosine being the only nucleoside involving in cell-to-cell signaling[72]. In this context, we successfully generated loss of function models by knockout cell lines via

CRISPR/Cas9 or RNAi to study the roles of our two targets in colorectal cancer. As seen in the expression profile, only two of the targets that had been checked was found to be highly relevant in colorectal cancer which might ease understanding the effects of purinergic signaling. Also, the expression level of two targets were shown under hypoxic conditions mimicked through HIF-1α induction by cobalt chloride hexahydrate ($CoCl_2.6H_2O$) as a stress factor on the cells since stress is one of the fundamental reasons of ATP release to extracellular environment and induced purinergic signaling. Moreover, hypoxia signaling has been reported to promote PSE002 transcriptionally[237] and both PSE002 and PSC003 have binding sites for the main regulator of hypoxia, HIF-1α, in the promoter sequences[81][238]. Interestingly, PSE002 levels were augmented or decreased in HT29 cells in a time-dependent manner whereas it diminished in SW480, RKO and HCT116 cell lines upon hypoxia (Fig. 10). Similarly, PSC003 levels on cell surface remained the same in HT29 cell line while it was strikingly upregulated in HCT116. In the line with these findings, it can be claimed that the regulation of purinergic signaling components might be context-dependent when there is stress induction in the environment, which requires to be explained mechanistically.

Furthermore, the lack of PSE001 expression in CRC cell lines was confirmed at both mRNA and protein level meaning that the level of ATP hydrolysis via PSE001 activity is not high. This might give rise to the question that how PSE002 and PSC003 can be highly expressed and effectively function in these cell lines. However, many studies showed an alternative enzymatic pathways to the canonical pathway for ADO production in which CD38 converts NAD^+ to cADPR and it is followed by ecto-nucleotide pyrophosphatase phosphodiesterase 1 (NPP1) function to metabolize it until AMP[239][240]. Additionally, adenosine and adenine nucleotides have been reported to be directly released upon inflammatory tissue damage claiming that AMP or adenosine can induce PSE002 or PSC003 activity directly through uncontrolled leakage, respectively[236][241].

Despite the presence of limited number of studies for adenosine signaling in colon cancer, recent literature claims that the elevated purinergic signaling promotes cancer initiation by enhancing cell proliferation. However, cell proliferation data that we had obtained from HT29, DLD1 and SW480 showed advanced cell proliferative capacity

upon PSE002-silencing. The repeatability of the results on different colorectal cancer cell lines by two different loss-of-function methods have raised the reliability of the findings. Moreover, colony-forming ability of these cells was also shown to be increased by clonogenic assay. Apart from the growth ability, we could show that PSE002 depletion could provide more migratory capabilities to the cells. Similar to PSE002, loss of PSC003 also resulted in induced cell growth and colony-forming ability and promoted migration capacity in HT29 cell line. These findings had not been comprehensively shown in the literature regarding colorectal cancer before, however, one of the studies showed similar effects in breast cancer upon PSC003 depletion which was refuted by Caglar C. et. al. in metastatic breast cancer cells[105]. Just as in these two studies, there are numerous contradictory findings in the literature about the role of these two target genes in cancer which proves the point that purinergic signaling is challenging to generalize and must be assessed in a context-dependent manner.

Furthermore, PSE002-depleted HT29 cell line showed significantly enhanced mesenchymal marker expression including N-cadherin, integrin α5, ZEB1 and alpha smooth muscle actin (Fig. 20). In a similar manner, PSC003-loss promoted ZEB1 and alpha smooth muscle actin expression. Despite the significant alteration towards mesenchymal features upon PSE002 or PSC003 depletion, phenotypical change in the cells was not observed. The effect observed in these cells might be possibly caused by hybrid EMT due to its epithelial plasticity and metastatic ability including increased migratory capacity. Importantly, enhanced EMT profile upon PSE002 depletion was consistent with obtained expression profile as SW480 and SW620 are derived from the same patient and metastatic version (SW620) did not show any PSE002 expression while it was considerably expressed by primary tumor cells (SW480). It was striking to show significantly advanced ERK and AKT phosphorylation upon both PSE002-depletion and PSC003-silencing. This finding is extremely compelling as GPCR-activated ERK and AKT phosphorylation is well-known and shown in many studies[232-235] and requires to be elucidated mechanistically. Indeed, increased phospho-ERK and phospho-AKT levels could explain enhanced cell growth. Also, CREB phosphorylation was induced upon PSC003-depletion which arises the same question as ERK and AKT phosphorylation.

These findings point out that there might be other regulators in this process to change activation between different proteins.

After providing that loss of PSE002 and PSC003 could provide the 2D growth advantage to the cells, we have assessed their 3D growth by utilizing a substance called polyHEMA to support anchorage-independent growth. As expected, for both targets, depleted cells could grow much more anchorage-independently. In addition, we reported that HT29 colorectal cancer cells became more invasive upon PSE002 depletion (Fig 20). Importantly, cell-derived xenograft (CDX) models showed increase tumor growth *in vivo* and corroborated *in vitro* findings in HT29 and SW480 cell lines. On the other hand, cell proliferation assays performed upon the treatment of PSE002 pharmacological inhibitor did not show any changes in cell growth, suggesting that PSE002 regulated cancer cell growth independently of its enzymatic activity. Furthermore, PSC003-selective agonist caused diminished cell growth whereas PSC003-selective antagonist resulted in augmented cell proliferation rate and colony-forming ability in HT29 cell line. However, it did not provide growth advantage to DLD1 and HCT116 cells under normal conditions. When the treatment was performed under hypoxic conditions, it improved the effect of PSC003-selective antagonist and led to enhanced cell growth.

As known, some cancers do not respond to conventional treatment approaches whereas adoptive immunotherapy engaging lymphokine-activated killer (LAK) cells seems promising to cure these certain cancers. However, colon adenocarcinomas are known to be unresponsive or poorly responsive towards LAK therapy[90]. It is claimed that this unresponsiveness, or the tendency to respond less efficiently, is because of immunosuppressive effects by tumors through anti-CD3-activated killer cell inhibition[207]. Moreover, adenosine has been implied as potential inhibitor for killer T-cell function in tumor microenvironment[208]. Hence, it has been thought that this strong inhibitory role of adenosine signaling may be pivotal for the resistance mechanism of colorectal cancer, and possibly other cancer types, to immunotherapy. On the other hand, as it is seen in our findings, disruption of this signaling causes enhanced tumor growth *in vitro* and *in vivo* which should be taken into consideration for selecting therapeutic strategies against colorectal cancer.

CHAPTER 5

Conclusion and Future Perspectives

Extracellular purinergic signaling may have growth-inhibiting or growth-promoting effects mostly depending on the cancer type. PSE002 was reported to show growth-limiting outcomes in pancreatic dual carcinoma[180], hepatocellular carcinoma[161], and breast cancer[84] as well as PSC003 in breast cancer[105], and lung carcinoma[128]. However, here, we provide a different perspective to extracellular adenosine signaling in colorectal carcinoma and claim that these extracellular purinergic signaling components function as tumor suppressor genes.

As colorectal cancer has a unique tumor microenvironment compared to other cancer types and purinergic signaling is highly regulated by immune cells in the surrounding environment, extracellular purinergic signaling requires to be further investigated in this context which may be done by utilizing co-culture systems. Also, spontaneous tumor models can be utilized for this purpose. Also, the activity of other purinergic signaling enzymes including CD38 and NPP should be investigated further in this context to enlighten how PSE002 and PSC003 are able to be extremely effective in colorectal cancer whereas PSE001 does not show any expression.

Additionally, the mechanism underlying significantly induced ERK and AKT phosphorylation upon PSE002 and PSC003 depletion as well as CREB phosphorylation upon PSC003 silencing requires further investigation to be clarified. Moreover, further analyses for enzymatic activity of PSE002 may be done *in vitro* or *in vivo* to further prove the point that the effect of PSE002 on the acquired abilities of the cells upon depletion is not depending on its enzymatic activity. It also might be a good idea to show the relation between these two target, PSE002 and PSC003 by double knockout models to demonstrate possible feedback loops as the response for a specific element of this signaling is mostly depending on the expression and activity level of other purinergic signaling components.

BIBLIOGRAPHY

[1] Nguyen, H. T., & Duong, H. Q. (2018). The molecular characteristics of colorectal cancer: Implications for diagnosis and therapy (review). *Oncology Letters*. https://doi.org/10.3892/ol.2018.8679

[2] Ferlay, J., Soerjomataram, I., Dikshit, R., Eser, S., Mathers, C., Rebelo, M., … Bray, F. (2015). Cancer incidence and mortality worldwide: Sources, methods and major patterns in GLOBOCAN 2012. *International Journal of Cancer*. https://doi.org/10.1002/ijc.29210

[3] Torre, L. A., Siegel, R. L., Ward, E. M., & Jemal, A. (2016). Global cancer incidence and mortality rates and trends - An update. *Cancer Epidemiology Biomarkers and Prevention*. https://doi.org/10.1158/1055-9965.EPI-15-0578

[4] Burt, R. (2007). Inheritance of colorectal cancer. *Drug Discovery Today: Disease Mechanisms*. https://doi.org/10.1016/j.ddmec.2008.05.004

[5] Hendon, S. E., & DiPalma, J. A. (2005). U.S. practices for colon cancer screening. *Keio Journal of Medicine*. https://doi.org/10.2302/kjm.54.179

[6] Lengauer, C., Kinzler, K. W., & Vogelstein, B. (1998). Genetic instabilities in human cancers. *Nature*. https://doi.org/10.1038/25292

[7] Markowitz, S. D., & Bertagnolli, M. M. (2009). Molecular origins of cancer: Molecular basis of colorectal cancer. *The New England Journal of Medicine*. https://doi.org/10.1056/NEJMra0804588

[8] Fransén, K., Klintenäs, M., Österström, A., Dimberg, J., Monstein, H. J., & Söderkvist, P. (2004). Mutation analysis of the BRAF, ARAF and RAF-1 genes in human colorectal adenocarcinomas. *Carcinogenesis*. https://doi.org/10.1093/carcin/bgh049

[9] Pino, M. S., & Chung, D. C. (2010). The Chromosomal Instability Pathway in Colon Cancer. *Gastroenterology*. https://doi.org/10.1053/j.gastro.2009.12.065

[10] Tsang, A. H. F., Cheng, K. H., Wong, A. S. P., Ng, S. S. M., Ma, B. B. Y., Chan, C. M. L., Tsui, N. B. Y., Chan, L. W. C., Yung, B. Y. M., & Wong, S. C. C. (2014). Current and future molecular diagnostics in colorectal cancer and colorectal adenoma. *World Journal of Gastroenterology*. https://doi.org/10.3748/wjg.v20.i14.3847

[11] Fearon, E. R., & Vogelstein, B. (1990). A genetic model for colorectal tumorigenesis. *Cell*. https://doi.org/10.1016/0092-8674(90)90186-I

[12] Markowitz, S., Wang, J., Myeroff, L., Parsons, R., Sun, L., Lutterbaugh, J., Fan, R. S., Zborowska, E., Kinzler, K. W., Vogelstein, B., Brattain, M., & Willson, J. K. V. (1995).

Inactivation of the type II TGF-β receptor in colon cancer cells with microsatellite instability. *Science*. https://doi.org/10.1126/science.7761852

[13] Baker, S. J., Fearon, E. R., Nigro, J. M., Hamilton, S. R., Preisinger, A. C., Jessup, J. M., Vantuinen, P., Ledbetter, D. H., Barker, D. F., Nakamura, Y., White, R., & Vogelstein, B. (1989). Chromosome 17 deletions and p53 gene mutations in colorectal carcinomas. *Science*. https://doi.org/10.1126/science.2649981

[14] Network, T. C. G. A., Muzny, D. M., Bainbridge, M. N., Chang, K., Dinh, H. H., Drummond, J. a., Fowler, G., Kovar, C. L., Lewis, L. R., Morgan, M. B., Newsham, I. F., Reid, J. G., Santibanez, J., Shinbrot, E., Trevino, L. R., Wu, Y.-Q., Wang, M., Gunaratne, P., Donehower, L. a., … Thomson., E. (2012). Comprehensive molecular characterization of human colon and rectal cancer. *Nature*. https://doi.org/10.1038/nature11252.Comprehensive

[15] Levine, A. J. (1997). p53, the cellular gatekeeper for growth and division. *Cell*. https://doi.org/10.1016/S0092-8674(00)81871-1

[16] Sigal, A., & Rotter, V. (2000). Oncogenic mutations of the p53 tumor suppressor: The demons of the guardian of the genome. *Cancer Research.*

[17] Conlin, A., Smith, G., Carey, F. A., Wolf, C. R., & Steele, R. J. C. (2005). The prognostic significance of K-ras, p53, and APC mutations in colorectal carcinoma. *Gut*. https://doi.org/10.1136/gut.2005.066514

[18] Phipps, A. I., Buchanan, D. D., Makar, K. W., Win, A. K., Baron, J. A., Lindor, N. M., Potter, J. D., & Newcomb, P. A. (2013). KRAS-mutation status in relation to colorectal cancer survival: The joint impact of correlated tumour markers. *British Journal of Cancer*. https://doi.org/10.1038/bjc.2013.118

[19] Vogelstein, B., Fearon, E. R., Hamilton, S. R., Kern, S. E., Preisinger, A. C., Leppert, M., Smits, A. M. m., & Bos, J. L. (1988). Genetic Alterations during Colorectal-Tumor Development. *New England Journal of Medicine*. https://doi.org/10.1056/NEJM198809013190901

[20] Kim, H. S., Heo, J. S., Lee, J., Lee, J. Y., Lee, M. Y., Lim, S. H., Lee, W. Y., Kim, S. H., Park, Y. A., Cho, Y. B., Yun, S. H., Kim, S. T., Park, J. O., Lim, H. Y., Choi, Y. S., Kwon, W. Il, Kim, H. C., & Park, Y. S. (2016). The impact of KRAS mutations on prognosis in surgically resected colorectal cancer patients with liver and lung metastases: A retrospective analysis. BMC Cancer. https://doi.org/10.1186/s12885-016-2141-4

[21] Irahara, N., Baba, Y., Nosho, K., Shima, K., Yan, L., Dias-Santagata, D., Iafrate, A. J., Fuchs, C. S., Haigis, K. M., & Ogino, S. (2010). NRAS mutations are rare in colorectal cancer. *Diagnostic Molecular Pathology*. https://doi.org/10.1097/PDM.0b013e3181c93fd1

[22] Vaughn, C. P., Zobell, S. D., Furtado, L. V., Baker, C. L., & Samowitz, W. S. (2011). Frequency of KRAS, BRAF, and NRAS mutations in colorectal cancer. *Genes Chromosomes and Cancer*. https://doi.org/10.1002/gcc.20854

[23] Abdel-Rahman, W. M., & Peltomäki, P. (2004). Molecular basis and diagnostics of hereditary colorectal cancers. *Annals of Medicine*. https://doi.org/10.1080/07853890410018222

[24] Boland, C. R., Thibodeau, S. N., Hamilton, S. R., Sidransky, D., Eshleman, J. R., Burt, R. W., Meltzer, S. J., Rodriguez-Bigas, M. A., Fodde, R., Ranzani, G. N., & Srivastava, S. (1998). A National Cancer Institute workshop on microsatellite instability for cancer detection and familial predisposition: Development of international criteria for the determination of microsatellite instability in colorectal cancer. *Cancer Research.*

[25] Findeisen, P., Kloor, M., Merx, S., Sutter, C., Woerner, S. M., Dostmann, N., Benner, A., Dondog, B., Pawlita, M., Dippold, W., Wagner, R., Gebert, J., & Von Knebel Doeberitz, M. (2005). T25 repeat in the 3′ untranslated region of the CASP2 gene: A sensitive and specific marker for microsatellite instability in colorectal cancer. *Cancer Research*. https://doi.org/10.1158/0008-5472.CAN-04-4146

[26] Toyota, M., Ahuja, N., Ohe-Toyota, M., Herman, J. G., Baylin, S. B., & Issa, J. P. J. (1999). CpG island methylator phenotype in colorectal cancer. *Proceedings of the National Academy of Sciences of the United States of America*. https://doi.org/10.1073/pnas.96.15.8681

[27] Lao, V. V., & Grady, W. M. (2011). Epigenetics and colorectal cancer. *Nature Reviews Gastroenterology and Hepatology*. https://doi.org/10.1038/nrgastro.2011.173

[28] Jones, P. A., & Laird, P. W. (1999). Cancer epigenetics comes of age. *Nature Genetics*. https://doi.org/10.1038/5947

[29] Jass, J. R. (2005). Serrated adenoma of the colorectum and the DNA-methylator phenotype. *Nature Clinical Practice Oncology*. https://doi.org/10.1038/ncponc0248

[30] Ku, J. L., Shin, Y. K., Kim, D. W., Kim, K. H., Choi, J. S., Hong, S. H., Jeon, Y. K., Kim, S. H., Kim, H. S., Park, J. H., Kim, I. J., & Park, J. G. (2010). Establishment and characterization of 13 human colorectal carcinoma cell lines: Mutations of genes and expressions of drug-sensitivity genes and cancer stem cell markers. *Carcinogenesis*. https://doi.org/10.1093/carcin/bgq043

[31] Ahmed, D., Eide, P. W., Eilertsen, I. A., Danielsen, S. A., Eknæs, M., Hektoen, M., Lind, G. E., & Lothe, R. A. (2013). Epigenetic and genetic features of 24 colon cancer cell lines. *Oncogenesis*. https://doi.org/10.1038/oncsis.2013.35

[32] Guinney, J., Dienstmann, R., Wang, X., De Reyniès, A., Schlicker, A., Soneson, C., Marisa, L., Roepman, P., Nyamundanda, G., Angelino, P., Bot, B. M., Morris, J. S.,

Simon, I. M., Gerster, S., Fessler, E., De Sousa .E Melo, F., Missiaglia, E., Ramay, H., Barras, D., … Tejpar, S. (2015). The consensus molecular subtypes of colorectal cancer. *Nature Medicine*. https://doi.org/10.1038/nm.3967

[33] Ronen, J., Hayat, S., & Akalin, A. (2018). Evaluation of colorectal cancer subtypes and cell lines using deep learning. *BioRxiv*. https://doi.org/10.1101/464743

[34] Müller, M. F., Ibrahim, A. E. K., & Arends, M. J. (2016). Molecular pathological classification of colorectal cancer. *Virchows Archiv*. https://doi.org/10.1007/s00428-016-1956-3

[35] Berg, K. C. G., Eide, P. W., Eilertsen, I. A., Johannessen, B., Bruun, J., Danielsen, S. A., Bjørnslett, M., Meza-Zepeda, L. A., Eknæs, M., Lind, G. E., Myklebost, O., Skotheim, R. I., Sveen, A., & Lothe, R. A. (2017). Multi-omics of 34 colorectal cancer cell lines - a resource for biomedical studies. *Molecular Cancer*. https://doi.org/10.1186/s12943-017-0691-y

[36] Vilar, E., & Gruber, S. B. (2010). Microsatellite instability in colorectal cancer the stable evidence. *Nature Reviews Clinical Oncology*. https://doi.org/10.1038/nrclinonc.2009.237

[37] Gupta, R., Sinha, S., & Paul, R. N. (2018). The impact of microsatellite stability status in colorectal cancer. *Current Problems in Cancer*. https://doi.org/10.1016/j.currproblcancer.2018.06.010

[38] Hanahan, D., & Weinberg, R. A. (2000). The hallmarks of cancer. *Cell*. https://doi.org/10.1016/S0092-8674(00)81683-9

[39] Bates, R. C., & Mercurio, A. M. (2005). The epithelial-mesenchymal transition (EMT) and colorectal cancer progression. *Cancer Biology and Therapy*. https://doi.org/10.4161/cbt.4.4.1655

[40] Hirohashi, S. (1998). Inactivation of the E-cadherin-mediated cell adhesion system in human cancers. *American Journal of Pathology*. https://doi.org/10.1016/S0002-9440(10)65575-7

[41] Yang, J., Mani, S. A., Donaher, J. L., Ramaswamy, S., Itzykson, R. A., Come, C., Savagner, P., Gitelman, I., Richardson, A., & Weinberg, R. A. (2004). Twist, a master regulator of morphogenesis, plays an essential role in tumor metastasis. *Cell*. https://doi.org/10.1016/j.cell.2004.06.006

[42] Bates, R. C., Bellovin, D. I., Brown, C., Maynard, E., Wu, B., Kawakatsu, H., Sheppard, D., Oettgen, P., & Mercurio, A. M. (2005). Transcriptional activation of integrin β6 during the epithelial-mesenchymal transition defines a novel prognostic indicator of aggressive colon carcinoma. *Journal of Clinical Investigation*. https://doi.org/10.1172/jci23183

[43] Busk, M., Pytela, R., & Sheppard, D. (1992). Characterization of the integrin αvβ6 as a fibronectin-binding protein. *Journal of Biological Chemistry*.

[44] Prieto, A. L., Edelman, G. M., & Crossin, K. L. (1993). Multiple integrins mediate cell attachment to cytotactin/tenascin. *Proceedings of the National Academy of Sciences of the United States of America*. https://doi.org/10.1073/pnas.90.21.10154

[45] Zhu, Q. C., Gao, R. Y., Wu, W., & Qin, H. L. (2013). Epithelial-mesenchymal transition and its role in the pathogenesis of colorectal cancer. *Asian Pacific Journal of Cancer Prevention*. https://doi.org/10.7314/APJCP.2013.14.5.2689

[46] Jing, Y., Han, Z., Zhang, S., Liu, Y., & Wei, L. (2011). Epithelial-Mesenchymal Transition in tumor microenvironment. *Cell and Bioscience*. https://doi.org/10.1186/2045-3701-1-29

[47] Lee, H., Herrmann, A., Deng, J. H., Kujawski, M., Niu, G., Li, Z., Forman, S., Jove, R., Pardoll, D. M., & Yu, H. (2009). Persistently Activated Stat3 Maintains Constitutive NF-κB Activity in Tumors. *Cancer Cell*. https://doi.org/10.1016/j.ccr.2009.02.015

[48] Micalizzi, D. S., Farabaugh, S. M., & Ford, H. L. (2010). Epithelial-mesenchymal transition in cancer: Parallels between normal development and tumor progression. *Journal of Mammary Gland Biology and Neoplasia*. https://doi.org/10.1007/s10911-010-9178-9

[49] Wang, H., Wang, H. S., Zhou, B. H., Li, C. L., Zhang, F., Wang, X. F., Zhang, G., Bu, X. Z., Cai, S. H., & Du, J. (2013). Epithelial-Mesenchymal Transition (EMT) Induced by TNF-α Requires AKT/GSK-3β-Mediated Stabilization of Snail in Colorectal Cancer. *PLoS ONE*. https://doi.org/10.1371/journal.pone.0056664

[50] Cano, C., Motoo, Y., & Iovanna, J. L. (2010). Epithelial-to-mesenchymal transition in pancreatic adenocarcinoma. *The Scientific World Journal*. https://doi.org/10.1100/tsw.2010.183

[51] Zhao, S., Venkatasubbarao, K., Lazor, J. W., Sperry, J., Jin, C., Cao, L., & Freeman, J. W. (2008). Inhibition of STAT3Tyr705 phosphorylation by Smad4 suppresses transforming growth factor β-mediated invasion and metastasis in pancreatic cancer cells. *Cancer Research*. https://doi.org/10.1158/0008-5472.CAN-07-5123

[52] Ono, Y., Hayashida, T., Konagai, A., Okazaki, H., Miyao, K., Kawachi, S., Tanabe, M., Shinoda, M., Jinno, H., Hasegawa, H., Kitajima, M., & Kitagawa, Y. (2012). Direct inhibition of the transforming growth factor-β pathway by protein-bound polysaccharide through inactivation of Smad2 signaling. *Cancer Science*. https://doi.org/10.1111/j.1349-7006.2011.02133.x

[53] Galliher, A. J., Neil, J. R., & Schiemann, W. P. (2006). Role of transforming growth factor-β in cancer progression. *Future Oncology*. https://doi.org/10.2217/14796694.2.6.743

[54] Neil, J. R., & Schiemann, W. P. (2008). Altered TAB1:IκB kinase interaction promotes transforming growth factor β-mediated nuclear factor-κB activation during breast cancer progression. *Cancer Research*. https://doi.org/10.1158/0008-5472.CAN-07-3094

[55] Cuevas, B. D., Uhlik, M. T., Garrington, T. P., & Johnson, G. L. (2005). MEKK1 regulates the AP-1 dimer repertoire via control of JunB transcription and Fra-2 protein stability. *Oncogene*. https://doi.org/10.1038/sj.onc.1208239

[56] Lemieux, É., Bergeron, S., Durand, V., Asselin, C., Saucier, C., & Rivard, N. (2009). Constitutively active MEK1 is sufficient to induce epithelial-to- mesenchymal transition in intestinal epithelial cells and to promote tumor invasion and metastasis. *International Journal of Cancer*. https://doi.org/10.1002/ijc.24485

[57] Guarino, M. (2007). Epithelial-mesenchymal transition and tumour invasion. *International Journal of Biochemistry and Cell Biology*. https://doi.org/10.1016/j.biocel.2007.07.011

[58] Tsai, J. H., & Yang, J. (2013). Epithelial-mesenchymal plasticity in carcinoma metastasis. *Genes and Development*. https://doi.org/10.1101/gad.225334.113

[59] Vu, T., & Datta, P. K. (2017). Regulation of EMT in colorectal cancer: A culprit in metastasis. *Cancers*. https://doi.org/10.3390/cancers9120171

[60] Stemmer, V., De Craene, B., Berx, G., & Behrens, J. (2008). Snail promotes Wnt target gene expression and interacts with β-catenin. *Oncogene*. https://doi.org/10.1038/onc.2008.140

[61] Saad, S., Stanners, S. R., Yong, R., Tang, O., & Pollock, C. A. (2010). Notch mediated epithelial to mesenchymal transformation is associated with increased expression of the Snail transcription factor. *International Journal of Biochemistry and Cell Biology*. https://doi.org/10.1016/j.biocel.2010.03.016

[62] Liu, C. W., Li, C. H., Peng, Y. J., Cheng, Y. W., Chen, H. W., Liao, P. L., Kang, J. J., & Yeng, M. H. (2014). Snail regulates Nanog status during the epithelial-mesenchymal transition via the Smad1/Akt/GSK3β signaling pathway in non-small-cell lung cancer. *Oncotarget*. https://doi.org/10.18632/oncotarget.2006

[63] Peinado, H., Ballestar, E., Esteller, M., & Cano, A. (2004). Snail Mediates E-Cadherin Repression by the Recruitment of the Sin3A/Histone Deacetylase 1 (HDAC1)/HDAC2 Complex. *Molecular and Cellular Biology*. https://doi.org/10.1128/mcb.24.1.306-319.2004

[64] Yang, F., Sun, L., Li, Q., Han, X., Lei, L., Zhang, H., & Shang, Y. (2012). SET8 promotes epithelial-mesenchymal transition and confers TWIST dual transcriptional activities. *EMBO Journal*. https://doi.org/10.1038/emboj.2011.364

[65] Postigo, A. A., & Dean, D. C. (1999). ZEB represses transcription through interaction with the corepressor CtBP. *Proceedings of the National Academy of Sciences of the United States of America*. https://doi.org/10.1073/pnas.96.12.6683

[66] He, X., Chen, Z., Jia, M., & Zhao, X. (2013). Downregulated E-Cadherin Expression Indicates Worse Prognosis in Asian Patients with Colorectal Cancer: Evidence from Meta-Analysis. *PLoS ONE*. https://doi.org/10.1371/journal.pone.0070858

[67] Postigo, A. A., Depp, J. L., Taylor, J. J., & Kroll, K. L. (2003). Regulation of Smad signaling through a differential recruitment of coactivators and corepressors by ZEB proteins. *EMBO Journal*. https://doi.org/10.1093/emboj/cdg226

[68] Pohl, M., Radacz, Y., Pawlik, N., Schoeneck, A., Baldus, S. E., Munding, J., Schmiegel, W., Schwarte-Waldhoff, I., & Reinacher-Schick, A. (2010). SMAD4 mediates mesenchymal-epithelial reversion in SW480 colon carcinoma cells. *Anticancer Research*.

[69] Abba, M., Patil, N., Rasheed, K., Nelson, L. D., Mudduluru, G., Leupold, J. H., & Allgayer, H. (2013). Unraveling the role of FOXQ1 in colorectal cancer metastasis. *Molecular Cancer Research*. https://doi.org/10.1158/1541-7786.MCR-13-0024

[70] Yang, C., Chen, H., Tan, G., Gao, W., Cheng, L., Jiang, X., Yu, L., & Tan, Y. (2013). FOXM1 promotes the epithelial to mesenchymal transition by stimulating the transcription of Slug in human breast cancer. *Cancer Letters*. https://doi.org/10.1016/j.canlet.2013.07.004

[71] Pino, M. S., Kikuchi, H., Zeng, M., Herraiz, M. T., Sperduti, I., Berger, D., Park, D. Y., Iafrate, A. J., Zukerberg, L. R., & Chung, D. C. (2010). Epithelial to Mesenchymal Transition Is Impaired in Colon Cancer Cells With Microsatellite Instability. *Gastroenterology*. https://doi.org/10.1053/j.gastro.2009.12.010

[72] Di Virgilio, F. (2012). Purines, purinergic receptors, and cancer. *Cancer Research*. https://doi.org/10.1158/0008-5472.CAN-12-1600

[73] von Kugelgen, I., & Harden, T. K. (2011). Molecular Pharmacology, Physiology, and Structure of the P2Y Receptors. *Advances in Pharmacology*. https://doi.org/10.1016/B978-0-12-385526-8.00012-6

[74] Coddou, C., Yan, Z., Obsil, T., Pablo Huidobro-Toro, J., & Stojilkovic, S. S. (2011). Activation and regulation of purinergic P2X receptor channels. *Pharmacological Reviews*. https://doi.org/10.1124/pr.110.003129

[75] Compan, V., Ulmann, L., Stelmashenko, O., Chemin, J., Chaumont, S., & Rassendren, F. (2012). P2X2 and P2X5 subunits define a new heteromeric receptor with P2X7-like properties. *Journal of Neuroscience*. https://doi.org/10.1523/JNEUROSCI.6332-11.2012

[76] North, R. A. (2002). Molecular physiology of P2X receptors. *Physiological Reviews*. https://doi.org/10.1152/physrev.00015.2002

[77] Ferrari, D., Pizzirani, C., Adinolfi, E., Forchap, S., Sitta, B., Turchet, L., Falzoni, S., Minelli, M., Baricordi, R., & Di Virgilio, F. (2004). The Antibiotic Polymyxin B Modulates P2X 7 Receptor Function. *The Journal of Immunology*. https://doi.org/10.4049/jimmunol.173.7.4652

[78] Ghiringhelli, F., Apetoh, L., Tesniere, A., Aymeric, L., Ma, Y., Ortiz, C., Vermaelen, K., Panaretakis, T., Mignot, G., Ullrich, E., Perfettini, J. L., Schlemmer, F., Tasdemir, E., Uhl, M., Génin, P., Civas, A., Ryffel, B., Kanellopoulos, J., Tschopp, J., … Zitvogel, L. (2009). Activation of the NLRP3 inflammasome in dendritic cells induces IL-1B-dependent adaptive immunity against tumors. *Nature Medicine*. https://doi.org/10.1038/nm.2028

[79] Aymeric, L., Apetoh, L., Ghiringhelli, F., Tesniere, A., Martins, I., Kroemer, G., Smyth, M. J., & Zitvogel, L. (2010). Tumor cell death and ATP release prime dendritic cells and efficient anticancer immunity. C*ancer Research*. https://doi.org/10.1158/0008-5472.CAN-09-3566

[80] Zitvogel, L., Kepp, O., & Kroemer, G. (2011). Immune parameters affecting the efficacy of chemotherapeutic regimens. *Nature Reviews Clinical Oncology*. https://doi.org/10.1038/nrclinonc.2010.223

[81] Synnestvedt, K., Furuta, G. T., Comerford, K. M., Louis, N., Karhausen, J., Eltzschig, H. K., Hansen, K. R., Thompson, L. F., & Colgan, S. P. (2002). Ecto-5′-nucleotidase (CD73) regulation by hypoxia-inducible factor-1 mediates permeability changes in intestinal epithelia. *Journal of Clinical Investigation*. https://doi.org/10.1172/jci15337

[82] Eltzschig, H. K., Kö hler, D., Eckle, T., Kong, T., Robson, S. C., & Colgan, S. P. (2009). Central role of Sp1-regulated CD39 in hypoxia/ischemia protection. *Blood*. https://doi.org/10.1182/blood-2008-06-165746

[83] Künzli, B. M., Bernlochner, M. I., Rath, S., Käser, S., Csizmadia, E., Enjyoji, K., Cowan, P., d'Apice, A., Dwyer, K., Rosenberg, R., Perren, A., Friess, H., Maurer, C. A., & Robson, S. C. (2011). Impact of CD39 and purinergic signalling on the growth and metastasis of colorectal cancer. *Purinergic Signalling*. https://doi.org/10.1007/s11302-011-9228-9

[84] Stagg, J., Divisekera, U., McLaughlin, N., Sharkey, J., Pommey, S., Denoyer, D., Dwyer, K. M., & Smyth, M. J. (2010). Anti-CD73 antibody therapy inhibits breast tumor growth and metastasis. *Proceedings of the National Academy of Sciences of the United States of America*. https://doi.org/10.1073/pnas.0908801107

[85] Stagg, J., Divisekera, U., Duret, H., Sparwasser, T., Teng, M. W. L., Darcy, P. K., & Smyth, M. J. (2011). CD73-deficient mice have increased antitumor immunity and are resistant to experimental metastasis. *Cancer Research*. https://doi.org/10.1158/0008-5472.CAN-10-4246

[86] Stagg, J., Beavis, P. A., Divisekera, U., Liu, M. C. P., Möller, A., Darcy, P. K., & Smyth, M. J. (2012). CD73-Deficient mice are resistant to carcinogenesis. *Cancer Research*. https://doi.org/10.1158/0008-5472.CAN-12-0420

[87] Deaglio, S., Dwyer, K. M., Gao, W., Friedman, D., Usheva, A., Erat, A., Chen, J. F., Enjyoji, K., Linden, J., Oukka, M., Kuchroo, V. K., Strom, T. B., & Robson, S. C. (2007). Adenosine generation catalyzed by CD39 and CD73 expressed on regulatory T cells mediates immune suppression. *Journal of Experimental Medicine*. https://doi.org/10.1084/jem.20062512

[88] Chalmin, F., Mignot, G., Bruchard, M., Chevriaux, A., Végran, F., Hichami, A., Ladoire, S., Derangère, V., Vincent, J., Masson, D., Robson, S. C., Eberl, G., Pallandre, J. R., Borg, C., Ryffel, B., Apetoh, L., Rébé, C., & Ghiringhelli, F. (2012). Stat3 and Gfi-1 Transcription Factors Control Th17 Cell Immunosuppressive Activity via the Regulation of Ectonucleotidase Expression. *Immunity*. https://doi.org/10.1016/j.immuni.2011.12.019

[89] Pro, B., & Dang, N. H. (2004). CD26/dipeptidyl peptidase IV and its role in cancer. *Histology and Histopathology*. https://doi.org/10.14670/HH-19.1345

[90] Gessi, S., Merighi, S., Sacchetto, V., Simioni, C., & Borea, P. A. (2011). Adenosine receptors and cancer. In *Biochimica et Biophysica Acta - Biomembranes*. https://doi.org/10.1016/j.bbamem.2010.09.020

[91] Fishman, P., Bar-Yehuda, S., Madi, L., & Cohn, I. (2002). A3 adenosine receptor as a target for cancer therapy. *Anti-Cancer Drugs*. https://doi.org/10.1097/00001813-200206000-00001

[92] Burnstock, G. (1972). Purinergic nerves. *Pharmacological Reviews*.

[93] Rapaport, E. (1983). Treatment of human tumor cells with ADP or ATP yields arrest of growth in the S phase of the cell cycle. *Journal of Cellular Physiology*. https://doi.org/10.1002/jcp.1041140305

[94] Spychala, J. (2000). Tumor-promoting functions of adenosine. *Pharmacology and Therapeutics*. https://doi.org/10.1016/S0163-7258(00)00053-X

[95] Burnstock, G., & Di Virgilio, F. (2013). Purinergic signalling and cancer. *Purinergic Signalling*. https://doi.org/10.1007/s11302-013-9372-5

[96] Maaser, K., Höpfner, M., Kap, H., Sutter, A. P., Barthel, B., Von Lampe, B., Zeitz, M., & Scherübl, H. (2002). Extracellular nucleotides inhibit growth of human oesophageal cancer cells via P2Y2-receptors. *British Journal of Cancer*. https://doi.org/10.1038/sj.bjc.6600100

[97] Yuahasi, K. K., Demasi, M. A., Tamajusuku, A. S. K., Lenz, G., Sogayar, M. C., Fornazari, M., Lameu, C., Nascimento, I. C., Glaser, T., Schwindt, T. T., Negraes, P. D., & Ulrich, H. (2012). Regulation of neurogenesis and gliogenesis of retinoic acid-induced P19 embryonal carcinoma cells by P2X2 and P2X7 receptors studied by RNA interference. *International Journal of Developmental Neuroscience*. https://doi.org/10.1016/j.ijdevneu.2011.12.010

[98] Li, S., Huang, S., & Peng, S. Bin. (2005). Overexpression of G protein-coupled receptors in cancer cells: Involvement in tumor progression. *International Journal of Oncology*. https://doi.org/10.3892/ijo.27.5.1329

[99] Madi, L., Ochaion, A., Rath-Wolfson, L., Bar-Yehuda, S., Erlanger, A., Ohana, G., Harish, A., Merimski, O., Barer, F., & Fishman, P. (2004). The A3 adenosine receptor is highly expressed in tumor versus normal cells: Potential target for tumor growth inhibition. *Clinical Cancer Research*. https://doi.org/10.1158/1078-0432.CCR-03-0651

[100] Varani, K., Vincenzi, F., Targa, M., Paradiso, B., Parrilli, A., Fini, M., Lanza, G., & Borea, P. A. (2013). The stimulation of A3 adenosine receptors reduces bone-residing breast cancer in a rat preclinical model. *European Journal of Cancer*. https://doi.org/10.1016/j.ejca.2012.06.005

[101] Tafani, M., Schito, L., Pellegrini, L., Villanova, L., Marfe, G., Anwar, T., Rosa, R., Indelicato, M., Fini, M., Pucci, B., & Russo, M. A. (2011). Hypoxia-increased RAGE and P2X7R expression regulates tumor cell invasion through phosphorylation of Erk1/2 and Akt and nuclear translocation of NF-κB. *Carcinogenesis*. https://doi.org/10.1093/carcin/bgr101

[102] Mujoomdar, M., Bennett, A., Hoskin, D., & Blay, J. (2004). Adenosine stimulation of proliferation of breast carcinoma cell lines: Evaluation of the [3H]thymidine assay system and modulatory effects of the cellular microenvironment in vitro. *Journal of Cellular Physiology*. https://doi.org/10.1002/jcp.20089

[103] Lu, J., Pierron, A., & Ravid, K. (2003). An adenosine analogue, IB-MECA, down-regulates estrogen receptor α and suppresses human breast cancer cell proliferation. *Cancer Research*.

[104] Panjehpour, M., & Karami-Tehrani, F. (2004). An adenosine analog (IB-MECA) inhibits anchorage-dependent cell growth of various human breast cancer cell lines. *International Journal of Biochemistry and Cell Biology*. https://doi.org/10.1016/j.biocel.2003.12.001

[105] Cekic, C., Sag, D., Li, Y., Theodorescu, D., Strieter, R. M., & Linden, J. (2012). Adenosine A2B Receptor Blockade Slows Growth of Bladder and Breast Tumors. *The Journal of Immunology*. https://doi.org/10.4049/jimmunol.1101845

[106] Ye, Z. wei, Ghalali, A., Högberg, J., & Stenius, U. (2011). Silencing p110β prevents rapid depletion of nuclear pAkt. *Biochemical and Biophysical Research Communications*. https://doi.org/10.1016/j.bbrc.2011.10.120

[107] Chen, L., He, H. Y., Li, H. M., Zheng, J., Heng, W. J., You, J. F., & Fang, W. G. (2004). ERK1/2 and p38 pathways are required for P2Y receptor-mediated prostate cancer invasion. *Cancer Letters*. https://doi.org/10.1016/j.canlet.2004.05.023

[108] Jajoo, S., Mukherjea, D., Watabe, K., & Ramkumar, V. (2009). Adenosine A3 receptor suppresses prostate cancer metastasis by inhibiting NADPH oxidase activity. *Neoplasia*. https://doi.org/10.1593/neo.09744

[109] Rapaport, E., Fishman, R. F., & Gercel, C. (1983). Growth Inhibition of Human Tumor Cells in Soft-Agar Cultures by Treatment with Low Levels of Adenosine 5'-Triphosphate. *Cancer Research*.

[110] Hinoshita, E., Uchiumi, T., Taguchi, K. I., Kinukawa, N., Tsuneyoshi, M., Maehara, Y., Sugimachi, K., & Kuwano, M. (2000). Increased expression of an ATP-binding cassette superfamily transporter, multidrug resistance protein 2, in human colorectal carcinomas. *Clinical Cancer Research*. https://doi.org/10.11501/3178943

[111] Eroğlu, A., Canbolat, O., Demirci, S., Kocaoglu, H., Eryavuz, Y., & Akgul, H. (2000). Activities of adenosine deaminase and 5'-nucleotidase in cancerous and noncancerous human colorectal tissues. *Medical Oncology*. https://doi.org/10.1007/BF02782198

[112] Höpfner, M., Lemmer, K., Jansen, A., Hanski, C., Riecken, E. O., Gavish, M., Mann, B., Buhr, H., Glassmeier, G., & Scherübl, H. (1998). Expression of functional P2-purinergic receptors in primary cultures of human colorectal carcinoma cells. *Biochemical and Biophysical Research Communications*. https://doi.org/10.1006/bbrc.1998.9555

[113] Höpfner, M., Maaser, K., Barthel, B., von Lampe, B., Hanski, C., Riecken, E. O., Zeitz, M., & Scherübl, H. (2001). Growth inhibition and apoptosis induced by P2Y2 receptors in human colorectal carcinoma cells: Involvement of intracellular calcium and cyclic adenosine monophosphate. *International Journal of Colorectal Disease*. https://doi.org/10.1007/s003840100302

[114] Yaguchi, T., Saito, M., Yasuda, Y., Kanno, T., Nakano, T., & Nishizaki, T. (2010). Higher concentrations of extracellular ATP suppress proliferation of Caco-2 human colonic cancer cells via an unknown receptor involving PKC inhibition. *Cellular Physiology and Biochemistry*. https://doi.org/10.1159/000320518

[115] Tan, E. Y., Mujoomdar, M., & Blay, J. (2004). Adenosine down-regulates the surface expression of dipeptidyl peptidase IV on HT-29 human colorectal carcinoma cells: Implications for cancer cell behavior. *American Journal of Pathology*. https://doi.org/10.1016/S0002-9440(10)63299-3

[116] Giglioni, S., Leoncini, R., Aceto, E., Chessa, A., Civitelli, S., Bernini, A., Tanzini, G., Carraro, F., Pucci, A., & Vannoni, D. (2008). Adenosine kinase gene expression in human colorectal cancer. *Nucleosides Nucleotides Nucleic Acids.* https://doi.org/10.1080/15257770802145629

[117] Lelièvre, V., Muller, J. M., & Falcón, J. (1998). Adenosine modulates cell proliferation in human colonic adenocarcinoma. I. Possible involvement of adenosine A1 receptor subtypes in HT29 cells. *European Journal of Pharmacology*. https://doi.org/10.1016/S0014-2999(97)01462-3

[118] Lelièvre, V., Muller, J. M., & Falcòn, J. (1998). Adenosine modulates cell proliferation in human colonic carcinoma. II. Differential behavior of HT29, DLD-1, Caco-2 and SW403 cell lines. *European Journal of Pharmacology*. https://doi.org/10.1016/S0014-2999(97)01463-5

[119] Mujoomdar, M., Hoskin, D., & Blay, J. (2003). Adenosine stimulation of the proliferation of colorectal carcinoma cell lines: Roles of cell density and adenosine metabolism. *Biochemical Pharmacology*. https://doi.org/10.1016/S0006-2952(03)00548-3

[120] Ma, D. F., Kondo, T., Nakazawa, T., Niu, D. F., Mochizuki, K., Kawasaki, T., Yamane, T., & Katoh, R. (2010). Hypoxia-inducible adenosine A2B receptor modulates proliferation of colon carcinoma cells. *Human Pathology*. https://doi.org/10.1016/j.humpath.2010.04.008

[121] Yasuda, Y., Saito, M., Yamamura, T., Yaguchi, T., & Nishizaki, T. (2009). Extracellular adenosine induces apoptosis in Caco-2 human colonic cancer cells by activating caspase-9/-3 via A2a adenosine receptors. *Journal of Gastroenterology*. https://doi.org/10.1007/s00535-008-2273-7

[122] Ohana, G., Bar-Yehuda, S., Arich, A., Madi, L., Dreznick, Z., Rath-Wolfson, L., Silberman, D., Slosman, G., & Fishman, P. (2003). Inhibition of primary colon carcinoma growth and liver metastasis by the A3 adenosine receptor agonist CF101. *British Journal of Cancer*. https://doi.org/10.1038/sj.bjc.6601315

[123] Fishman, P., Bar-Yehuda, S., Ohana, G., Barer, F., Ochaion, A., Erlanger, A., & Madi, L. (2004). An agonist to the A3 adenosine receptor inhibits colon carcinoma growth in mice via modulation of GSK-3β and NF-κB. *Oncogene*. https://doi.org/10.1038/sj.onc.1207355

[124] Tan, E. Y., Richard, C. L., Zhang, H., Hoskin, D. W., & Blay, J. (2006). Adenosine downregulates DPPIV on HT-29 colon cancer cells by stimulating protein tyrosine phosphatase(s) and reducing ERK1/2 activity via a novel pathway. *American Journal of Physiology - Cell Physiology*. https://doi.org/10.1152/ajpcell.00238.2005

[125] Saitoh, M., Nagai, K., Nakagawa, K., Yamamura, T., Yamamoto, S., & Nishizaki, T. (2004). Adenosine induces apoptosis in the human gastric cancer cells via an intrinsic pathway relevant to activation of AMP-activated protein kinase. *Biochemical Pharmacology*. https://doi.org/10.1016/j.bcp.2004.01.020

[126] Wang, M. X., & Ren, L. M. (2006). Growth inhibitory effect and apoptosis induced by extracellular ATP and adenosine on human gastric carcinoma cells: Involvement of intracellular uptake of adenosine. *Acta Pharmacologica Sinica*. https://doi.org/10.1111/j.1745-7254.2006.00342.x

[127] Agteresch, H. J., van Rooijen, M. H. C., van den Berg, J. W. O., Minderman-Voortman, G. J., Wilson, J. H. P , Dagnelie, P.C. (2003) Growth inhibition of lung cancer cells by adenosine 5'-triphosphate. *Drug Dev Res* https://doi.org/10.1002/ddr.10296

[128] Ryzhov, S., Novitskiy, S. V, Zaynagetdinov, R., Goldstein, A. E., Carbone, D. P., Biaggioni, I., Dikov, M. M., & Feoktistov, I. (2008). Host A(2B) adenosine receptors promote carcinoma growth. *Neoplasia*.

[129] Wu, Y., Sun, X., Imai, M., Sultan, B., Csizmadia, E., Enjyoji, K., Jackson, S., Usheva, A., Robson, S. C. (2005) Modulation of RAS/ERK signaling by CD39/ENTPD1 during liver regeneration. *Hepatology*

[130] Hargrove, J. L., & Granner, D. K. (1982). Inhibition of hepatoma cell growth by analogs of adenosine and cyclic AMP and the influence of enzymes in mammalian sera. *Journal of Cellular Physiology*. https://doi.org/10.1002/jcp.1041110303

[131] Bar-Yehuda, S., Stemmer, S. M., Madi, L., Castel, D., Ochaion, A., Cohen, S., Barer, F., Zabutti, A., Perez-Liz, G., Del Valle, L., & Fishman, P. (2008). The A3 adenosine receptor agonist CF102 induces apoptosis of hepatocellular carcinoma via de-regulation of the Wnt and NF-κB signal transduction pathways. *International Journal of Oncology*. https://doi.org/10.3892/ijo_00000008

[132] Wen, L. T., & Knowles, A. F. (2003). Extracellular ATP and adenosine induce cell apoptosis of human hepatoma Li-7A cells via the A3 adenosine receptor. *British Journal of Pharmacology*. https://doi.org/10.1038/sj.bjp.0705523

[133] Xiang, H. jun, Liu, Z. cai, Wang, D. sheng, Chen, Y., Yang, Y. ling, & Dou, K. feng. (2006). Adenosine A2b receptor is highly expressed in human hepatocellular carcinoma. *Hepatology Research*. https://doi.org/10.1016/j.hepres.2006.06.008

[134] Sun, X., Han, L., Seth, P., Bian, S., Li, L., Csizmadia, E., Junger, W. G., Schmelzle, M., Usheva, A., Tapper, E. B., Baffy, G., Sukhatme, V. P., Wu, Y., & Robson, S. C. (2013). Disordered purinergic signaling and abnormal cellular metabolism are associated with development of liver cancer in Cd39/Entpd1 null Mice. *Hepatology*. https://doi.org/10.1002/hep.25989

[135] Zeng, D., Maa, T., Wang, U., Feoktistov, I., Biaggioni, I., Belardinelli, L. (2004) Expression and function of A2B adenosine receptors in the U87MG tumor cells. *Drug Dev Res* https://doi.org/10.1002/ddr.10212

[136] Ferrari, D., McNamee, E. N., Idzko, M., Gambari, R., & Eltzschig, H. K. (2016). Purinergic Signaling During Immune Cell Trafficking. *Trends in Immunology*. https://doi.org/10.1016/j.it.2016.04.004

[137] Fredholm, B. B., Ijzerman, A. P., Jacobson, K. A., Klotz, K. N., & Linden, J. (2001). International Union of Pharmacology. XXV. Nomenclature and classification of adenosine receptors. *Pharmacological Reviews*.

[138] Cekic, C., & Linden, J. (2016). Purinergic regulation of the immune system. *Nature Reviews Immunology*. https://doi.org/10.1038/nri.2016.4

[139] Eckle, T., Kewley, E. M., Brodsky, K. S., Tak, E., Bonney, S., Gobel, M., Anderson, D., Glover, L. E., Riegel, A. K., Colgan, S. P., & Eltzschig, H. K. (2014). Identification of Hypoxia-Inducible Factor HIF-1A as Transcriptional Regulator of the A2B Adenosine Receptor during Acute Lung Injury. *The Journal of Immunology*. https://doi.org/10.4049/jimmunol.1100593

[140] Linden, J., Thai, T., Figler, H., Jin, X., & Robeva, A. S. (1999). Characterization of human A(2B) adenosine receptors: Radioligand binding, Western blotting, and coupling to G(q) in human embryonic kidney 293 cells and HMC-1 mast cells. *Molecular Pharmacology*.

[141] Sorrentino, C., Miele, L., Porta, A., Pinto, A., & Morello, S. (2015). Myeloid-derived suppressor cells contribute to A2B adenosine receptor-induced VEGF production and angiogenesis in a mouse melanoma model. *Oncotarget*. https://doi.org/10.18632/oncotarget.4393

[142] Zhou, Y., Schneider, D. J., Morschl, E., Song, L., Pedroza, M., Karmouty-Quintana, H., Sun, C.-X., & Blackburn, M. R. (2011). Distinct Roles for the A2B Adenosine Receptor in Acute and Chronic Stages of Bleomycin-Induced Lung Injury. *The Journal of Immunology*. https://doi.org/10.4049/jimmunol.1002907

[143] Ohta, A., Gorelik, E., Prasad, S. J., Ronchese, F., Lukashev, D., Wong, M. K. K., Huang, X., Caldwell, S., Liu, K., Smith, P., Chen, J. F., Jackson, E. K., Apasov, S., Abrams, S., & Sitkovsky, M. (2006). A2A adenosine receptor protects tumors from antitumor T cells. *Proceedings of the National Academy of Sciences of the United States of America*. https://doi.org/10.1073/pnas.0605251103

[144] Cekic, C., & Linden, J. (2014). Adenosine A2A receptors intrinsically regulate CD8+ T cells in the tumor microenvironment. *Cancer Research*. https://doi.org/10.1158/0008-5472.CAN-13-3581

[145] Leo Bours, M. J., Dagnelie, P. C., Giuliani, A. L., Wesselius, A., & Di Virgilio, F. (2011). P2 receptors and extracellular ATP: A novel homeostatic pathway in inflammation. *Frontiers in Bioscience - Scholar*. https://doi.org/10.2741/s235

[146] Khakh, B. S., & Alan North, R. (2006). P2X receptors as cell-surface ATP sensors in health and disease. *Nature*. https://doi.org/10.1038/nature04886

[147] Idzko, M., Ferrari, D., & Eltzschig, H. K. (2014). Nucleotide signalling during inflammation. *Nature*. https://doi.org/10.1038/nature13085

[148] Antonioli, L., Blandizzi, C., Pacher, P., & Haskó, G. (2013). Immunity, inflammation and cancer: A leading role for adenosine. *Nature Reviews Cancer*. https://doi.org/10.1038/nrc3613

[149] Di Virgilio, F., & Adinolfi, E. (2017). Extracellular purines, purinergic receptors and tumor growth. *Oncogene*. https://doi.org/10.1038/onc.2016.206

[150] Zimmermann, H. (2000). Extracellular metabolism of ATP and other nucleotides. *Naunyn-Schmiedeberg's Archives of Pharmacology*. https://doi.org/10.1007/s002100000309

[151] Leclerc, B. G., Charlebois, R., Chouinard, G., Allard, B., Pommey, S., Saad, F., & Stagg, J. (2016). CD73 expression is an independent prognostic factor in prostate cancer. *Clinical Cancer Research*. https://doi.org/10.1158/1078-0432.CCR-15-1181

[152] Campos-Contreras, A. D. R., Díaz-Muñoz, M., & Vázquez-Cuevas, F. G. (2020). Purinergic Signaling in the Hallmarks of Cancer. *Cells*. https://doi.org/10.3390/cells9071612

[153] Corriden, R., & Insel, P. A. (2010). Basal release of ATP: An autocrine-paracrine mechanism for cell regulation. *Science Signaling*. https://doi.org/10.1126/scisignal.3104re1

[154] Di Virgilio, F., Sarti, A. C., Falzoni, S., De Marchi, E., & Adinolfi, E. (2018). Extracellular ATP and P2 purinergic signalling in the tumour microenvironment. *Nature Reviews Cancer*. https://doi.org/10.1038/s41568-018-0037-0

[155] Zhou, P., Zhi, X., Zhou, T., Chen, S., Li, X., Wang, L., Yin, L., Shao, Z., & Ou, Z. (2007). Overexpression of ecto-5′-nucleotidase (CD73) promotes T-47D human breast cancer cells invasion and adhesion to extracellular matrix. *Cancer Biology and Therapy*. https://doi.org/10.4161/cbt.6.3.3762

[156] Wang, L., Zhou, X., Zhou, T., Ma, D., Chen, S., Zhi, X., Yin, L., Shao, Z., Ou, Z., & Zhou, P. (2008). Ecto-5′-nucleotidase promotes invasion, migration and adhesion of human breast cancer cells. *Journal of Cancer Research and Clinical Oncology*. https://doi.org/10.1007/s00432-007-0292-z

[157] Gao, Z. W., Wang, H. P., Dong, K., Lin, F., Wang, X., & Zhang, H. Z. (2016). Adenosine inhibits migration, invasion and induces apoptosis of human cervical cancer cells. *Neoplasma*. https://doi.org/10.4149/204_150723N407

[158] Bowser, J. L., & Broaddus, R. R. (2016). CD73s protection of epithelial integrity: Thinking beyond the barrier. *Tissue Barriers*. https://doi.org/10.1080/21688370.2016.1224963

[159] Ren, Z. H., Lin, C. Z., Cao, W., Yang, R., Lu, W., Liu, Z. Q., Chen, Y. M., Yang, X., Tian, Z., Wang, L. Z., Li, J., Wang, X., Chen, W. T., Ji, T., & Zhang, C. P. (2016). CD73 is associated with poor prognosis in HNSCC. *Oncotarget*. https://doi.org/10.18632/oncotarget.11435

[160] Lupia, M., Angiolini, F., Bertalot, G., Freddi, S., Sachsenmeier, K. F., Chisci, E., Kutryb-Zajac, B., Confalonieri, S., Smolenski, R. T., Giovannoni, R., Colombo, N., Bianchi, F., & Cavallaro, U. (2018). CD73 Regulates Stemness and Epithelial-Mesenchymal Transition in Ovarian Cancer-Initiating Cells. *Stem Cell Reports*. https://doi.org/10.1016/j.stemcr.2018.02.009

[161] Ma, X. L., Shen, M. N., Hu, B., Wang, B. L., Yang, W. J., Lv, L. H., Wang, H., Zhou, Y., Jin, A. L., Sun, Y. F., Zhang, C. Y., Qiu, S. J., Pan, B. S., Zhou, J., Fan, J., Yang, X. R., & Guo, W. (2019). CD73 promotes hepatocellular carcinoma progression and metastasis via activating PI3K/AKT signaling by inducing Rap1-mediated membrane localization of P110β and predicts poor prognosis. *Journal of Hematology and Oncology*. https://doi.org/10.1186/s13045-019-0724-7

[162] Virtanen, S. S., Kukkonen-Macchi, A., Vainio, M., Elima, K., Härkönen, P. L., Jalkanen, S., & Yegutkin, G. G. (2014). Adenosine inhibits tumor cell invasion via receptor-independent mechanisms. *Molecular Cancer Research*. https://doi.org/10.1158/1541-7786.MCR-14-0302-T

[163] Martínez-Ramírez, A. S., Díaz-Muñoz, M., Battastini, A. M., Campos-Contreras, A., Olvera, A., Bergamin, L., Glaser, T., Jacintho Moritz, C. E., Ulrich, H., & Vázquez-Cuevas, F. G. (2017). Cellular Migration Ability Is Modulated by Extracellular Purines

in Ovarian Carcinoma SKOV-3 Cells. *Journal of Cellular Biochemistry*. https://doi.org/10.1002/jcb.26104

[164] Giacomelli, C., Daniele, S., Romei, C., Tavanti, L., Neri, T., Piano, I., Celi, A., Martini, C., & Trincavelli, M. L. (2018). The A2B adenosine receptor modulates the epithelial- mesenchymal transition through the balance of cAMP/PKA and MAPK/ERK pathway activation in human epithelial lung cells. *Frontiers in Pharmacology*. https://doi.org/10.3389/fphar.2018.00054

[165] Marucci, G., Santinelli, C., Buccioni, M., Navia, A. M., Lambertucci, C., Zhurina, A., Yli-Harja, O., Volpini, R., & Kandhavelu, M. (2018). Anticancer activity study of A3 adenosine receptor agonists. *Life Sciences*. https://doi.org/10.1016/j.lfs.2018.05.028

[166] Maliszewski, C. R., Delespesse, G. J., Schoenborn, M. A., Armitage, R. J., Fanslow, W. C., Nakajima, T., Baker, E., Sutherland, G. R., Poindexter, K., & Birks, C. (1994). The CD39 lymphoid cell activation antigen. Molecular cloning and structural characterization. *Journal of Immunology (Baltimore, Md. : 1950)*.

[167] Heine, P., Braun, N., Sévigny, J., Robson, S. C., Servos, J., & Zimmermann, H. (2001). The C-terminal cysteine-rich region dictates specific catalytic properties in chimeras of the ectonucleotidases NTPDase1 and NTPDase2. *European Journal of Biochemistry*. https://doi.org/10.1046/j.1432-1033.2001.01896.x

[168] Antonioli, L., Pacher, P., Vizi, E. S., & Haskó, G. (2013). CD39 and CD73 in immunity and inflammation. *Trends in Molecular Medicine*. https://doi.org/10.1016/j.molmed.2013.03.005

[169] Smith, T. M., & Kirley, T. L. (1998). Cloning, sequencing, and expression of a human brain ecto-apyrase related to both the ecto-ATPases and CD39 ecto-apyrases1. *Biochimica et Biophysica Acta - Protein Structure and Molecular Enzymology*. https://doi.org/10.1016/S0167-4838(98)00063-6

[170] Sträter, N. (2006). Ecto-5′-nucleotidase: Structure function relationships. *Purinergic Signalling*. https://doi.org/10.1007/s11302-006-9000-8

[171] Yegutkin, G. G. (2008). Nucleotide- and nucleoside-converting ectoenzymes: Important modulators of purinergic signalling cascade. *Biochimica et Biophysica Acta - Molecular Cell Research*. https://doi.org/10.1016/j.bbamcr.2008.01.024

[172] Heuts, D. P. H. M., Weissenborn, M. J., Olkhov, R. V., Shaw, A. M., Gummadova, J., Levy, C., & Scrutton, N. S. (2012). Crystal Structure of a Soluble Form of Human CD73 with Ecto-5′-Nucleotidase Activity. *ChemBioChem*. https://doi.org/10.1002/cbic.201200426

[173] Bastid, J., Regairaz, A., Bonnefoy, N., Dejou, C., Giustiniani, J., Laheurte, C., Cochaud, S., Laprevotte, E., Funck-Brentano, E., Hemon, P., Gros, L., Bec, N.,

Larroque, C., Alberici, G., Bensussan, A., & Eliaou, J. F. (2015). Inhibition of CD39 enzymatic function at the surface of tumor cells alleviates their immunosuppressive activity. *Cancer Immunology Research*. https://doi.org/10.1158/2326-6066.CIR-14-0018

[174] Xu, Z., Gu, C., Yao, X., Guo, W., Wang, H., Lin, T., Li, F., Chen, D., Wu, J., Ye, G., Zhao, L., Hu, Y., Yu, J., Shi, J., Li, G., & Liu, H. (2020). CD73 promotes tumor metastasis by modulating RICS/RhoA signaling and EMT in gastric cancer. *Cell Death and Disease*. https://doi.org/10.1038/s41419-020-2403-6

[175] Yu, M., Guo, G., Huang, L., Deng, L., Chang, C. S., Achyut, B. R., Canning, M., Xu, N., Arbab, A. S., Bollag, R. J., Rodriguez, P. C., Mellor, A. L., Shi, H., Munn, D. H., & Cui, Y. (2020). CD73 on cancer-associated fibroblasts enhanced by the A2B-mediated feedforward circuit enforces an immune checkpoint. *Nature Communications*. https://doi.org/10.1038/s41467-019-14060-x

[176] Knöfel, T., & Sträter, N. (2001). Mechanism of hydrolysis of phosphate esters by the dimetal center of 5′-nucleotidase based on crystal structures. *Journal of Molecular Biology*. https://doi.org/10.1006/jmbi.2001.4656

[177] Ripphausen, P., Freundlieb, M., Brunschweiger, A., Zimmermann, H., Müller, C. E., & Bajorath, J. (2012). Virtual screening identifies novel sulfonamide inhibitors of ecto -5′-nucleotidase. *Journal of Medicinal Chemistry*. https://doi.org/10.1021/jm300658n

[178] Qiao, Z., Li, X., Kang, N., Yang, Y., Chen, C., Wu, T., Zhao, M., Liu, Y., & Ji, X. (2019). A novel specific anti-cd73 antibody inhibits triple-negative breast cancer cell motility by regulating autophagy. *International Journal of Molecular Sciences*. https://doi.org/10.3390/ijms20051057

[179] Perrot, I., Michaud, H. A., Giraudon-Paoli, M., Augier, S., Docquier, A., Gros, L., Courtois, R., Déjou, C., Jecko, D., Becquart, O., Rispaud-Blanc, H., Gauthier, L., Rossi, B., Chanteux, S., Gourdin, N., Amigues, B., Roussel, A., Bensussan, A., Eliaou, J. F., … Bonnefoy, N. (2019). Blocking Antibodies Targeting the CD39/CD73 Immunosuppressive Pathway Unleash Immune Responses in Combination Cancer Therapies. *Cell Reports*. https://doi.org/10.1016/j.celrep.2019.04.091

[180] Zhou, L., Jia, S., Chen, Y., Wang, W., Wu, Z., Yu, W., Zhang, M., Ding, G., & Cao, L. (2019). The distinct role of CD73 in the progression of pancreatic cancer. *Journal of Molecular Medicine*. https://doi.org/10.1007/s00109-018-01742-0

[181] Kordaß, T., Osen, W., & Eichmüller, S. B. (2018). Controlling the immune suppressor: Transcription factors and MicroRNAs regulating CD73/NT5E. *Frontiers in Immunology*. https://doi.org/10.3389/fimmu.2018.00813

[182] Samanta, D., Park, Y., Ni, X., Li, H., Zahnow, C. A., Gabrielson, E., Pan, F., & Semenza, G. L. (2018). Chemotherapy induces enrichment of CD47+/CD73+/PDL1+ immune evasive triple-negative breast cancer cells. *Proceedings of the National Academy of Sciences of the United States of America*. https://doi.org/10.1073/pnas.1718197115

[183] Gao, Z. wei, Wang, H. ping, Lin, F., Wang, X., Long, M., Zhang, H. zhong, & Dong, K. (2017). CD73 promotes proliferation and migration of human cervical cancer cells independent of its enzyme activity. *BMC Cancer*. https://doi.org/10.1186/s12885-017-3128-5

[184] Adzic, M., & Nedeljkovic, N. (2018). Unveiling the role of Ecto-5'-nucleotidase/CD73 in astrocyte migration by using pharmacological tools. *Frontiers in Pharmacology*. https://doi.org/10.3389/fphar.2018.00153

[185] Yu, J., Wang, X., Lu, Q., Wang, J., Li, L., Liao, X., Zhu, W., Lv, L., Zhi, X., Yu, J., Jin, Y., Zou, Q., Ou, Z., Liu, X., & Zhou, P. (2018). Extracellular 5′-nucleotidase (CD73) promotes human breast cancer cells growth through AKT/GSK-3β/β-catenin/cyclinD1 signaling pathway. *International Journal of Cancer*. https://doi.org/10.1002/ijc.31112

[186] Zimmermann, H. (1992). 5'-Nucleotidase: Molecular structure and functional aspects. *Biochemical Journal*. https://doi.org/10.1042/bj2850345

[187] Knapp, K., Zebisch, M., Pippel, J., El-Tayeb, A., Müller, C. E., & Sträter, N. (2012). Crystal structure of the human ecto-5′-nucleotidase (CD73): Insights into the regulation of purinergic signaling. *Structure*. https://doi.org/10.1016/j.str.2012.10.001

[188] Ohana, G., Bar-Yehuda, S., Barer, F., & Fishman, P. (2001). Differential effect of adenosine on tumor and normal cell growth: Focus on the A3 adenosine receptor. *Journal of Cellular Physiology*. https://doi.org/10.1002/1097-4652(200101)186:1<19::AID-JCP1011>3.0.CO;2-3

[189] Merighi, S., Mirandola, P., Milani, D., Varani, K., Gessi, S., Klotz, K. N., Leung, E., Baraldi, P. G., & Borea, P. A. (2002). Adenosine receptors as mediators of both cell proliferation and cell death of cultured human melanoma cells. *Journal of Investigative Dermatology*. https://doi.org/10.1046/j.1523-1747.2002.00111.x

[190] Gessi, S., Varani, K., Merighi, S., Morelli, A., Ferrari, D., Leung, E., Baraldi, P. G., Spalluto, G., & Borea, P. A. (2001). Pharmacological and biochemical characterization of A3 adenosine receptors in Jurkat T cells. *British Journal of Pharmacology*. https://doi.org/10.1038/sj.bjp.0704254

[191] Merighi, S., Varani, K., Gessi, S., Cattabriga, E., Iannotta, V., Ulouglu, C., Leung, E., & Borea, P. A. (2001). Pharmacological and biochemical characterization of

adenosine receptors in the human malignant melanoma A375 cell line. *British Journal of Pharmacology*. https://doi.org/10.1038/sj.bjp.0704352

[192] Fishman, P., Bar-Yehuda, S., Synowitz, M., Powell, J. D., Klotz, K. N., Gessi, S., & Borea, P. A. (2009). Adenosine receptors and cancer. *Handbook of Experimental Pharmacology*. https://doi.org/10.1007/978-3-540-89615-9_14

[193] Salmon, J. E., & Cronstein, B. N. (1990). Fc gamma receptor-mediated functions in neutrophils are modulated by adenosine receptor occupancy. A1 receptors are stimulatory and A2 receptors are inhibitory. *Journal of Immunology (Baltimore, Md. : 1950)*.

[194] Salmon, J. E., Brogle, N., Brownlie, C., Edberg, J. C., Kimberly, R. P., Chen, B. X., & Erlanger, B. F. (1993). Human mononuclear phagocytes express adenosine A1 receptors. A novel mechanism for differential regulation of Fc gamma receptor function. *Journal of Immunology (Baltimore, Md. : 1950)*.

[195] Tsutsui, S., Schnermann, J., Noorbakhsh, F., Henry, S., Yong, V. W., Winston, B. W., Warren, K., & Power, C. (2004). A1 Adenosine Receptor Upregulation and Activation Attenuates Neuroinflammation and Demyelination in a Model of Multiple Sclerosis. *Journal of Neuroscience*. https://doi.org/10.1523/JNEUROSCI.4271-03.2004

[196] Liao, Y., Takashima, S., Asano, Y., Asakura, M., Ogai, A., Shintani, Y., Minamino, T., Asanuma, H., Sanada, S., Kim, J., Ogita, H., Tomoike, H., Hori, M., & Kitakaze, M. (2003). Activation of Adenosine A1 Receptor Attenuates Cardiac Hypertrophy and Prevents Heart Failure in Murine Left Ventricular Pressure-Overload Model. *Circulation Research*. https://doi.org/10.1161/01.RES.0000094744.88220.62

[197] Johansson, B., Halldner, L., Dunwiddie, T. V., Masino, S. A., Poelchen, W., Giménez-Llort, L., Escorihuela, R. M., Fernández-Teruel, A., Wiesenfeld-Hallin, Z., Xu, X. J., Hårdemark, A., Betsholtz, C., Herlenius, E., & Fredholm, B. B. (2001). Hyperalgesia, anxiety, and decreased hypoxic neuroprotection in mice lacking the adenosine A1 receptor. *Proceedings of the National Academy of Sciences of the United States of America*. https://doi.org/10.1073/pnas.161292398

[198] Giménez-Llort, L., Fernández-Teruel, A., Escorihuela, R. M., Fredholm, B. B., Tobeña, A., Pekny, M., & Johansson, B. (2002). Mice lacking the adenosine A1 receptor are anxious and aggressive, but are normal learners with reduced muscle strength and survival rate. *European Journal of Neuroscience*. https://doi.org/10.1046/j.1460-9568.2002.02122.x

[199] Synowitz, M., Glass, R., Färber, K., Markovic, D., Kronenberg, G., Herrmann, K., Schnermann, J., Nolte, C., Van Rooijen, N., Kiwit, J., & Kettenmann, H. (2006). A1 adenosine receptors in microglia control glioblastoma-host interaction. *Cancer Research*. https://doi.org/10.1158/0008-5472.CAN-06-0365

[200] Sullivan, G. W. (2003). Adenosine A2A receptor agonists as anti-inflammatory agents. *Current Opinion in Investigational Drugs*.

[201] Erdmann, A. A., Gao, Z. G., Jung, U., Foley, J., Borenstein, T., Jacobson, K. A., & Fowler, D. H. (2005). Activation of Th1 and Tc1 cell adenosine A2A receptors directly inhibits IL-2 secretion in vitro and IL-2-driven expansion in vivo. *Blood*. https://doi.org/10.1182/blood-2004-04-1407

[202] Zarek, P. E., Huang, C. T., Lutz, E. R., Kowalski, J., Horton, M. R., Linden, J., Drake, C. G., & Powell, J. D. (2008). A2A receptor signaling promotes peripheral tolerance by inducing T-cell anergy and the generation of adaptive regulatory T cells. *Blood*. https://doi.org/10.1182/blood-2007-03-081646

[203] Raskovalova, T., Lokshin, A., Huang, X., Jackson, E. K., & Gorelik, E. (2006). Adenosine-mediated inhibition of cytotoxic activity and cytokine production by IL-2/NKp46-activated NK cells: Involvement of protein kinase A isozyme I (PKA I). *Immunologic Research*. https://doi.org/10.1385/ir:36:1:91

[204] Fredholm, B. B., Irenius, E., Kull, B., & Schulte, G. (2001). Comparison of the potency of adenosine as an agonist at human adenosine receptors expressed in Chinese hamster ovary cells. *Biochemical Pharmacology*. https://doi.org/10.1016/S0006-2952(00)00570-0

[205] Illes, P., Klotz, K. N., & Lohse, M. J. (2000). Signaling by extracellular nucleotides and nucleosides. *Naunyn-Schmiedeberg's Archives of Pharmacology*. https://doi.org/10.1007/s002100000308

[206] Merighi, S., Mirandola, P., Varani, K., Gessi, S., Leung, E., Baraldi, P. G., Tabrizi, M. A., & Borea, P. A. (2003). A glance at adenosine receptors: Novel target for antitumor therapy. *Pharmacology and Therapeutics*. https://doi.org/10.1016/S0163-7258(03)00084-6

[207] Hoskin, D. W., Reynolds, T., & Blay, J. (1994). Colon adenocarcinoma cells inhibit anti-CD3-activated killer cell induction. *Cancer Immunology Immunotherapy*. https://doi.org/10.1007/BF01525642

[208] Hoskin, D. W., Reynolds, T., & Blay, J. (1994). Adenosine as a possible inhibitor of killer T-cell activation in the microenvironment of solid tumours. *International Journal of Cancer*. https://doi.org/10.1002/ijc.2910590625

[209] D'Ancona, S., Ragazzi, E., Fassina, G., Mazzo, M., Gusella, M., & Berti, T. (1994). Effect of dipyridamole, 5'-(N-ethyl)-carboxamidoadenosine and 1,3-dipropyl-8-(2-amino-4-chlorophenyl)-xanthine on LoVo cell growth and morphology. *Anticancer Research*.

[210] Shaban, M., Smith, R. A., & Stone, T. W. (1995). Purine suppression of proliferation of Sertoli-like TM4 cells in culture. *Cell Proliferation*. https://doi.org/10.1111/j.1365-2184.1995.tb00053.x

[211] Mirza, A., Basso, A., Black, S., Malkowski, M., Kwee, L., Pachter, J. A., Lachowicz, J. E., Wang, Y., & Liu, S. (2005). RNA interference targeting of A1 receptor-overexpressing breast carcinoma cells leads to diminished rates of cell proliferation and induction of apoptosis. *Cancer Biology and Therapy*. https://doi.org/10.4161/cbt.4.12.2196

[212] Koshiba, M., Kojima, H., Huang, S., Apasov, S., & Sitkovsky, M. V. (1997). Memory of extracellular adenosine A(2a) purinergic receptor-mediated signaling in murine T cells. *Journal of Biological Chemistry*. https://doi.org/10.1074/jbc.272.41.25881

[213] Gessi, S., Merighi, S., Varani, K., Cattabriga, E., Benini, A., Mirandola, P., Leung, E., Mac Lennan, S., Feo, C., Baraldi, S., & Borea, P. A. (2007). Adenosine receptors in colon carcinoma tissues and colon tumoral cell lines: Focus on the A3 adenosine subtype. *Journal of Cellular Physiology*. https://doi.org/10.1002/jcp.20994

[214] Yao, Y., Sei, Y., Abbracchio, M. P., Jiang, J. L., Kim, Y. C., & Jacobson, K. A. (1997). Adenosine A3 receptor agonists protect HL-60 and U-937 cells from apoptosis induced by A3 antagonists. *Biochemical and Biophysical Research Communications*. https://doi.org/10.1006/bbrc.1997.6290

[215] Fishman, P., Bar-Yehuda, S., Ohana, G., Pathak, S., Wasserman, L., Barer, F., & Multani, A. S. (2000). Adenosine acts as an inhibitor of lymphoma cell growtha major role for the A3 adenosine receptor. *European Journal of Cancer*. https://doi.org/10.1016/S0959-8049(00)00130-1

[216] Doench, J. G., Fusi, N., Sullender, M., Hegde, M., Vaimberg, E. W., Donovan, K. F., Smith, I., Tothova, Z., Wilen, C., Orchard, R., Virgin, H. W., Listgarten, J., & Root, D. E. (2016). Optimized sgRNA design to maximize activity and minimize off-target effects of CRISPR-Cas9. *Nature Biotechnology*. https://doi.org/10.1038/nbt.3437

[217] Hsu, P. D., Scott, D. A., Weinstein, J. A., Ran, F. A., Konermann, S., Agarwala, V., Li, Y., Fine, E. J., Wu, X., Shalem, O., Cradick, T. J., Marraffini, L. A., Bao, G., & Zhang, F. (2013). DNA targeting specificity of RNA-guided Cas9 nucleases. *Nature Biotechnology*. https://doi.org/10.1038/nbt.2647

[218] Horizon Discovery, 2019, CRISPR Design Tools. Retrieved from https://horizondiscovery.com/en/ordering-and-calculation-tools/crispr-design-tool

[219] Synthego, 2019, Knockout Guide Design. Retrieved from https://design.synthego.com

[220] Heigwer, F. , Kerr, G. & Boutros, M. (2014). E-CRISP: fast CRISPR target site identification. *Nat. Methods* 11, 122-123 https://doi.org/10.1038/nmeth.2812

[221] Liu, H., Wei, Z., Dominguez, A., Li, Y., Wang, X., Qi, L.S. (2015) CRISPR-ERA: a comprehensive design tool for CRISPR-mediated gene editing, repression and activation. *Bioinformatics.* https://doi.org/10.1093/bioinformatics/btv423

[222] Labun, K., Montague, T. G., Krause, M., Torres Cleuren, Y. N., Tjeldnes, H., & Valen, E. (0-2019) CHOPCHOP v3: expanding the CRISPR web toolbox beyond genome editing. *Nucleic Acids Research.* https://doi.org/10.1093/nar/gkz365

[223] Jean-Paul, C., Maximilian, H. (2018) CRISPOR: intuitive guide selection for CRISPR/Cas9 genome editing experiments and screens. *Nucleic Acids Research*. https://doi.org/10.1093/nar/gky354

[224] Benchling, 2019, CRISPR Guide RNA Design. Retrieved from https://benchling.com

[225] Deskgen, 2019, CRISPR Design Tool, Retrieved from https://deskgen.com

[226] Bae, S., Park, J., & Kim, J.-S. (2014) Cas-OFFinder: A fast and versatile algorithm that searches for potential off-target sites of Cas9 RNA-guided endonucleases. *Bioinformatics* https://doi.org/10.1093/bioinformatics/btu048

[227] Ran, F. A., Hsu, P. D., Wright, J., Agarwala, V., Scott, D. A., & Zhang, F. (2013). Genome engineering using the CRISPR-Cas9 system. *Nature Protocols*. https://doi.org/10.1038/nprot.2013.143

[228] Doench, J. G., Hartenian, E., Graham, D. B., Tothova, Z., Hegde, M., Smith, I., Sullender, M., Ebert, B. L., Xavier, R. J., & Root, D. E. (2014). Rational design of highly active sgRNAs for CRISPR-Cas9-mediated gene inactivation. *Nature Biotechnology*. https://doi.org/10.1038/nbt.3026

[229] Sanjana, N. E., Shalem, O., & Zhang, F. (2014). Improved vectors and genome-wide libraries for CRISPR screening. *Nature Methods*. https://doi.org/10.1038/nmeth.3047

[230] Shalem, O., Sanjana, N. E., Hartenian, E., Shi, X., Scott, D. A., Mikkelsen, T. S., Heckl, D., Ebert, B. L., Root, D. E., Doench, J. G., & Zhang, F. (2014). Genome-scale CRISPR-Cas9 knockout screening in human cells. *Science*. https://doi.org/10.1126/science.1247005

[231] Ferlay J, Ervik M, Lam F, Colombet M, Mery L, Piñeros M, Znaor A, Soerjomataram I, Bray F (2020). Global Cancer Observatory: Cancer Today. Lyon, France: International Agency for Research on Cancer. Available from: https://gco.iarc.fr/today, accessed [12.01.2021].

[232] Nakano, N., Matsuda, S., Ichimura, M., Minami, A., Ogino, M., Murai, T., & Kitagishi, Y. (2017). PI3K/AKT signaling mediated by G protein-coupled receptors is involved in neurodegenerative Parkinson's disease (Review). In *International Journal of Molecular Medicine*. https://doi.org/10.3892/ijmm.2016.2833

[233] New, D. C., Wu, K., Kwok, A. W. S., & Wong, Y. H. (2007). G protein-coupled receptor-induced Akt activity in cellular proliferation and apoptosis. *In FEBS Journal*. https://doi.org/10.1111/j.1742-4658.2007.06116.x

[234] Eishingdrelo, H. (2013). Minireview: Targeting GPCR Activated ERK Pathways for Drug Discovery. *Current Chemical Genomics and Translational Medicine*. https://doi.org/10.2174/2213988501307010009

[235] Leroy, D., Missotten, M., Waltzinger, C., Martin, T., & Scheer, A. (2007). G protein-coupled receptor-mediated ERK1/2 phosphorylation: Towards a generic sensor of GPCR activation. *Journal of Receptors and Signal Transduction*. https://doi.org/10.1080/10799890601112244

[236] Lennon, P. F., Taylor, C. T., Stahl, G. L., & Colgan, S. P. (1998). Neutrophil-derived 5'-adenosine monophosphate promotes endothelial barrier function via CD73-mediated conversion to adenosine and endothelial A(2B) receptor activation. *Journal of Experimental Medicine*. https://doi.org/10.1084/jem.188.8.1433

[237] Eltzschig, H. K., Sitkovsky, M. V., & Robson, S. C. (2012). Purinergic Signaling during Inflammation. *New England Journal of Medicine.* https://doi.org/10.1056/nejmra1205750

[238] Kong, T., Westerman, K. A., Faigle, M., Eltzschig, H. K., & Colgan, S. P. (2006). HIF-dependent induction of adenosine A2B receptor in hypoxia. *The FASEB Journal*. https://doi.org/10.1096/fj.06-6419com

[239] Horenstein, A. L., Chillemi, A., Zaccarello, G., Bruzzone, S., Quarona, V., Zito, A., Serra, S., & Malavasi, F. (2013). A CD38/CD203A/CD73 ectoenzymatic pathway independent of CD39 drives a novel adenosinergic loop in human T lymphocytes. *OncoImmunology*. https://doi.org/10.4161/onci.26246

[240] Peola, S., Borrione, P., Matera, L., Malavasi, F., Pileri, A., & Massaia, M. (1996). Selective induction of CD73 expression in human lymphocytes by CD38 ligation: a novel pathway linking signal transducers with ecto-enzyme activities. *Journal of Immunology* (Baltimore, Md. : 1950).

[241] Mizumoto, N., Kumamoto, T., Robson, S. C., Sévigny, J., Matsue, H., Enjyoji, K., & Takashima, A. (2002). CD39 is the dominant Langerhans cell-associated ecto-NTPDase: Modulatory roles in inflammation and immune responsiveness. *Nature Medicine*. https://doi.org/10.1038/nm0402-358

APPENDIX

A. Mutation profiles of colorectal cancer cell lines[31]

Cell lines	MS-status	KRAS	BRAF	PIK3CA	TP53
DLD-1	MSI	Protein: p.G13D CDS: c.38G>A Alleles: heterozygous Codon change: GGC>GAC	-	Protein: p.E545K; D549N CDS: c.1633G>A; 1645G>A Alleles: heterozygous Codon change: GAG>AAG; GAT>AAT	Protein: p.S241F CDS: c.722C>T Alleles: heterozygous Codon change: TCC>TTC
HT-29	MSS	-	Protein: p.V600E CDS: c.1799T>A Alleles: heterozygous Codon change: GTG>GAG	Protein: p.P449T CDS: c.1345C>A Alleles: heterozygous Codon change: -	Protein: p.R273H CDS: c.818G>A Alleles: homozygous Codon change: CGT>CAT
LoVo	MSI	Protein: p.G13D;A14V CDS: c.38G>A;41C>T Alleles: heterozygous Codon change: GGC>GCA;GAC>GTC	-	-	-
RKO	MSI	-	Protein: p.V600E CDS: c.1799T>A Alleles: heterozygous Codon change: GTG>GAG	Protein: p.H1047R CDS: c.3140A>G Alleles: heterozygous Codon change: CAT>CGT	-
SW480	MSS	Protein: p.G12V CDS: c.35G>T Alleles: homozygous Codon change: GGT>GTT	-	-	Protein: p.R273H;P309S CDS: c.818G>A;925C>T Alleles: homozygous Codon change: CGT>CAT;CCC>TCC

SW620	MSS	Protein: p.G12V CDS: c.35G>T Alleles: homozygous Codon change: GGT>GTT	-	-	Protein: p.R273H;P309S CDS: c.818G>A;925C>T Alleles: homozygous Codon change: CGT>CAT;CCC>TCC

Colon-like cell lines			Undifferentiated cell lines		
CL-34	HT29/WiDr	NCI-H508	Caco2	DLD-1/HCT15	SW48
CL-40	IS3	SW1116	CL-11	IS1	SW480/SW620
Colo205	KM12	SW1463	Co115	LoVo	SW837
EB	LS1034	SW403	Colo678	RKO	HCT116
FRI	LS174T	SW948	TC71		
HCC2998	V9P				

B. Classification of colon cancer cells[35]. By using ssGSEA scores, colorectal cancer cell lines have been categorized in two different classes including colon-like cell lines and undifferentiated cell lines. *Adapted from "Multi-omics of 34 colorectal cancer cell lines – a resource for biomedical studies" by Berg K. C. G. et. al., 2017*

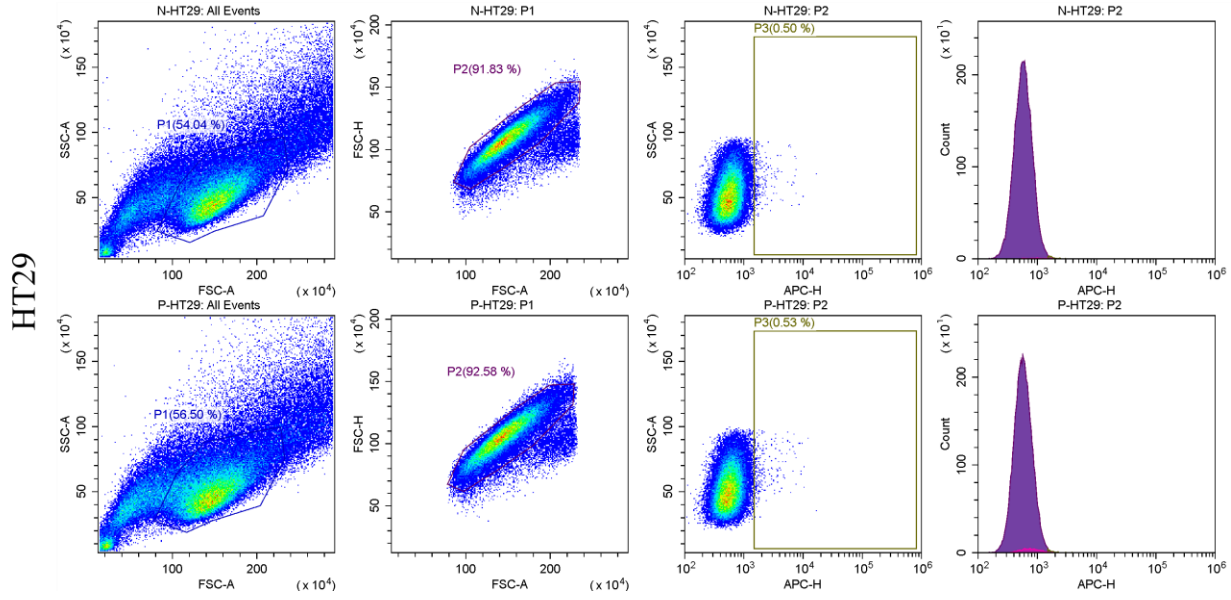

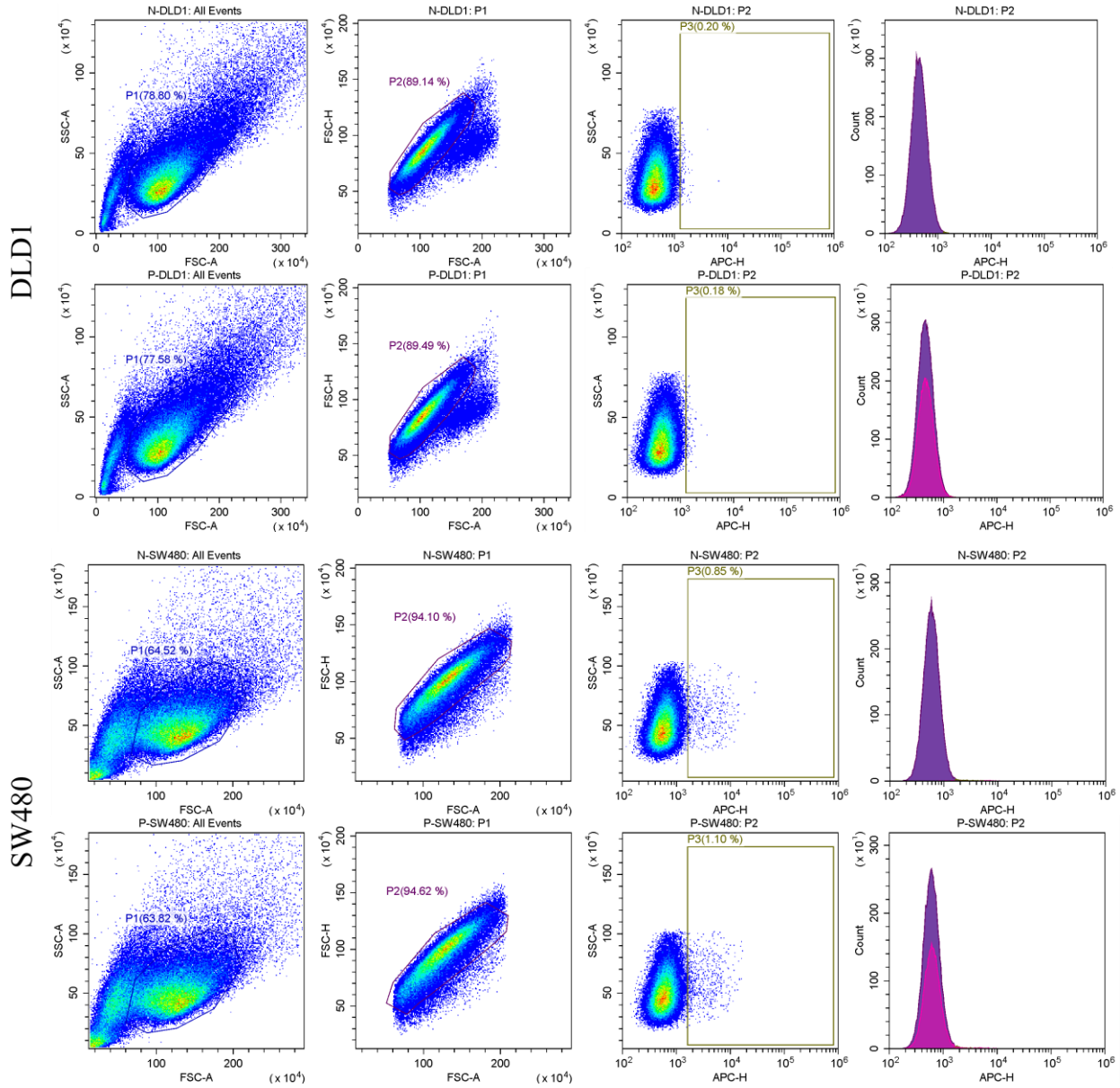
DLD1
SW480
N-DLD1: All Events
P1(78.80 %)
N-DLD1: P1
P2(89.14 %)
N-DLD1: P2
P3(0.20 %)
N-DLD1: P2
P-DLD1: All Events
P1(77.58 %)
P-DLD1: P1
P2(89.49 %)
P-DLD1: P2
P3(0.18 %)
P-DLD1: P2
N-SW480: All Events
P1(64.52 %)
N-SW480: P1
P2(94.10 %)
N-SW480: P2
P3(0.85 %)
N-SW480: P2
P-SW480: All Events
P1(63.82 %)
P-SW480: P1
P2(94.62 %)
P-SW480: P2
P3(1.10 %)
P-SW480: P2
SSC-A
FSC-A
FSC-H
APC-H
Count

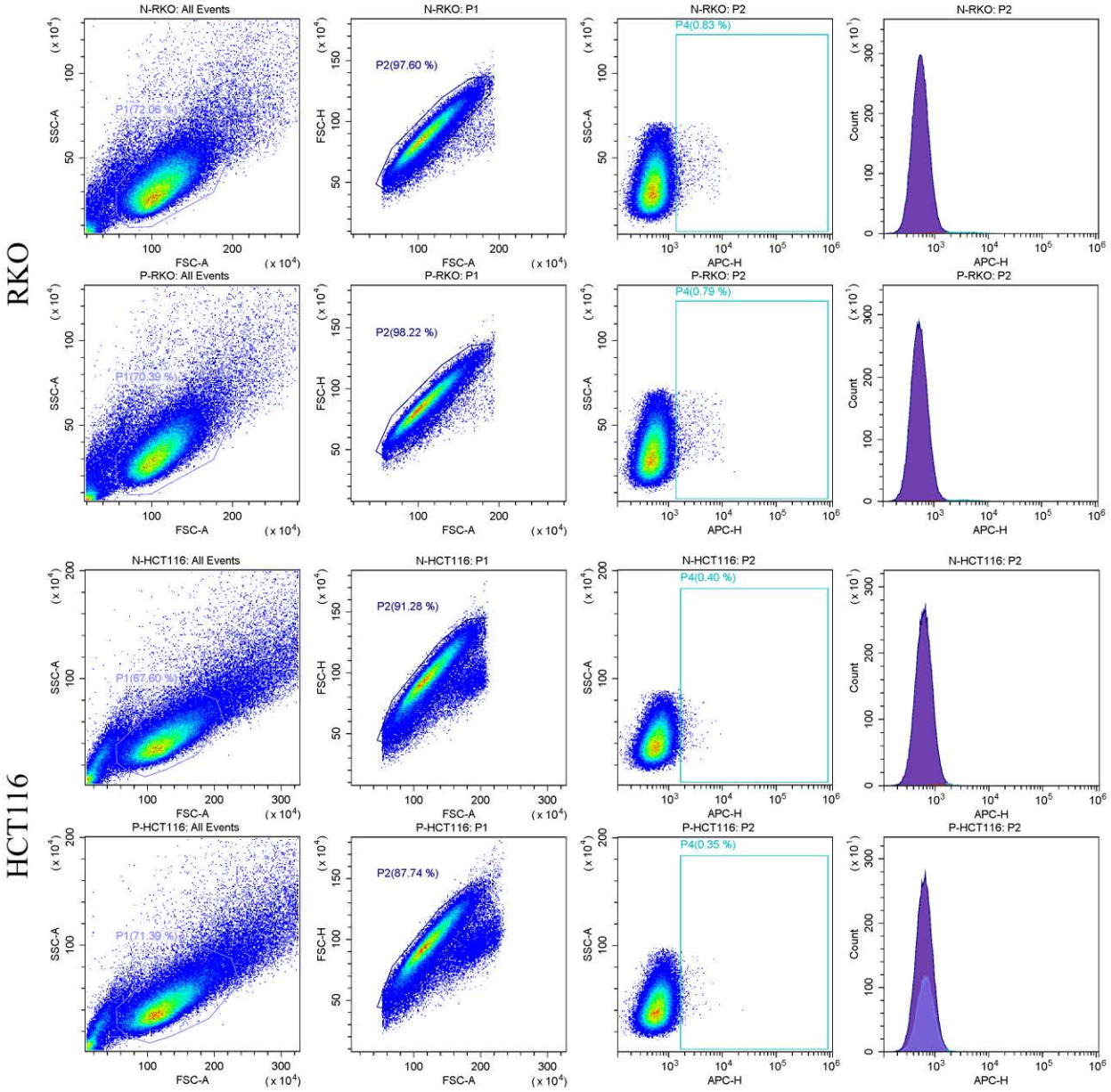
RKO
HCT116
N-RKO: All Events
N-RKO: P1
N-RKO: P2
N-RKO: P2
P2(97.60 %)
P4(0.83 %)
P-RKO: All Events
P-RKO: P1
P-RKO: P2
P-RKO: P2
P2(98.22 %)
P4(0.79 %)
N-HCT116: All Events
N-HCT116: P1
N-HCT116: P2
N-HCT116: P2
P2(91.28 %)
P4(0.40 %)
P-HCT116: All Events
P-HCT116: P1
P-HCT116: P2
P-HCT116: P2
P2(87.74 %)
P4(0.35 %)
SSC-A
FSC-A
FSC-H
APC-H
Count

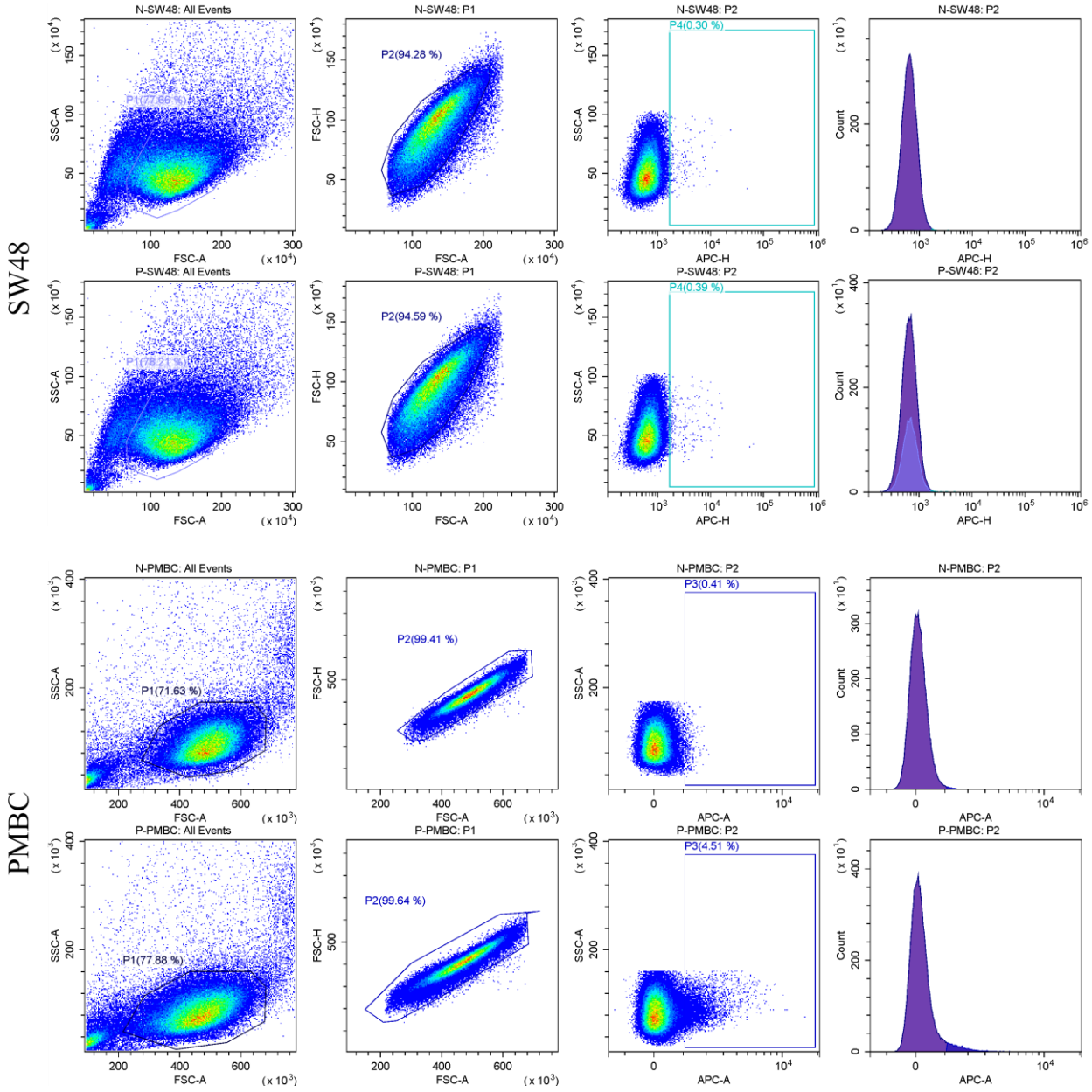

C. Expression level of PSE001 on the surface of CRC cell lines. PSE001 level was measured in six different CRC cell lines and in PBMC by flow cytometry. The results are provided together with their background staining. The first row for each cell line is representing the background for that specific cell line and the second row is showing the staining by APC-conjugated PSE001 antibody. The results belonging to HT29, DLD1, SW480, RKO, HCT116, SW620, and SW48 are shown, respectively.

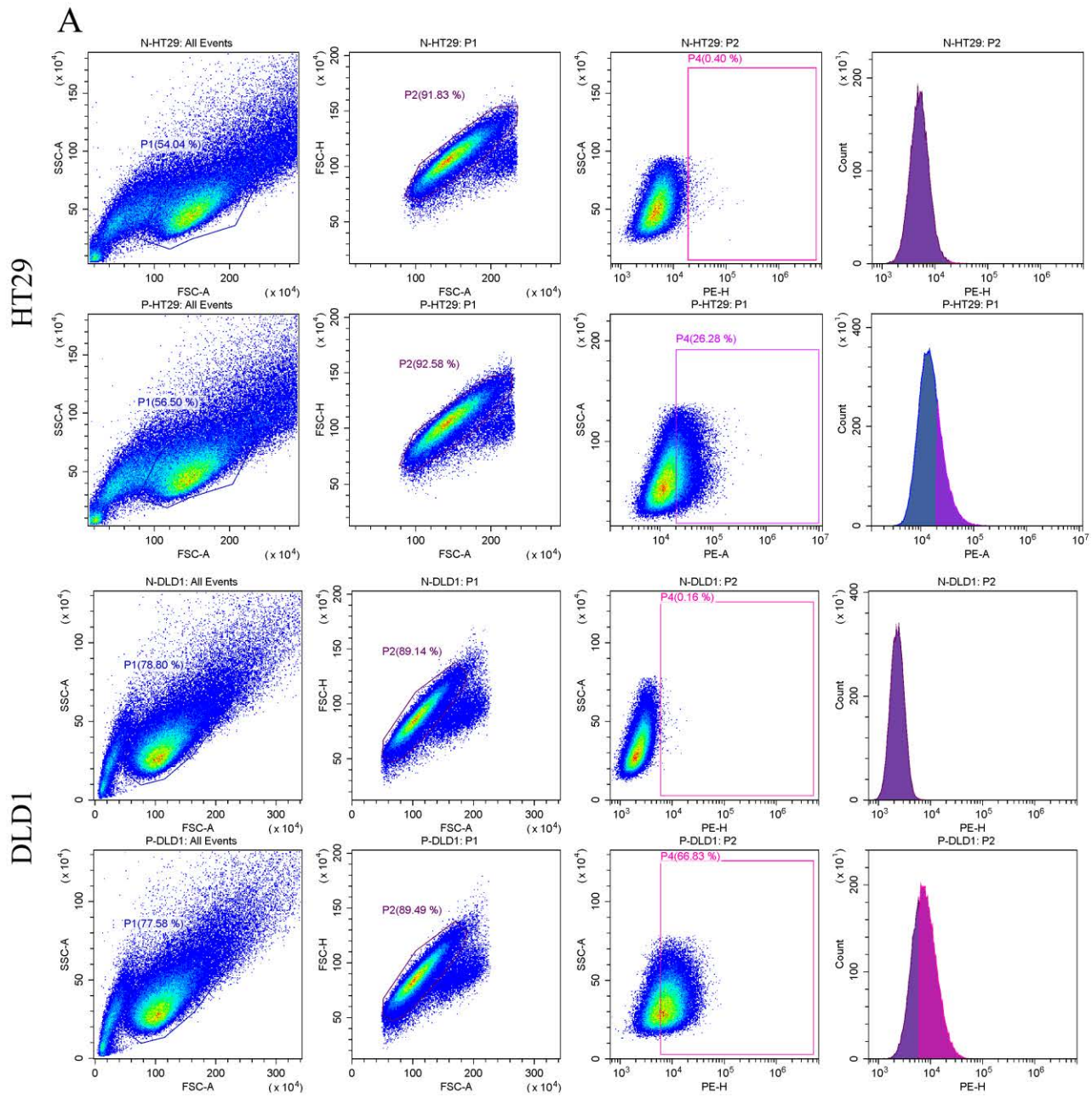
A
HT29
DLD1
N-HT29: All Events
P1(54.04 %)
N-HT29: P1
P2(91.83 %)
N-HT29: P2
P4(0.40 %)
P-HT29: All Events
P1(56.50 %)
P-HT29: P1
P2(92.58 %)
P-HT29: P1
P4(26.28 %)
N-DLD1: All Events
P1(78.80 %)
N-DLD1: P1
P2(89.14 %)
N-DLD1: P2
P4(0.16 %)
P-DLD1: All Events
P1(77.58 %)
P-DLD1: P1
P2(89.49 %)
P-DLD1: P2
P4(66.83 %)
SSC-A
FSC-A
FSC-H
PE-H
PE-A
Count

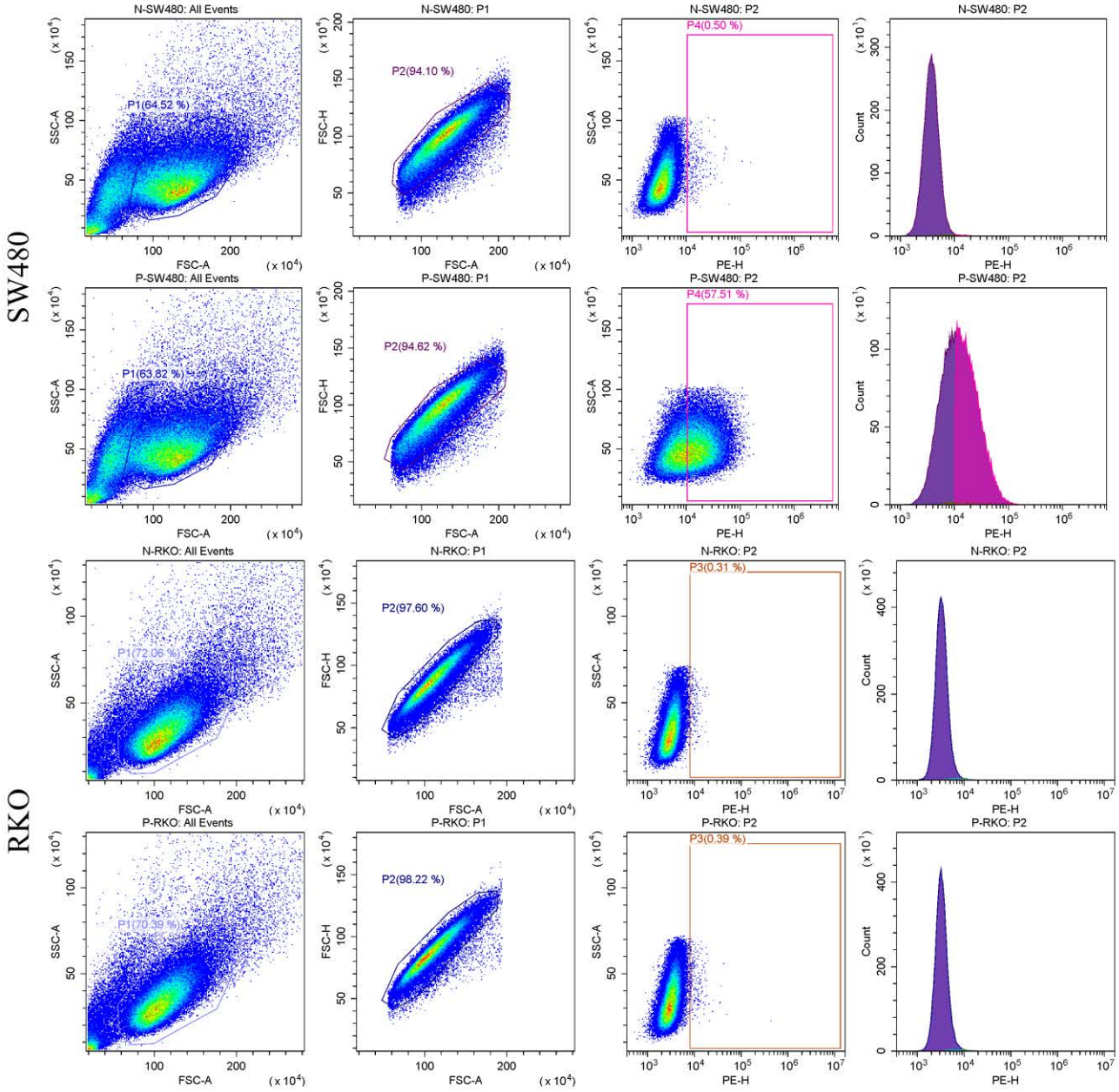
SW480
RKO
N-SW480: All Events
P1(64.52 %)
N-SW480: P1
P2(94.10 %)
N-SW480: P2
P4(0.50 %)
N-SW480: P2
P-SW480: All Events
P1(63.82 %)
P-SW480: P1
P2(94.62 %)
P-SW480: P2
P4(57.51 %)
P-SW480: P2
N-RKO: All Events
P1(72.06 %)
N-RKO: P1
P2(97.60 %)
N-RKO: P2
P3(0.31 %)
N-RKO: P2
P-RKO: All Events
P1(70.39 %)
P-RKO: P1
P2(98.22 %)
P-RKO: P2
P3(0.39 %)
P-RKO: P2
SSC-A
FSC-A
FSC-H
PE-H
Count
(x 10⁴)
(x 10³)
(x 10¹)

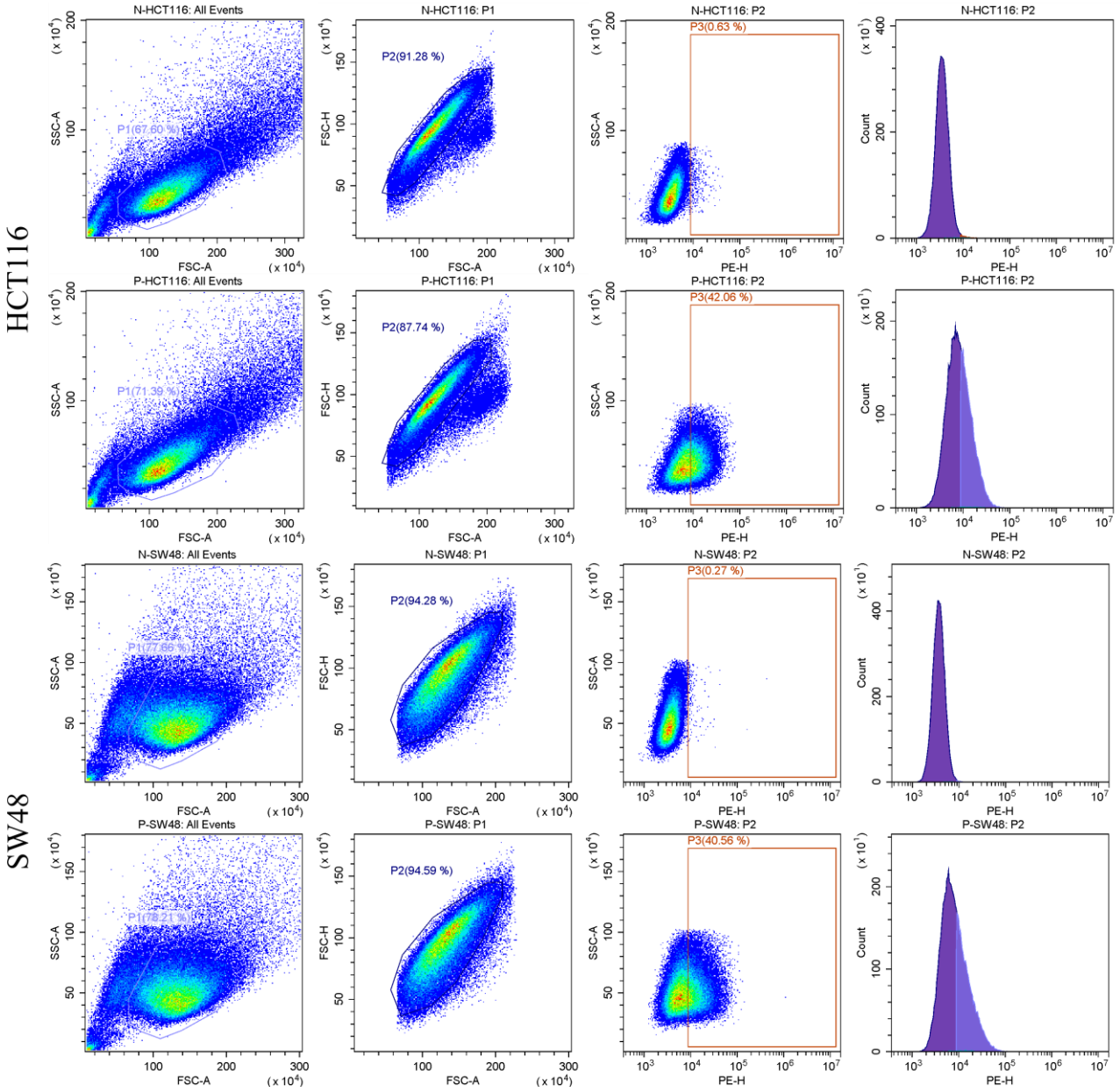

D. Expression level of PSE002 on the surface of CRC cell lines. PSE002 level was measured in six different CRC cell lines by flow cytometry. The results are provided together with their background staining. The first row for each cell line is representing the background for that specific cell line and the second row is showing the staining by PE-conjugated PSE002 antibody. The results belonging to HT29, DLD1, SW480, RKO, HCT116, SW620, and SW48 are shown, respectively.

A

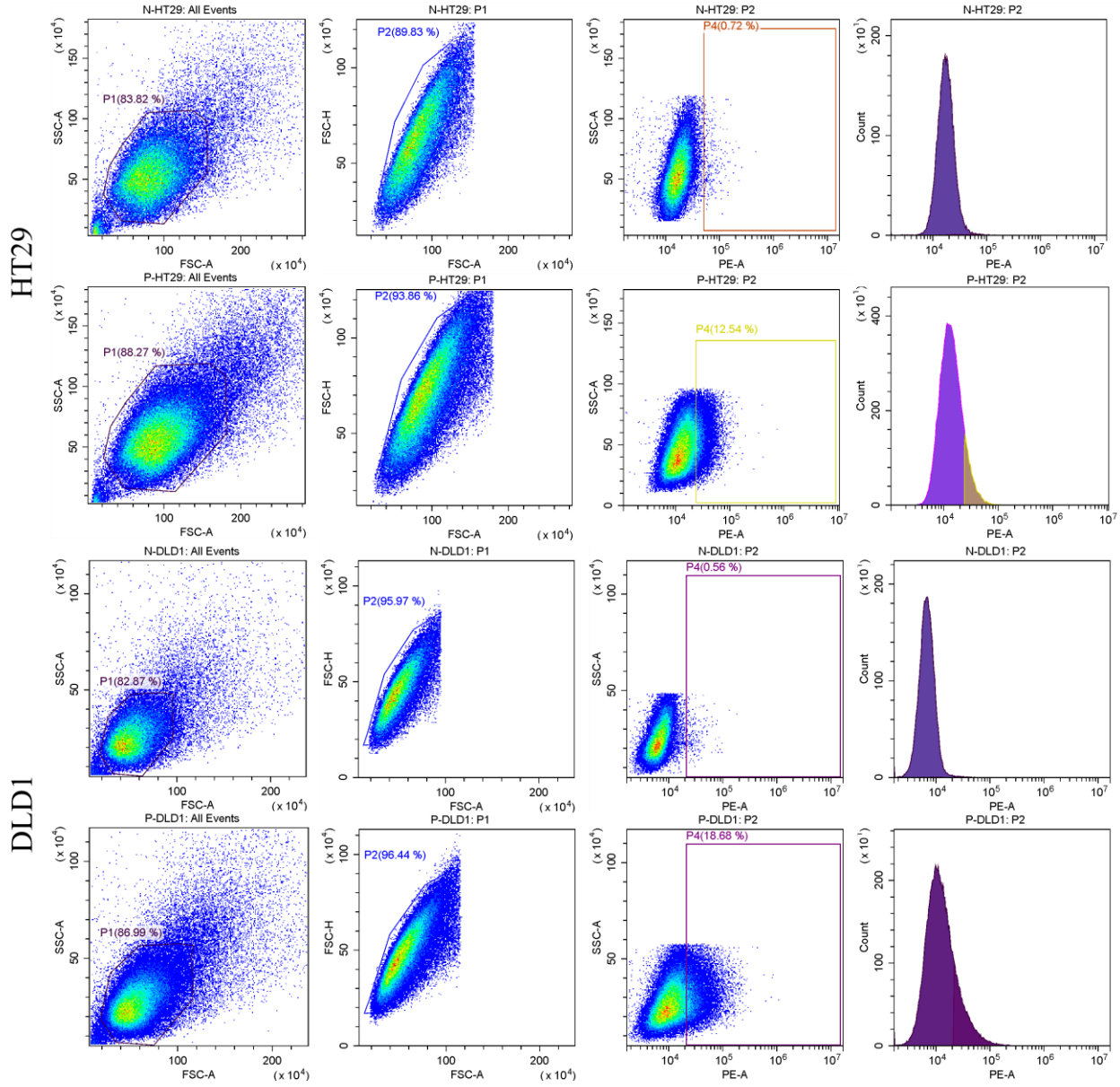
HT29
DLD1
N-HT29: All Events
P1(83.82 %)
N-HT29: P1
P2(89.83 %)
N-HT29: P2
P4(0.72 %)
N-HT29: P2
P-HT29: All Events
P1(88.27 %)
P-HT29: P1
P2(93.86 %)
P-HT29: P2
P4(12.54 %)
P-HT29: P2
N-DLD1: All Events
P1(82.87 %)
N-DLD1: P1
P2(95.97 %)
N-DLD1: P2
P4(0.56 %)
N-DLD1: P2
P-DLD1: All Events
P1(86.99 %)
P-DLD1: P1
P2(96.44 %)
P-DLD1: P2
P4(18.68 %)
P-DLD1: P2
SSC-A
FSC-A
FSC-H
PE-A
Count

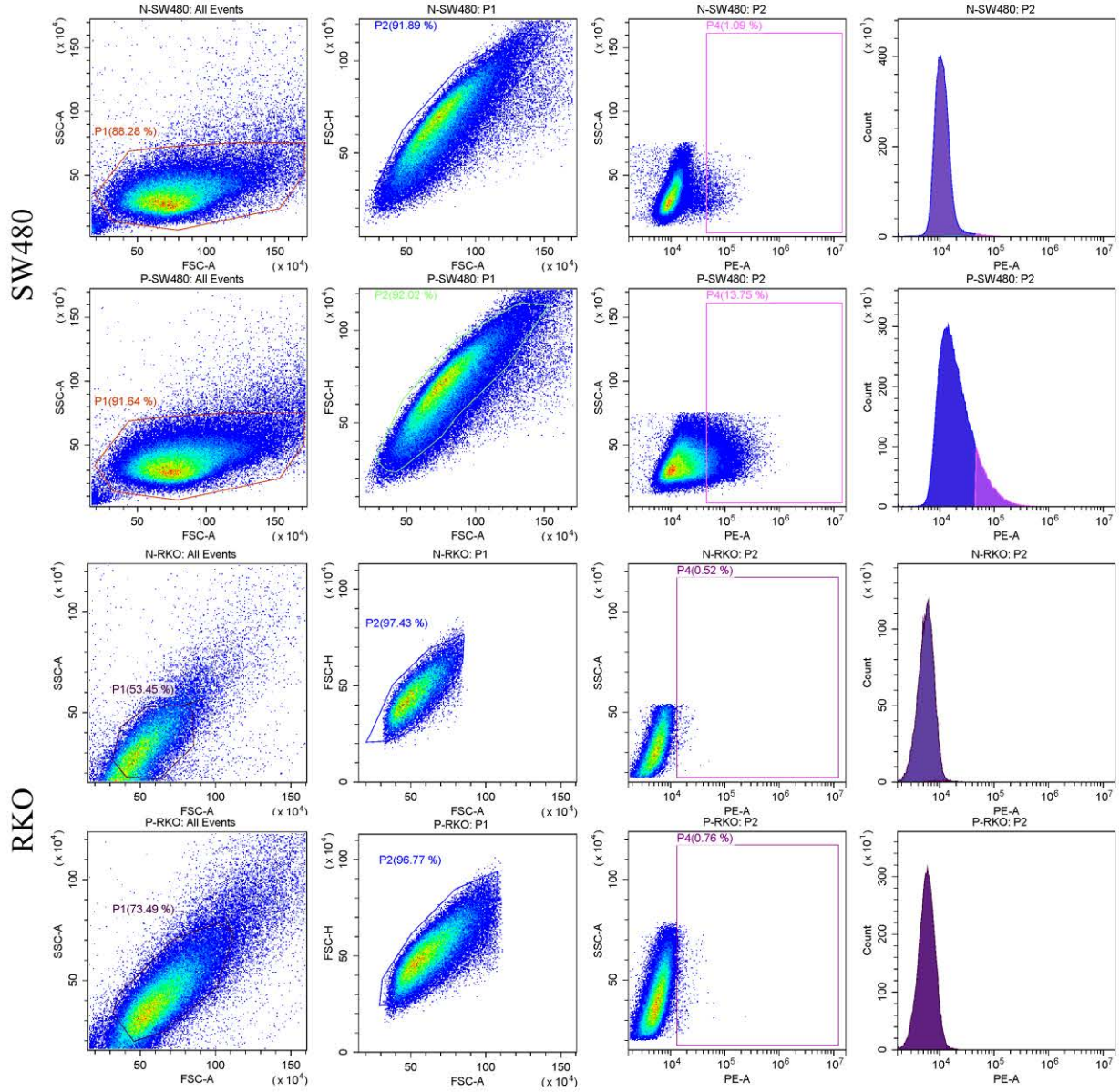
SW480
RKO
N-SW480: All Events
P1(88.28 %)
N-SW480: P1
P2(91.89 %)
N-SW480: P2
P4(1.09 %)
N-SW480: P2
P-SW480: All Events
P1(91.64 %)
P-SW480: P1
P2(92.02 %)
P-SW480: P2
P4(13.75 %)
P-SW480: P2
N-RKO: All Events
P1(53.45 %)
N-RKO: P1
P2(97.43 %)
N-RKO: P2
P4(0.52 %)
N-RKO: P2
P-RKO: All Events
P1(73.49 %)
P-RKO: P1
P2(96.77 %)
P-RKO: P2
P4(0.76 %)
P-RKO: P2
SSC-A
FSC-A
FSC-H
PE-A
Count

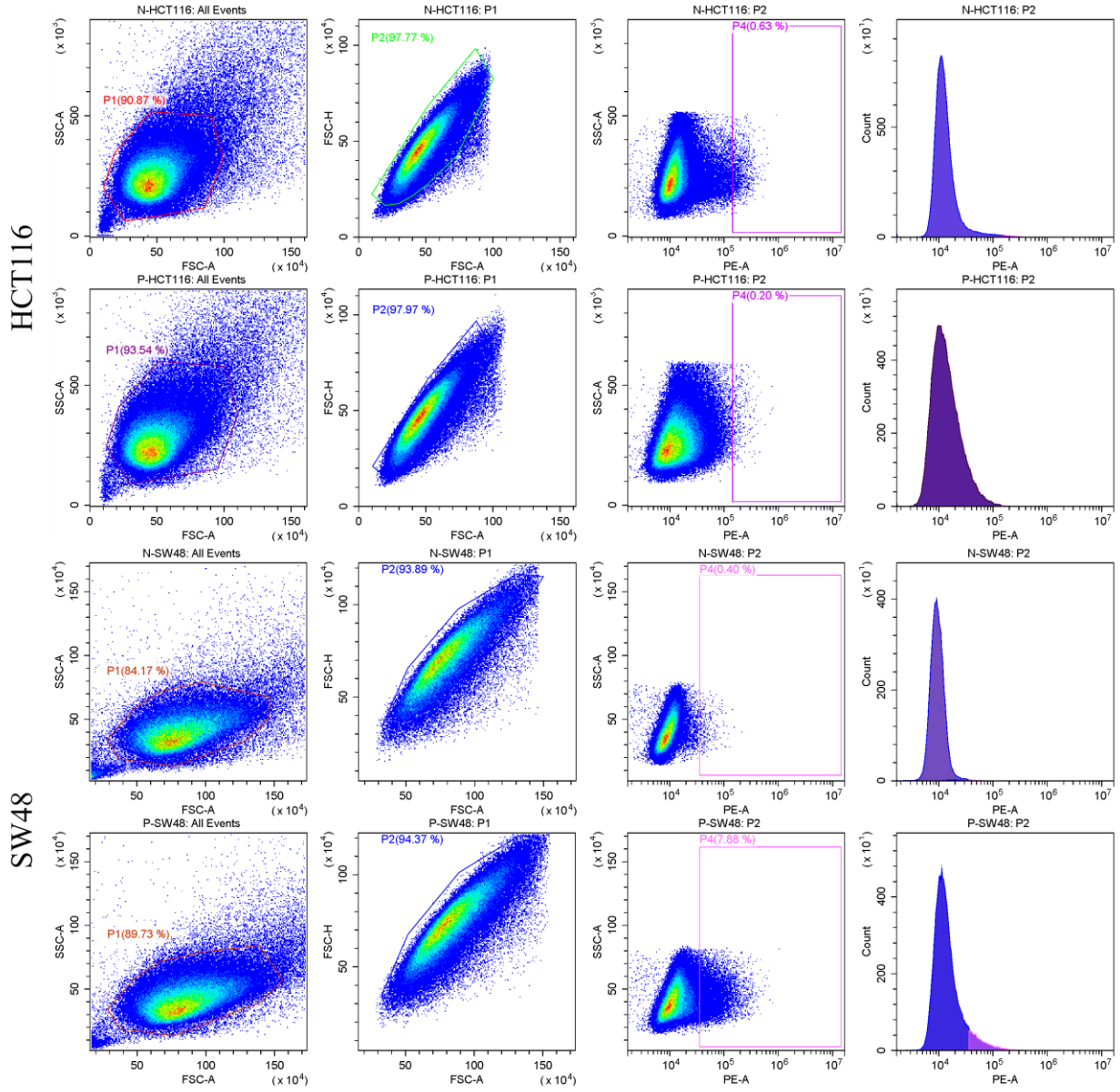

E. Expression level of PSE002 in the intracellular compartment of CRC cell lines. PSE002 level was measured in six different CRC cell lines by flow cytometry. The results are provided together with their background staining. The first row for each cell line is representing the background for that specific cell line and second row is showing the staining by PE-conjugated PSE002 antibody. The results belonging to HT29, DLD1, SW480, RKO, HCT116, SW620, and SW48 are shown, respectively.

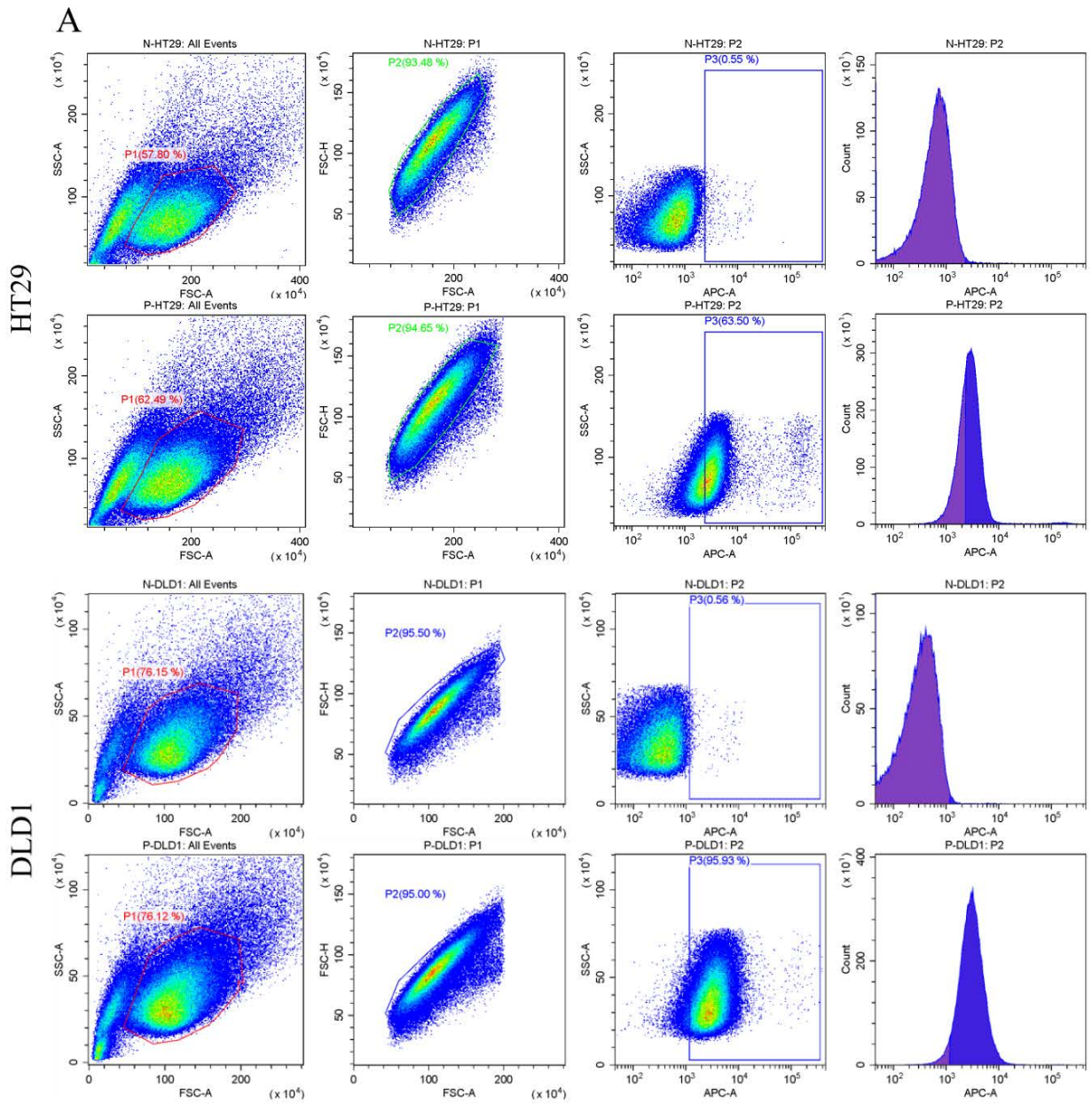
A
HT29
DLD1
N-HT29: All Events
P1(57.80 %)
N-HT29: P1
P2(93.48 %)
N-HT29: P2
P3(0.55 %)
N-HT29: P2
P-HT29: All Events
P1(62.49 %)
P-HT29: P1
P2(94.65 %)
P-HT29: P2
P3(63.50 %)
P-HT29: P2
N-DLD1: All Events
P1(76.15 %)
N-DLD1: P1
P2(95.50 %)
N-DLD1: P2
P3(0.56 %)
N-DLD1: P2
P-DLD1: All Events
P1(76.12 %)
P-DLD1: P1
P2(95.00 %)
P-DLD1: P2
P3(95.93 %)
P-DLD1: P2
SSC-A
FSC-A
FSC-H
APC-A
Count

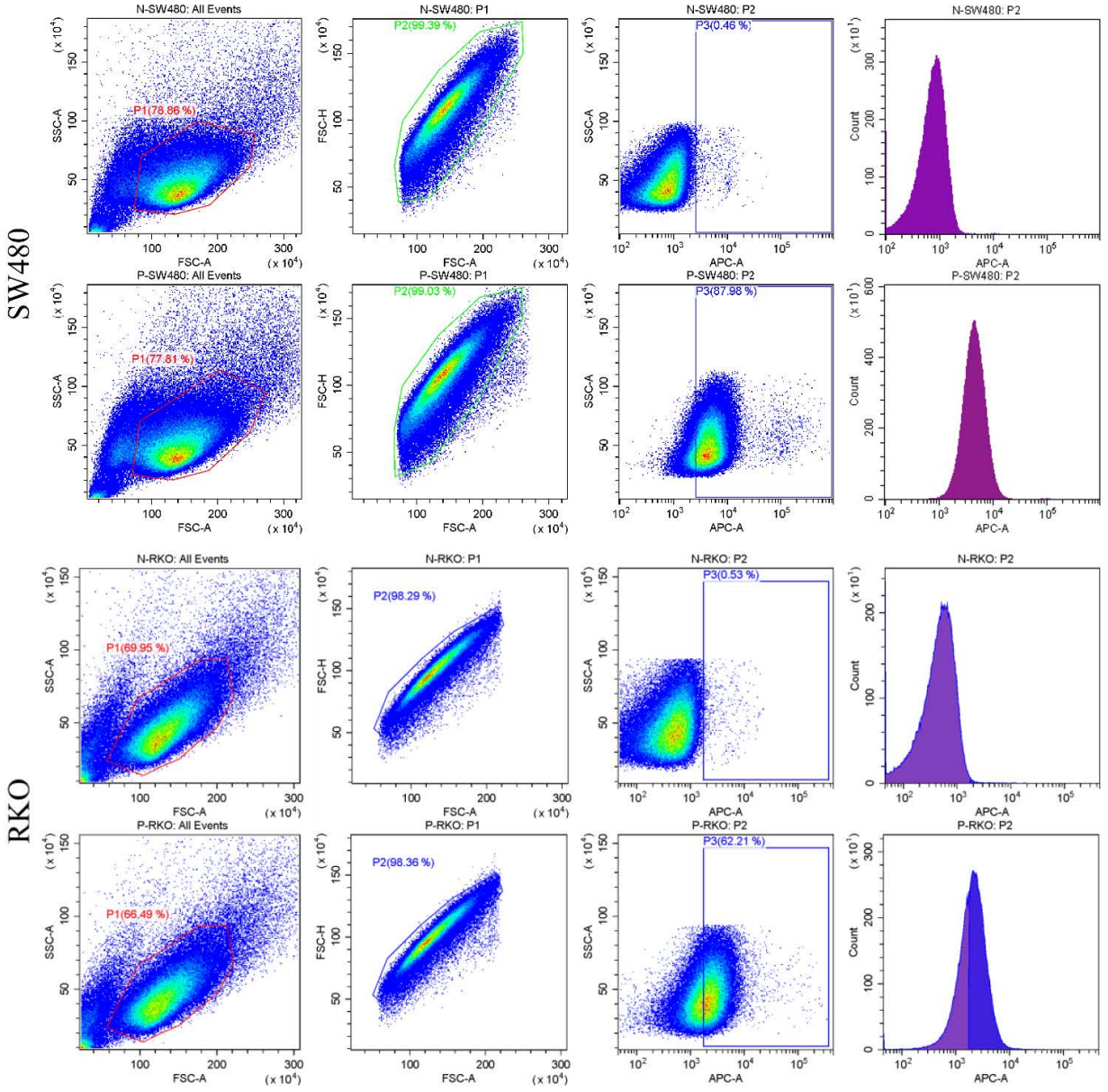
SW480
RKO
N-SW480: All Events
P1(78.86 %)
N-SW480: P1
P2(99.39 %)
N-SW480: P2
P3(0.46 %)
N-SW480: P2
P-SW480: All Events
P1(77.81 %)
P-SW480: P1
P2(99.03 %)
P-SW480: P2
P3(87.98 %)
P-SW480: P2
N-RKO: All Events
P1(69.95 %)
N-RKO: P1
P2(98.29 %)
N-RKO: P2
P3(0.53 %)
N-RKO: P2
P-RKO: All Events
P1(66.49 %)
P-RKO: P1
P2(98.36 %)
P-RKO: P2
P3(62.21 %)
P-RKO: P2
SSC-A
FSC-A
FSC-H
APC-A
Count

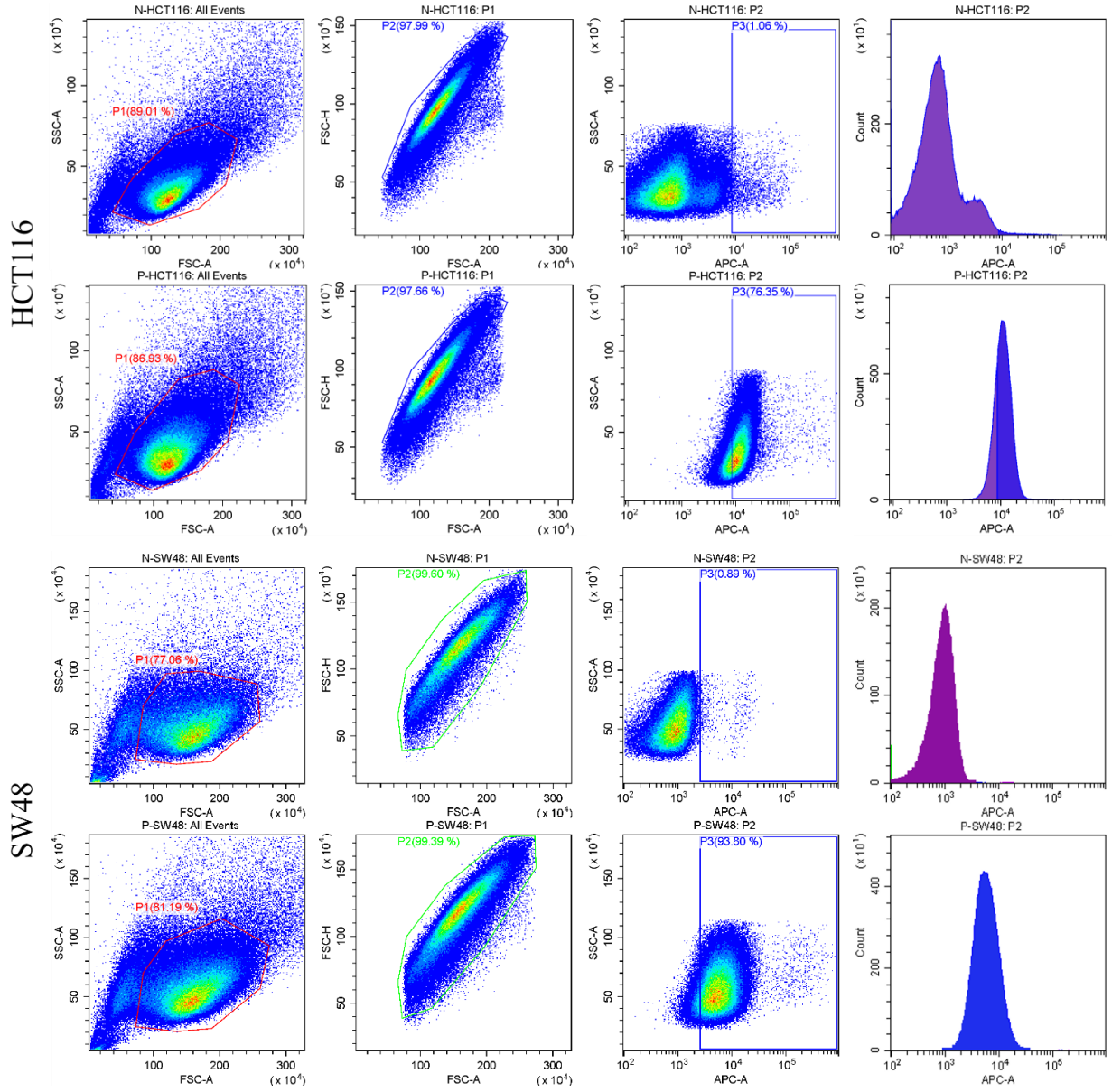

F. Expression level of PSC003 on the surface of CRC cell lines. PSC003 level was measured in six different CRC cell lines by flow cytometry. The results are provided together with their background staining. The first row for each cell line is representing the background for that specific cell line and second row is showing the staining by APC-conjugated PSC003 antibody. The results belonging to HT29, DLD1, SW480, RKO, HCT116, SW620, and SW48 are shown, respectively.

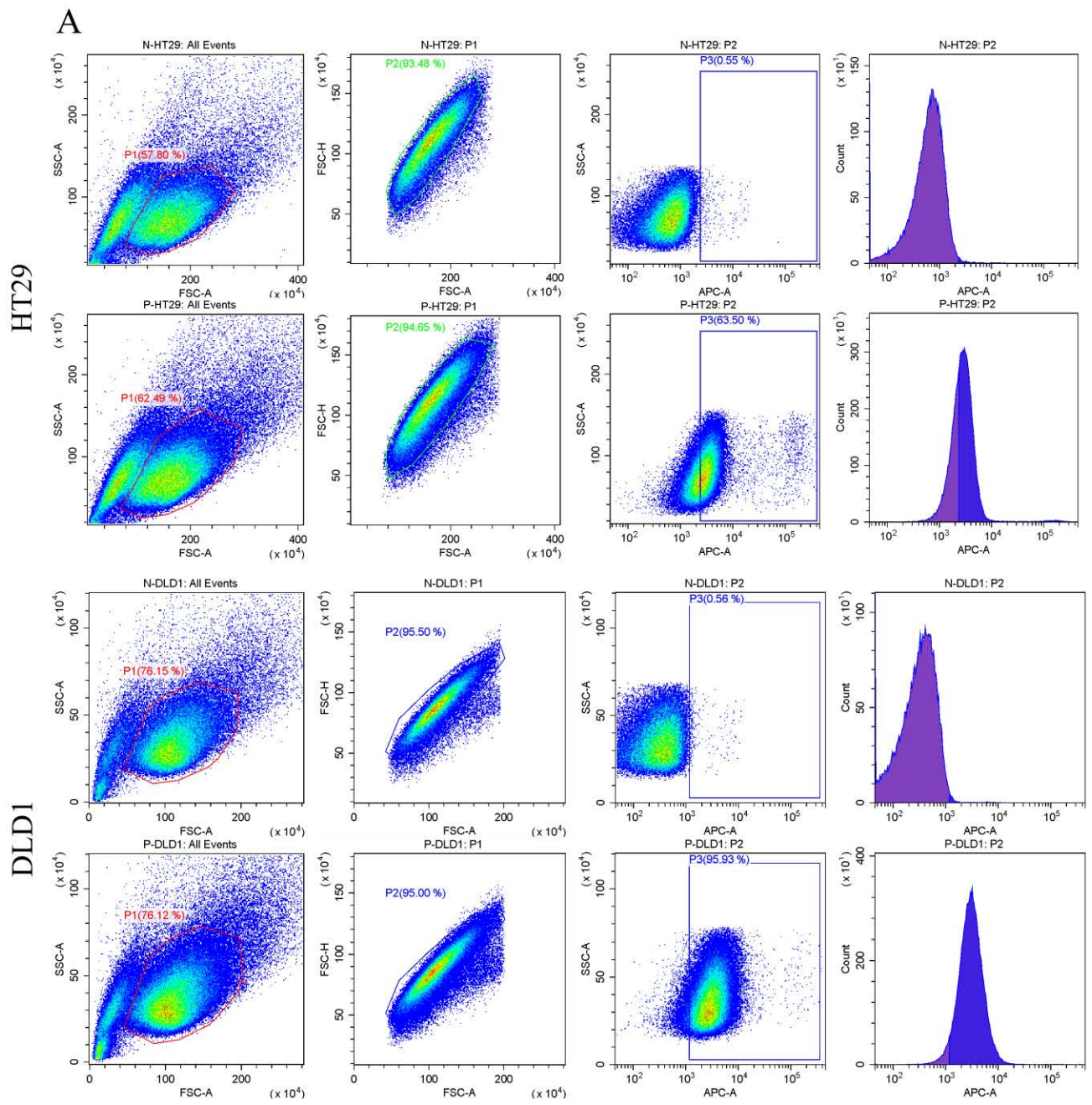
A
HT29
DLD1
N-HT29: All Events
P1(57.80 %)
N-HT29: P1
P2(93.48 %)
N-HT29: P2
P3(0.55 %)
N-HT29: P2
P-HT29: All Events
P1(62.49 %)
P-HT29: P1
P2(94.65 %)
P-HT29: P2
P3(63.50 %)
P-HT29: P2
N-DLD1: All Events
P1(76.15 %)
N-DLD1: P1
P2(95.50 %)
N-DLD1: P2
P3(0.56 %)
N-DLD1: P2
P-DLD1: All Events
P1(76.12 %)
P-DLD1: P1
P2(95.00 %)
P-DLD1: P2
P3(95.93 %)
P-DLD1: P2
SSC-A
FSC-A
FSC-H
APC-A
Count

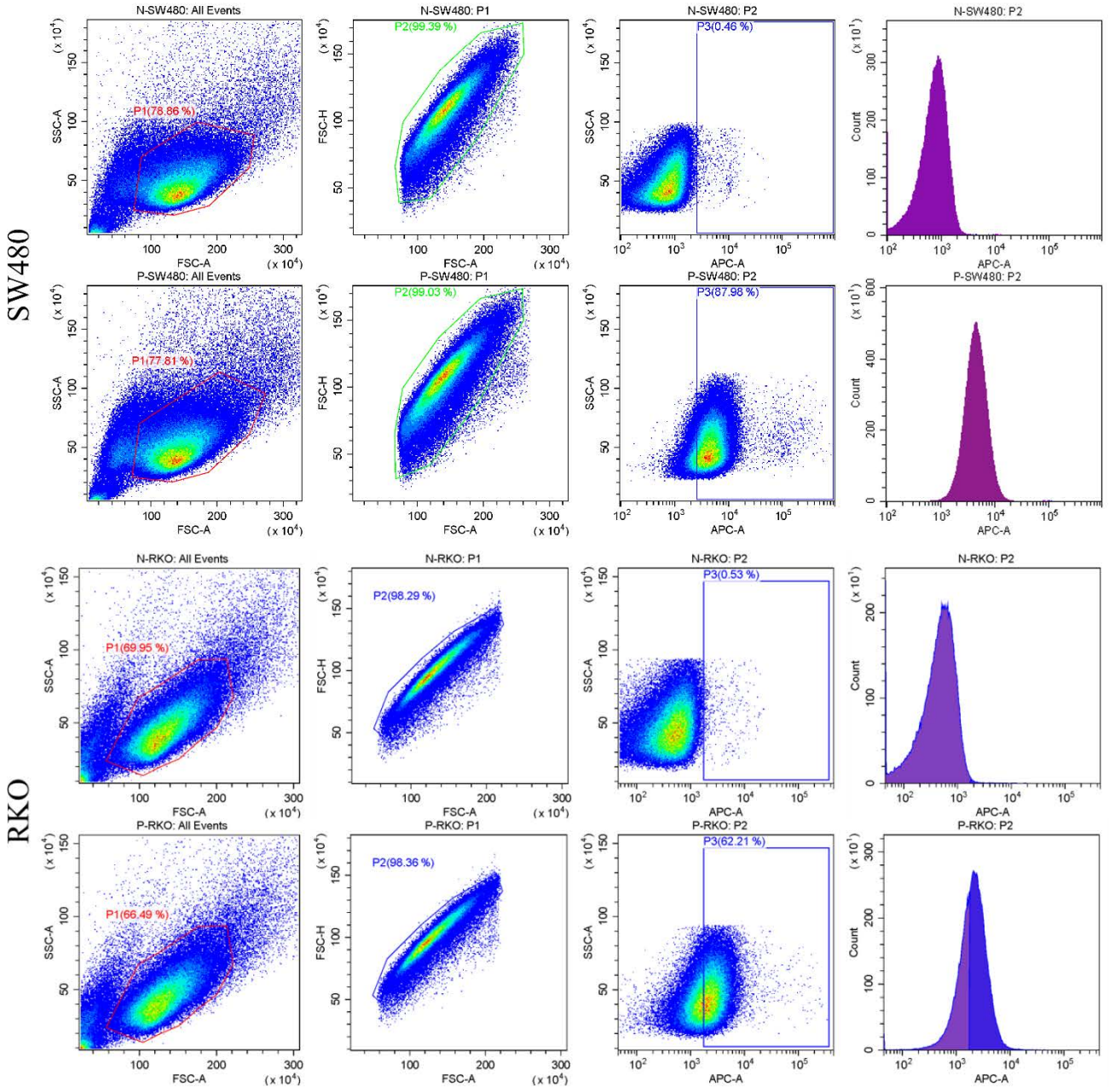
SW480
RKO
N-SW480: All Events
P1(78.86 %)
N-SW480: P1
P2(99.39 %)
N-SW480: P2
P3(0.46 %)
N-SW480: P2
P-SW480: All Events
P1(77.81 %)
P-SW480: P1
P2(99.03 %)
P-SW480: P2
P3(87.98 %)
P-SW480: P2
N-RKO: All Events
P1(69.95 %)
N-RKO: P1
P2(98.29 %)
N-RKO: P2
P3(0.53 %)
N-RKO: P2
P-RKO: All Events
P1(66.49 %)
P-RKO: P1
P2(98.36 %)
P-RKO: P2
P3(62.21 %)
P-RKO: P2
SSC-A
FSC-A
FSC-H
APC-A
Count

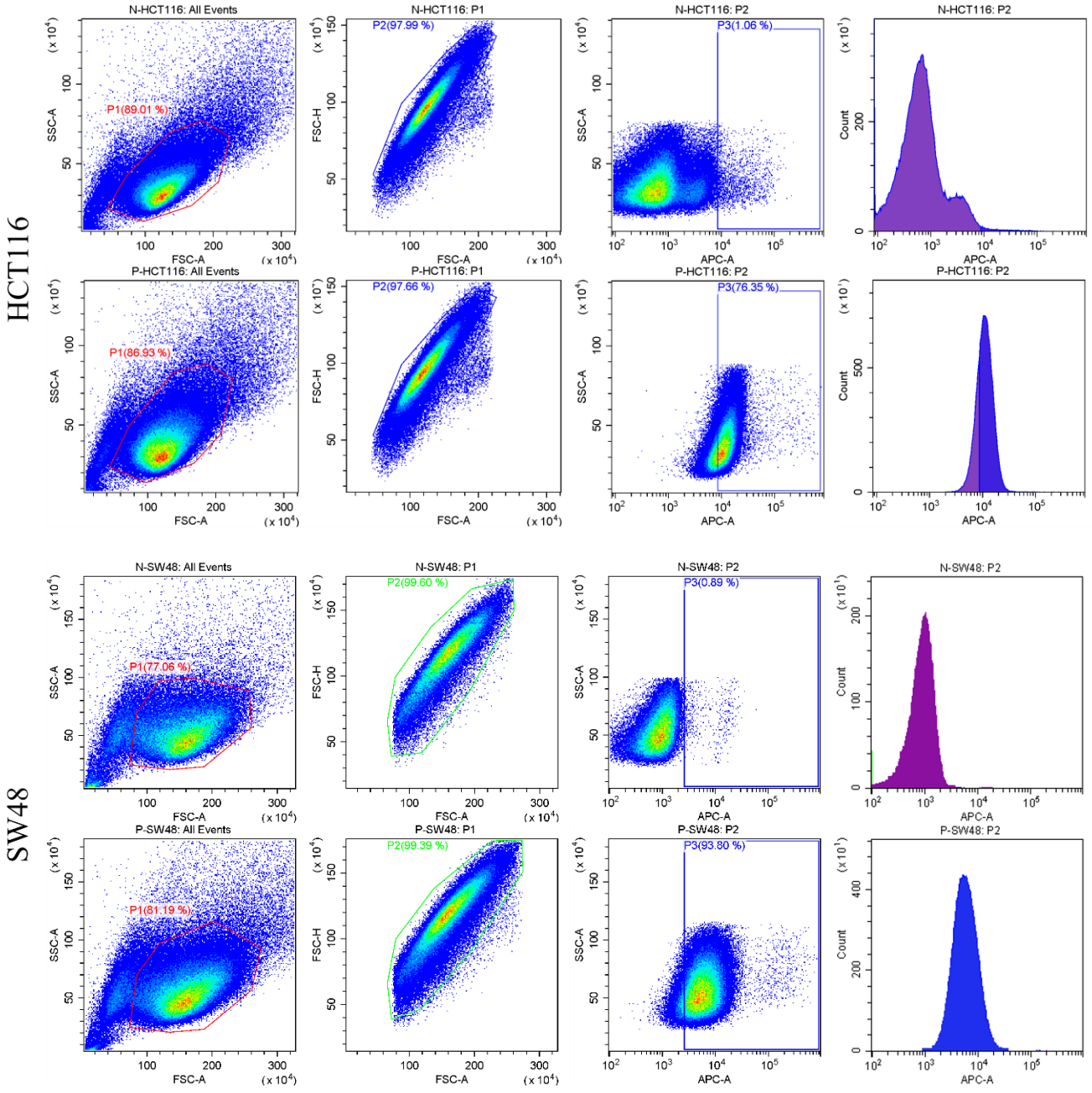

G. Expression level of PSC003 in the intracellular compartment of CRC cell lines. PSC003 level was measured in six different CRC cell lines by flow cytometry. The results are provided together with their background staining. The first row for each cell line is representing the background for that specific cell line and second row is showing the staining by APC-conjugated PSC003 antibody. The results belonging to HT29, DLD1, SW480, RKO, HCT116, SW620, and SW48 are shown, respectively.

H. sgRNA sequences for PSE002 and PSC003 with their specificity and efficiency scores.

PSE002

	Position	Strand	Sequence	PAM	Specificity Score	Efficiency Score
1	85450361	-1	GCA[redacted]CG	CGG	94.183	72.027
2	85450155	1	CTA[redacted]CG	CGG	90.717	74.641
3	85450427	1	ATC[redacted]AA	GGG	86.452	66.019

PSC003

	Position	Strand	Sequence	PAM	Specificity Score	Efficiency Score
1	15945307	-1	GTT[redacted]CG	CGG	94.74942	59.70475
2	15945277	1	GAC[redacted]CG	TGG	94.15003	66.14694
3	15945539	-1	TGT[redacted]GA	AGG	83.58106	59.37897

*The guide RNA sequences for target genes are not disclosed. These sequences would be revealed in the forthcoming manuscript.

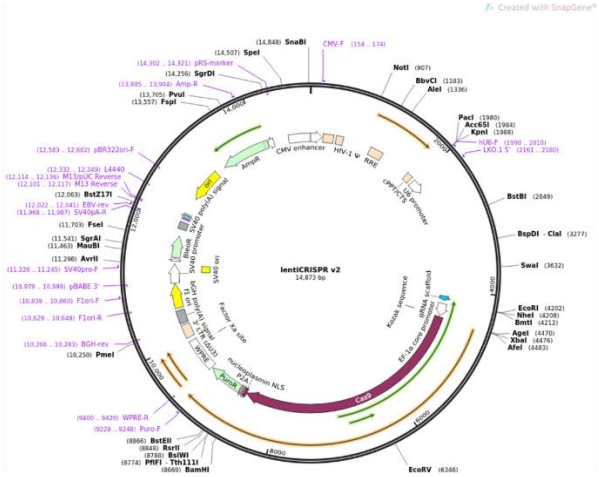

I. The map of lentiCRISPR v2 plasmid[129][130].

J. The format of oligos for cloning of sgRNA into lentiCRIPSRv2 plasmid after the restriction by *BsmBI*[129][130].

Permission for copyrights for the figures used in this thesis.

Copyrights permission for Figure 1.

SPRINGER NATURE LICENSE
TERMS AND CONDITIONS
Jan 28, 2021

This Agreement between Beste Uygur ("You") and Springer Nature ("Springer Nature") consists of your license details and the terms and conditions provided by Springer Nature and Copyright Clearance Center.

License Number	4997790578708
License date	Jan 28, 2021
Licensed Content Publisher	Springer Nature
Licensed Content Publication	Nature Reviews Cancer
Licensed Content Title	Genetic prognostic and predictive markers in colorectal cancer
Licensed Content Author	Axel Walther et al
Licensed Content Date	Jun 18, 2009
Type of Use	Thesis/Dissertation
Requestor type	non-commercial (non-profit)
Format	print and electronic
Portion	figures/tables/illustrations
Number of figures/tables/illustrations	1
High-res required	no
Will you be translating?	no
Circulation/distribution	500 - 999
Author of this Springer Nature content	no
Title	CHARACTERIZATION OF EXTRACELLULAR PURINERGIC SIGNALING COMPONENTS IN COLORECTAL CARCINOMA

Institution name	Bilkent University
Expected presentation date	Aug 2021
Portions	Figure 1
Requestor Location	Beste Uygur Universiteler Mahallesi Bilkent Universitesi Merkez Kampüs SB Binasi 2. Kat Ankara, 06800 Turkey Attn: Beste Uygur
Total	0.00 USD

Copyrights permission for Figure 2 and Appendix B.

SPRINGER NATURE

Multi-omics of 34 colorectal cancer cell lines - a resource for biomedical studies

Author: Kaja C. G. Berg et al

Publication: Molecular Cancer

Publisher: Springer Nature

Date: Jul 6, 2017

Copyrights permission for Figure 3.

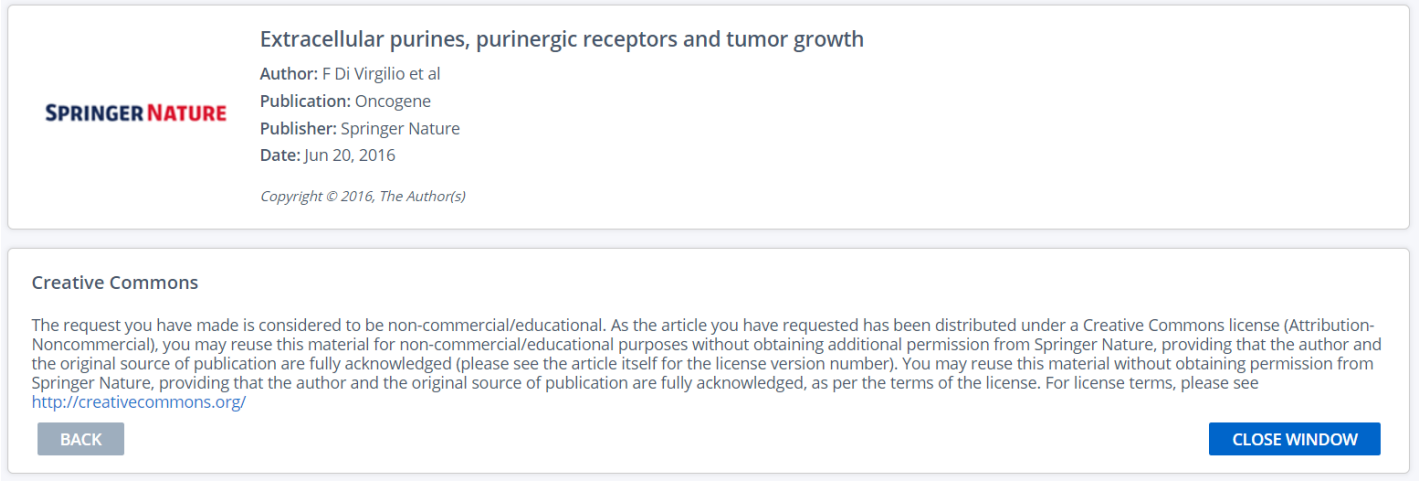

Extracellular purines, purinergic receptors and tumor growth

Author: F Di Virgilio et al
Publication: Oncogene
Publisher: Springer Nature
Date: Jun 20, 2016